Very/Ultra high energy cosmic rays

Measurements and interpreptation of the flux

Ioana C. Mariș

University of Granada, Spain

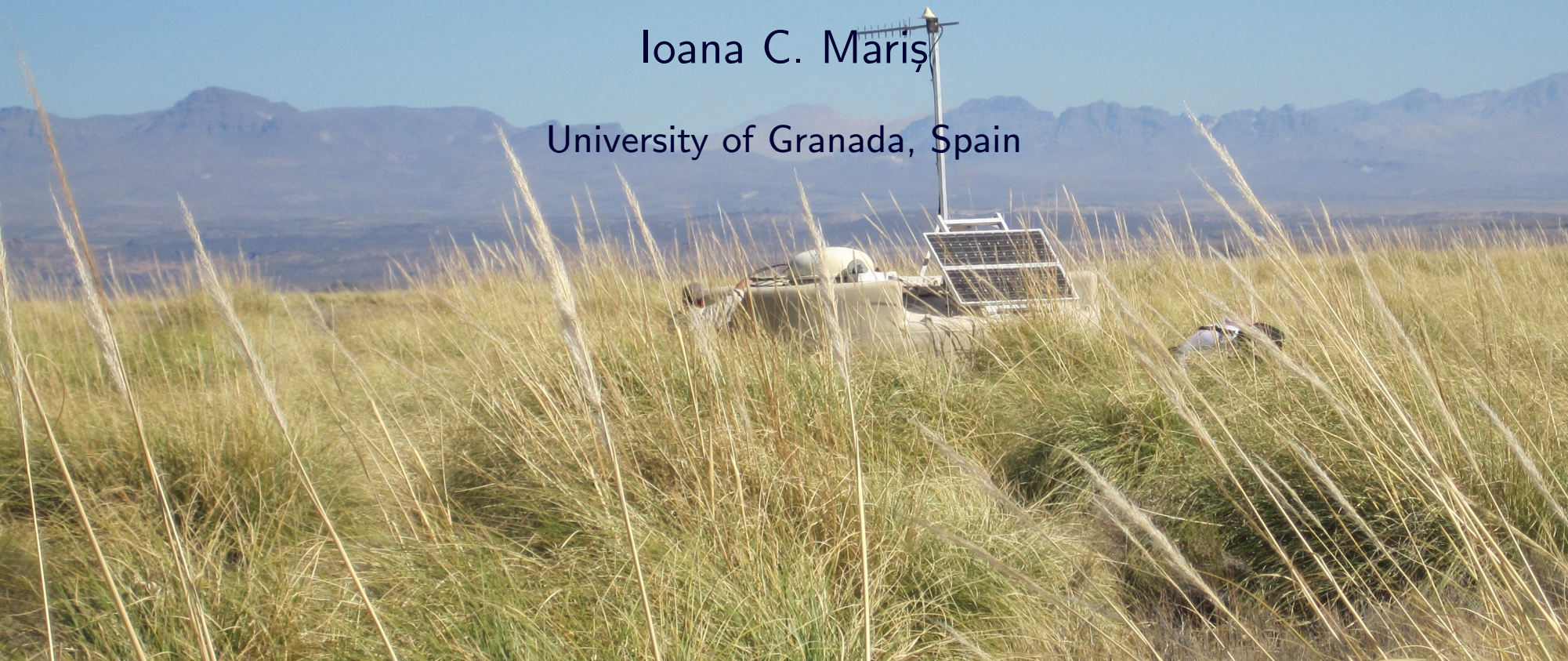

Ultra High Energy Cosmic Rays

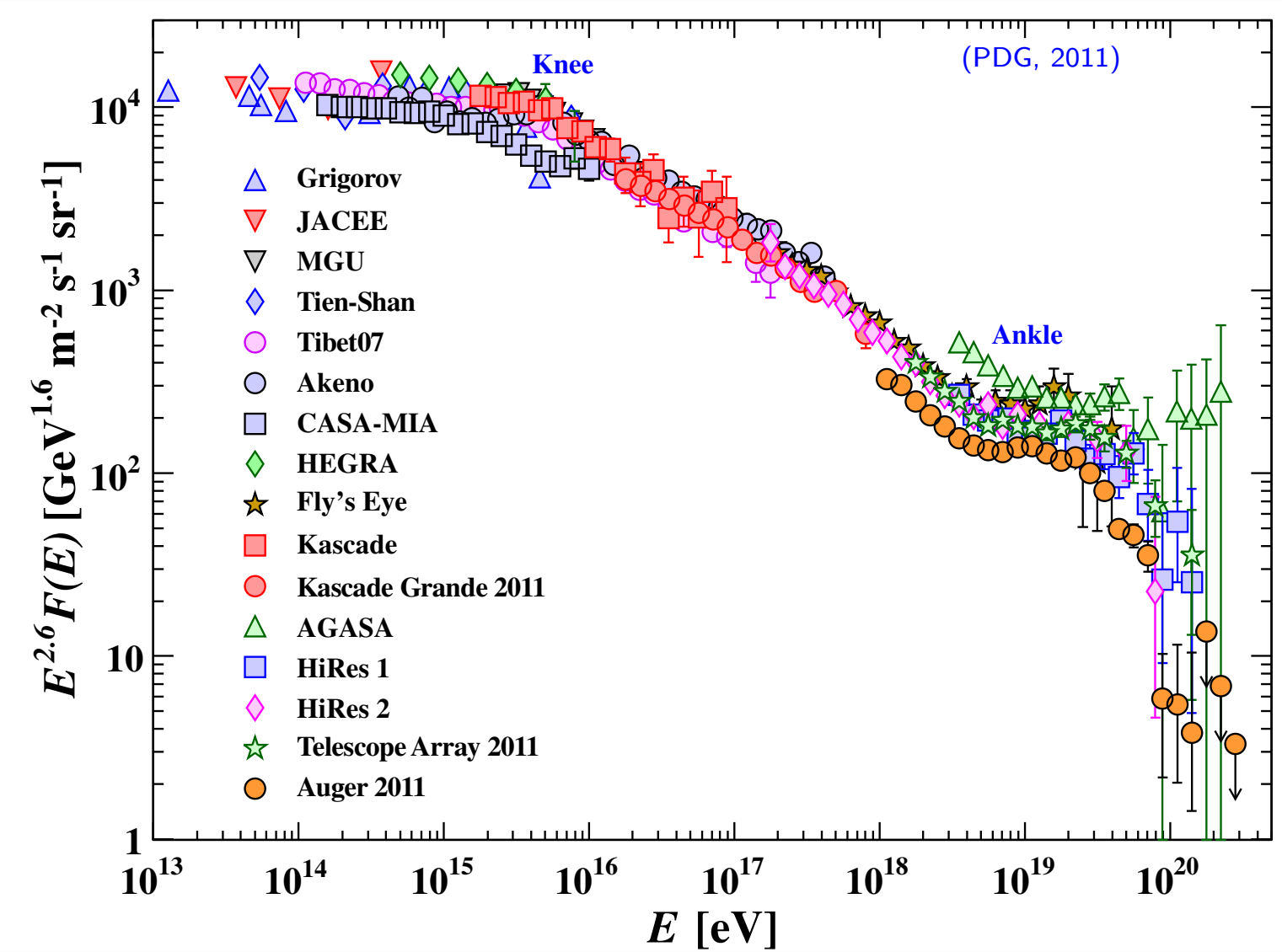

spectral features: propagation and acceleration effects

heavy or light composition (?), UHECRs sources(?), particle interactions (?)

Cosmic rays flux

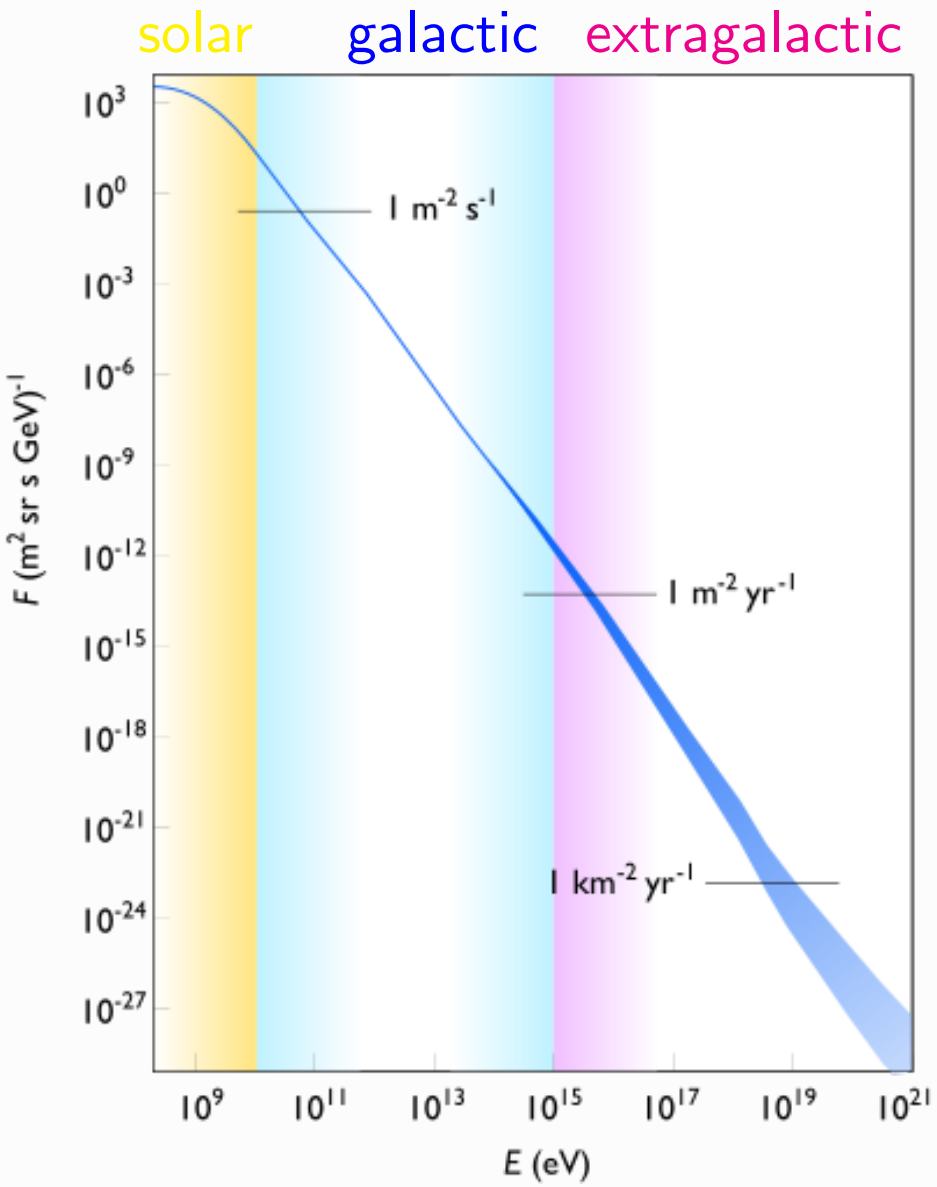

very high energies: 1 /km2 /10 años

- 1963, John Linsley (Volcano Ranch) finds UHECRs
- 1995, Fly's Eye detector confirms the existence of 100 EeV particles

Flux for different masses

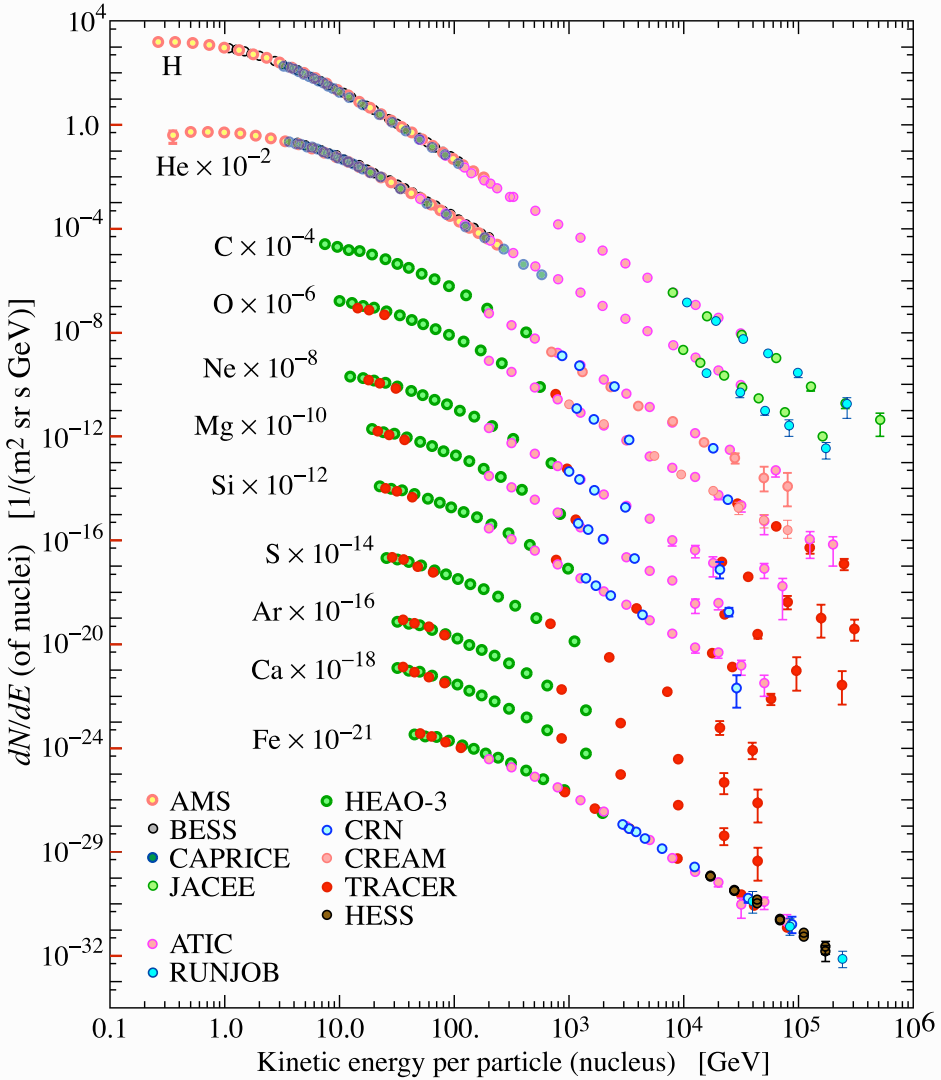

- flux exhibits a power-law behavior
- Power low also found for different elements
- Index of power law almost identical (heavier elements have slightly harder spectra)
- Relative abundances of nuclei: H:1 He:0.38 Z= (6-9):0.22 (10-20):0.15 (21-30):0.4

Low energy fluxes

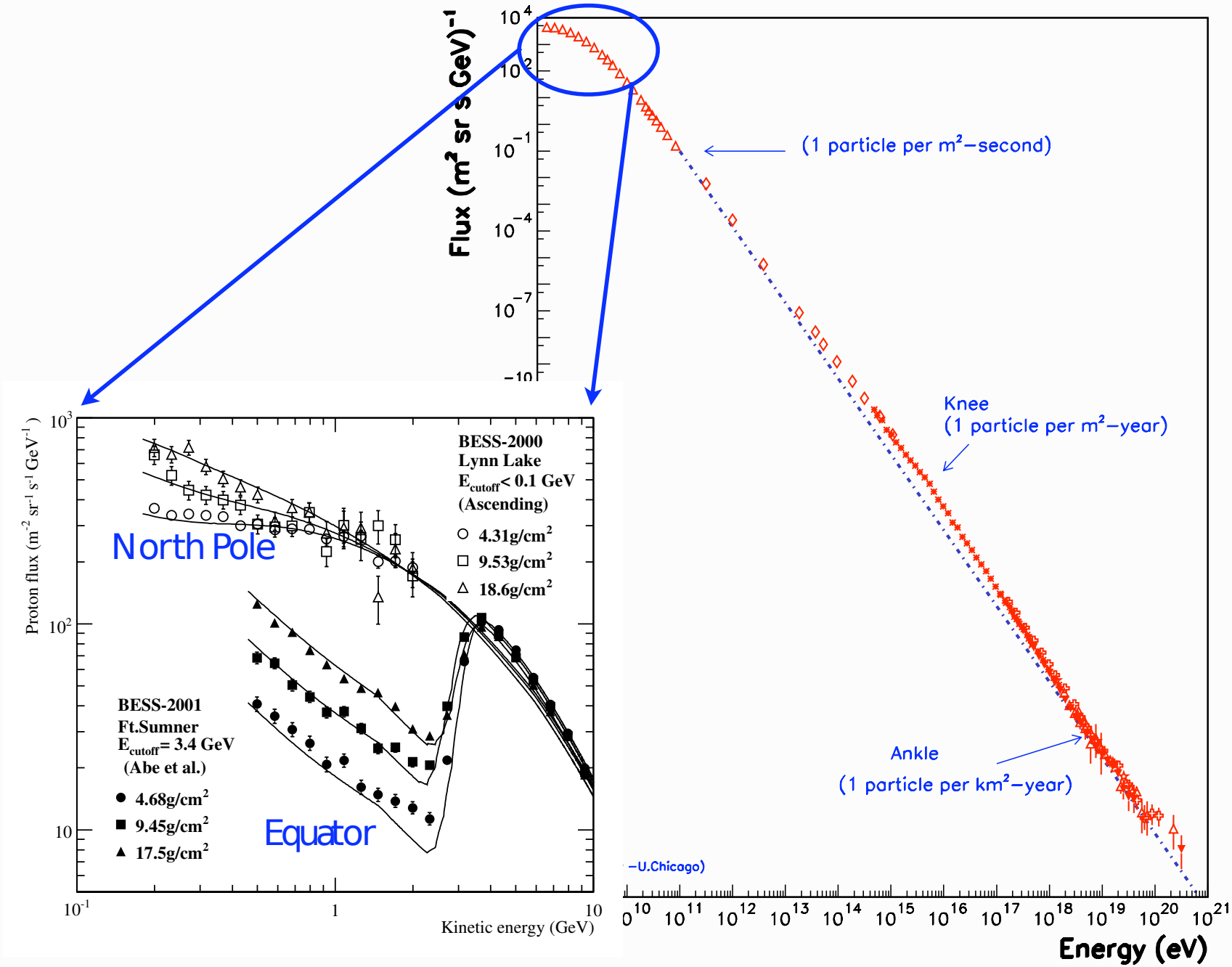

Magnetic field and East-west effect

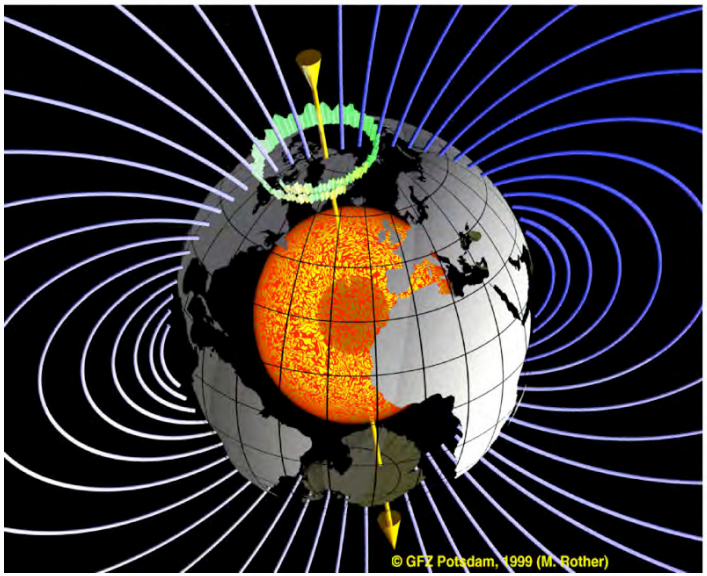

Earth's magnetic field

Vincinity of poles: $B \approx 60\,\mu T$
Equator: $B \approx 30\,\mu T$

$$R_L = 3 \times 10^3 \quad \frac{E}{\text{GeV}} \quad \frac{\mu T}{ZB} \quad \text{km}$$

East-West effect

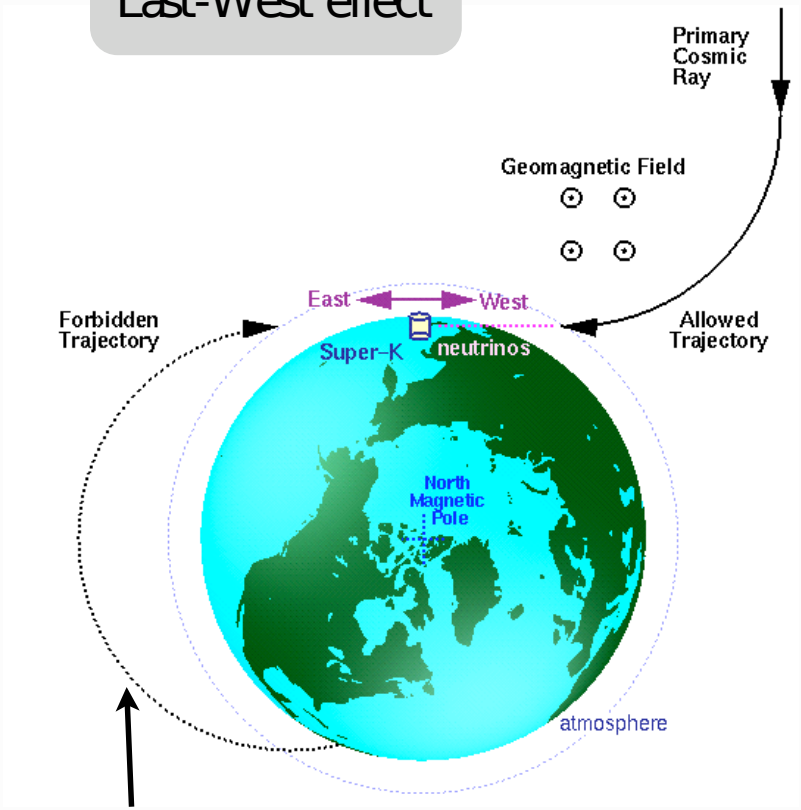

Radius of curvature
smaller than radius of Earth

Low energy fluxes

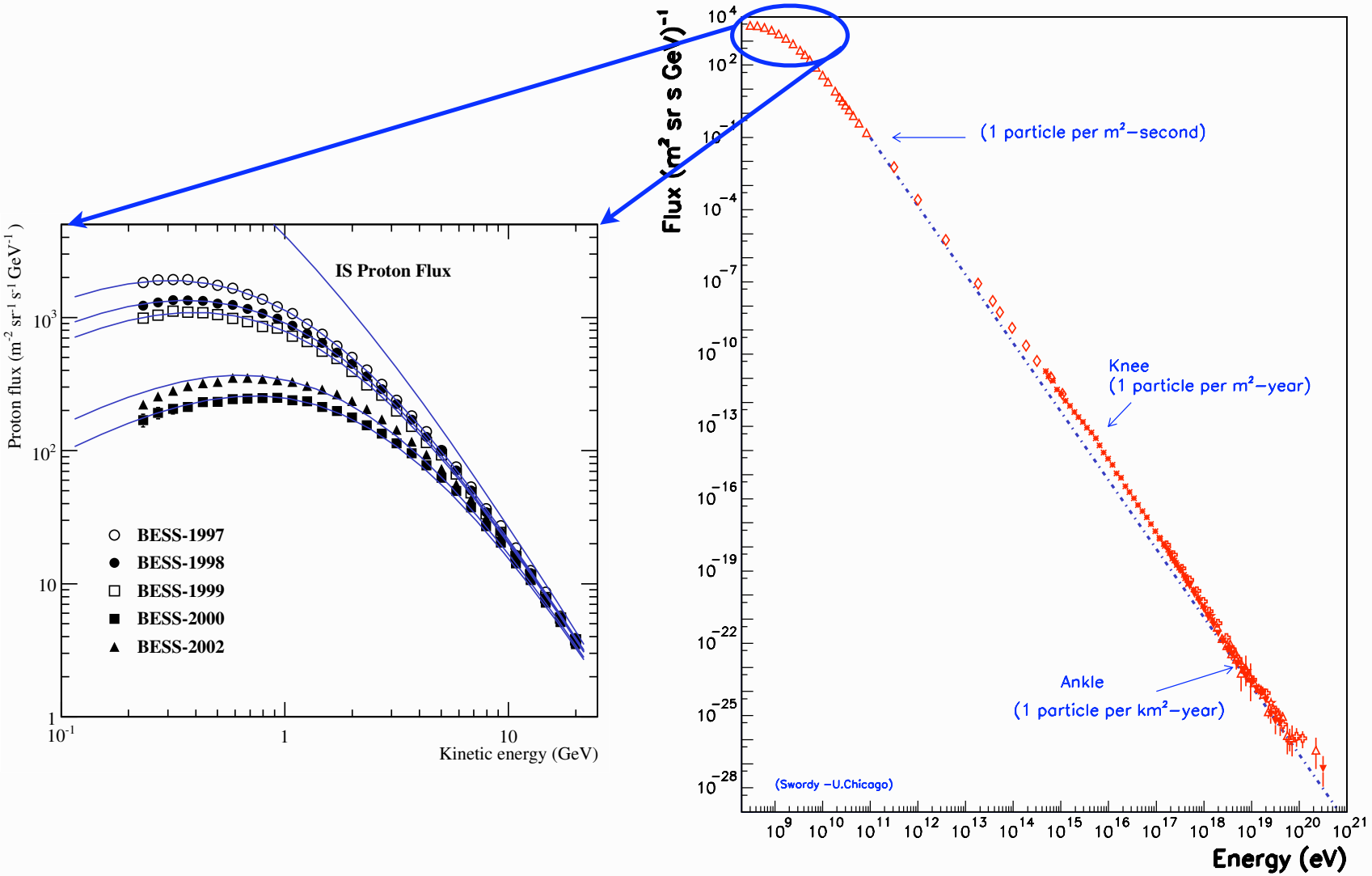

Anti-correlation with solar activity

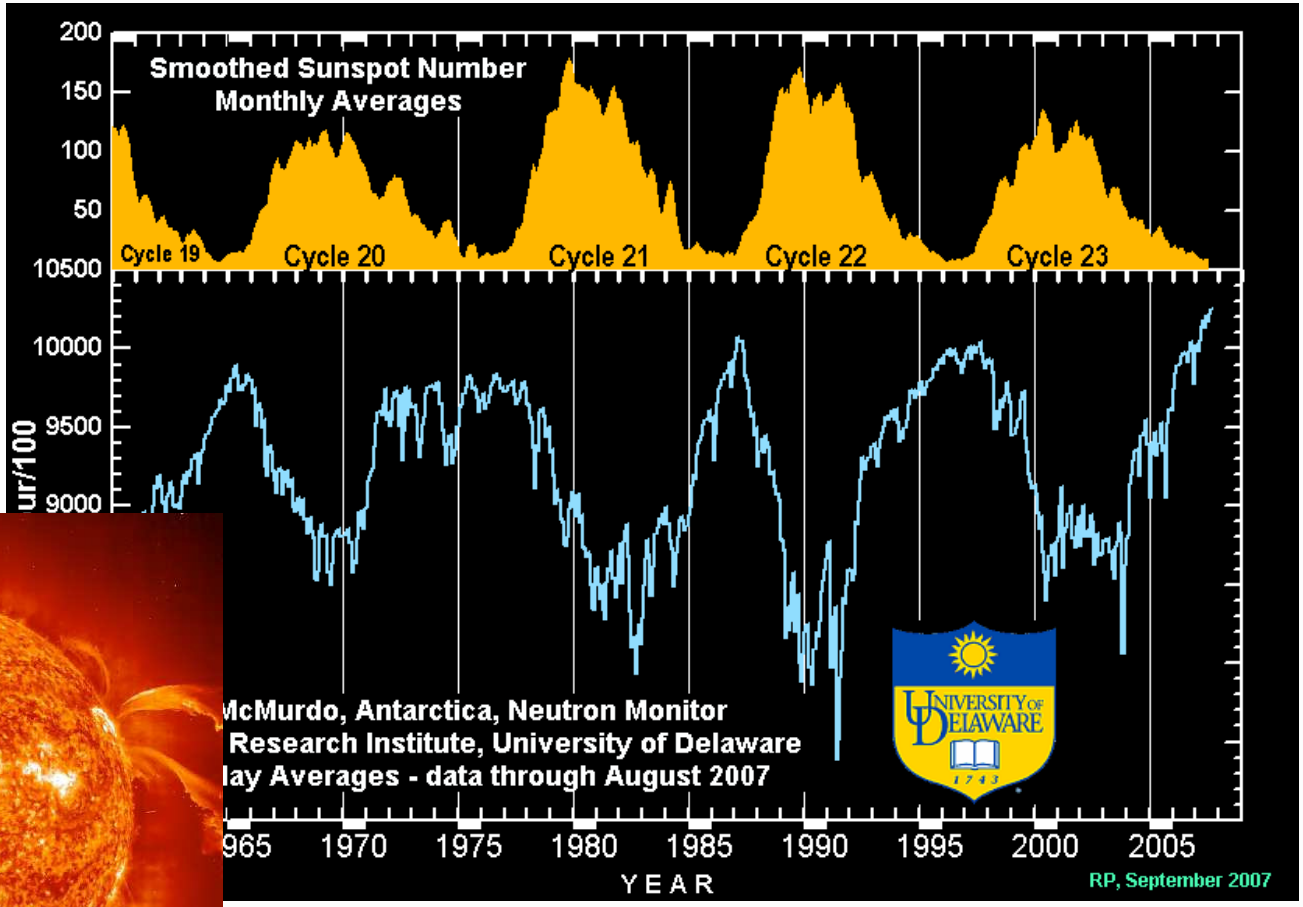

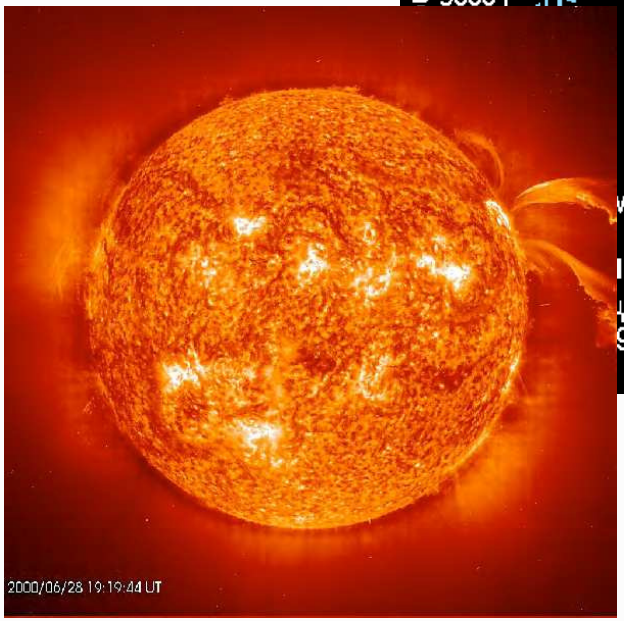

Differential rotation of sun: reversal of mag. field every 11 years (full period 22 years)

Nuclear abundances

Ballon direct measurements

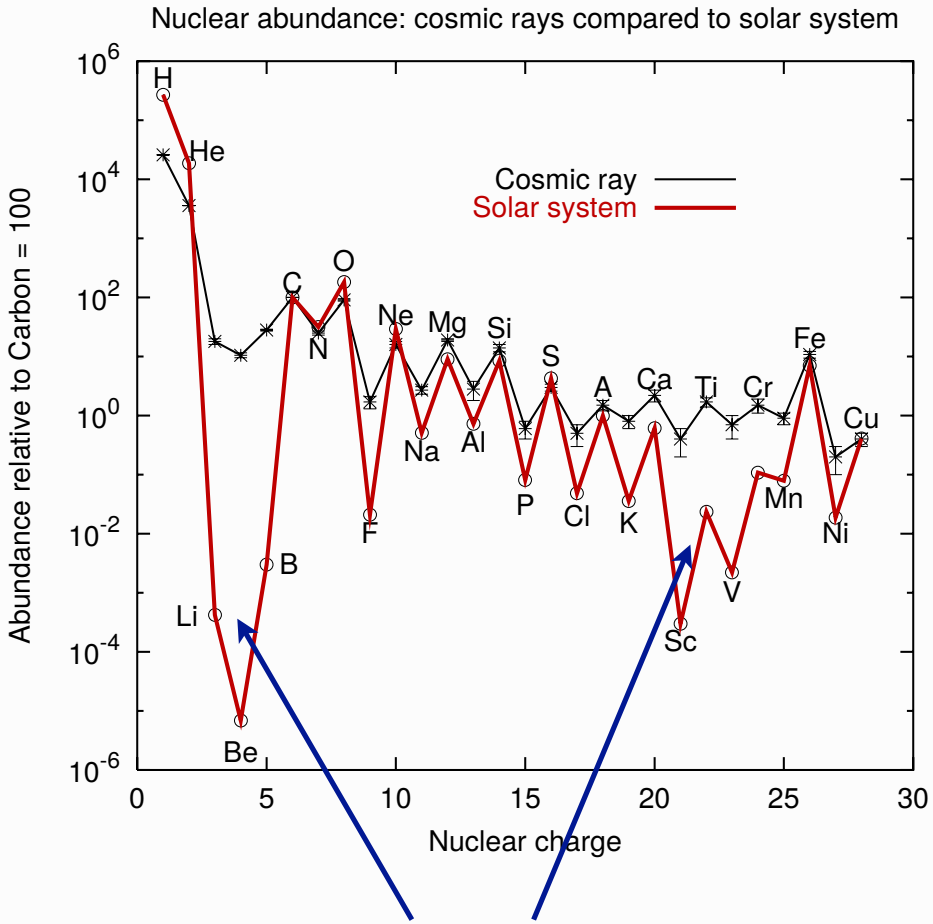

Not typical in supernova

Nuclear abundances, heavy elements

Elements heavier than Iron or Nickel hardly produced in SN explosions

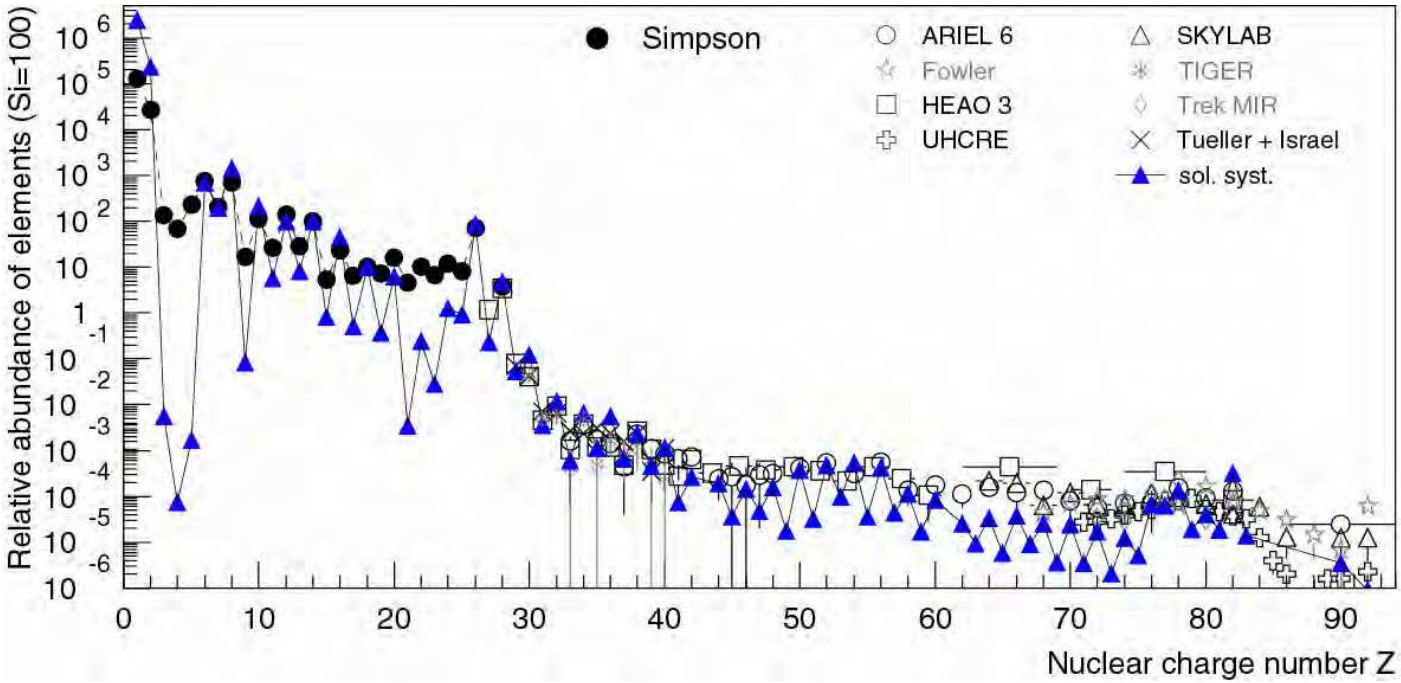

Supernova remants

Observed galactic SN explosions

- 1604(Kepler)
- 1572(Tycho)
- 1181 (Chinese astronomers)
- 1054 (Crab nebula)
- 1006 (CHinese and Arabian records)

General arguments

- $\approx$ 3SN / 100 years
- Kinetic energy: $\approx 10^{51}$ ergs
- Rate and energy budget
- Mass composition
- Acceleration theory

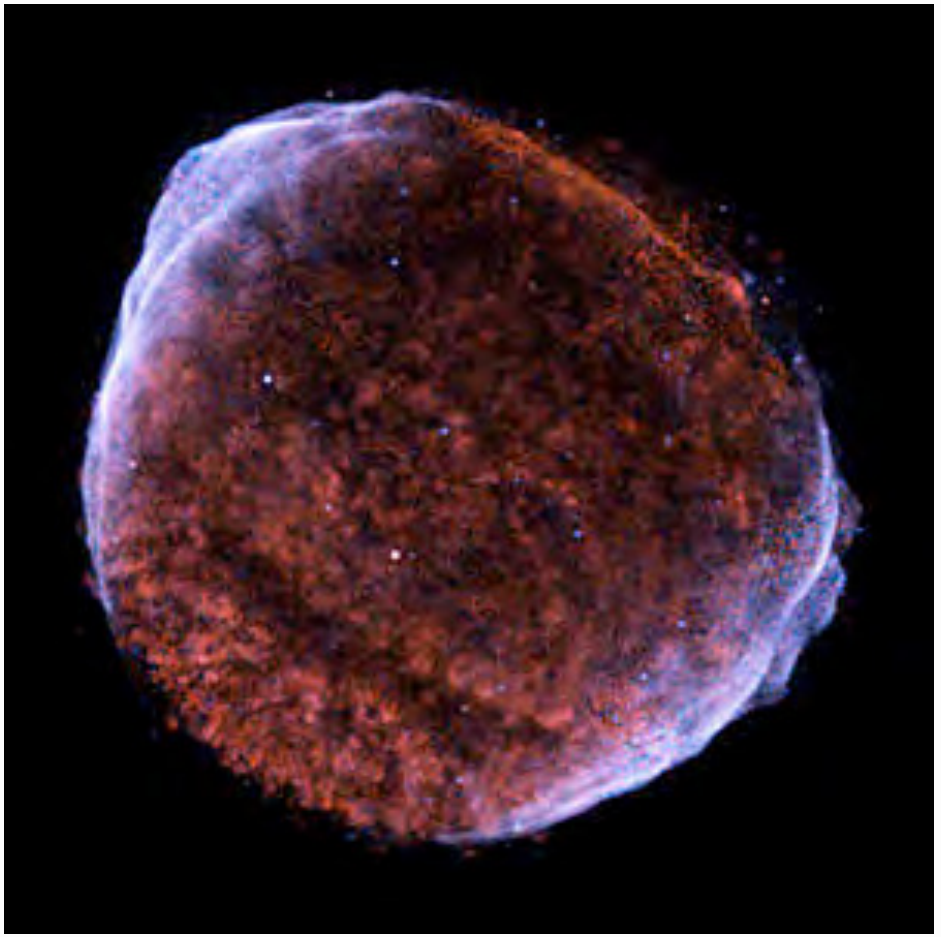

SN 1006

Stochastic (first order Fermi) acceleration in SN

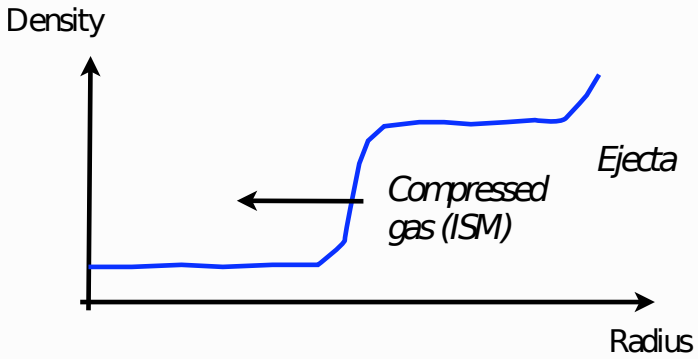

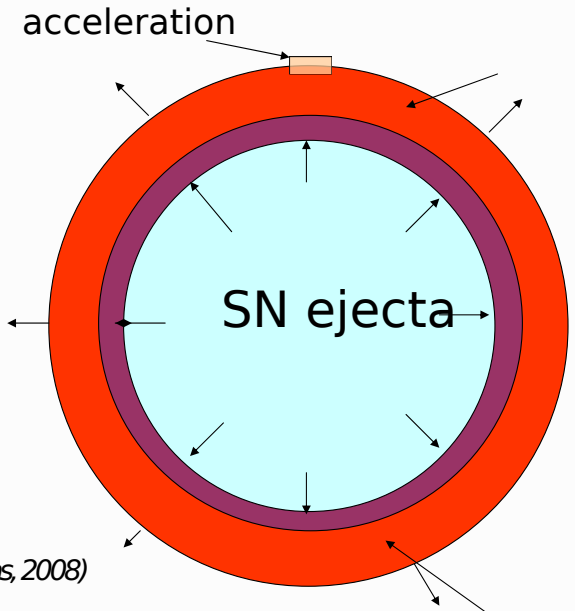

$4\rho_{ISM} \approx \rho_{shock}$

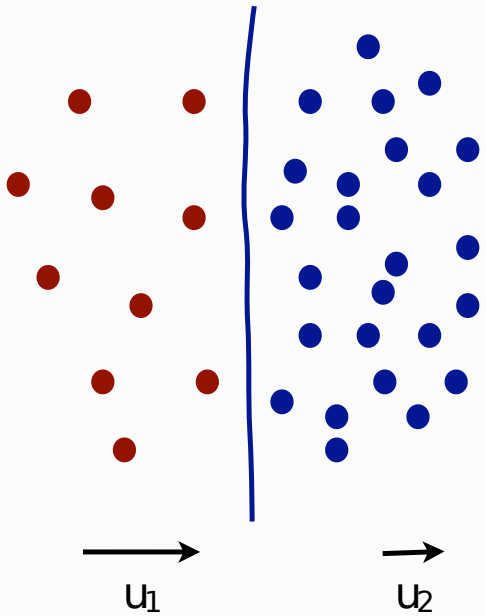

energy gain per crossing:

$$\frac{\Delta E}{E} = \frac{4}{3}\frac{u_1 - u_2}{c}$$

Energy distribution at sources and Earth

Energy independent escape probability: P_{esc}

Energy gain per cycle: $\frac{\Delta E}{E} = \epsilon$

Energy gain after k cicles: $E = E_0 \epsilon^k$

Number of particles for further acceleration: $N = N_0(1 - P_{esc})^k$

This lead to the flux of particles: $N(> E) = ctE^{\alpha}$, $\alpha = -\ln(1 - P_{esc})/ln\epsilon$

Numerical values: $\alpha = 1 \rightarrow dN/dE \propto E^{-2}$

Confinement in the galaxy ($t_{esc} \approx 10^7$ years, energy and 1/Z dependent)
$\rightarrow dN/dE \propto E^{-2.7}$

Comic rays at higher energies escape faster, have a smaller chance to interact

Energy Spectrum at the Knee

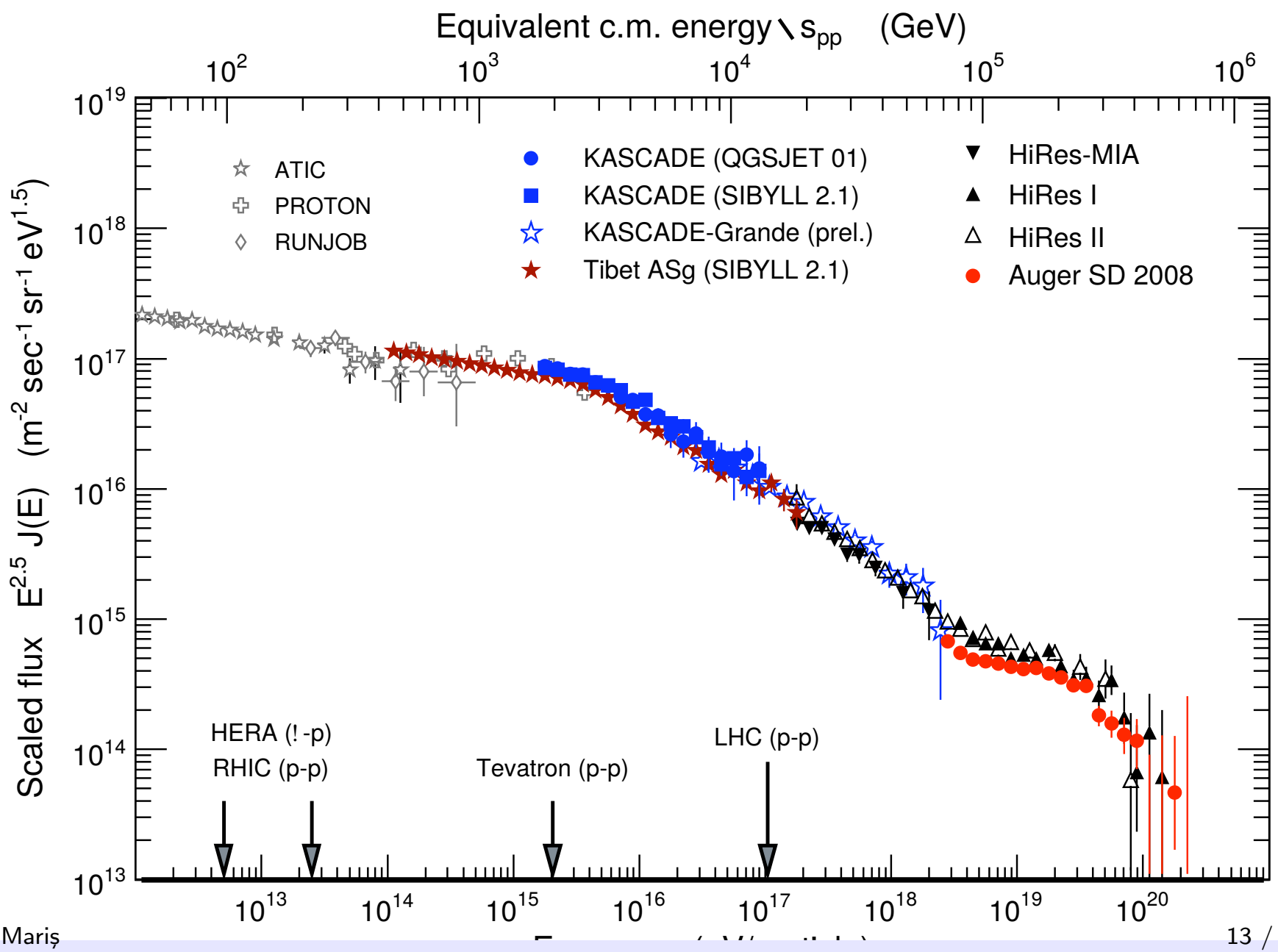

Energy Spectrum at the Knee

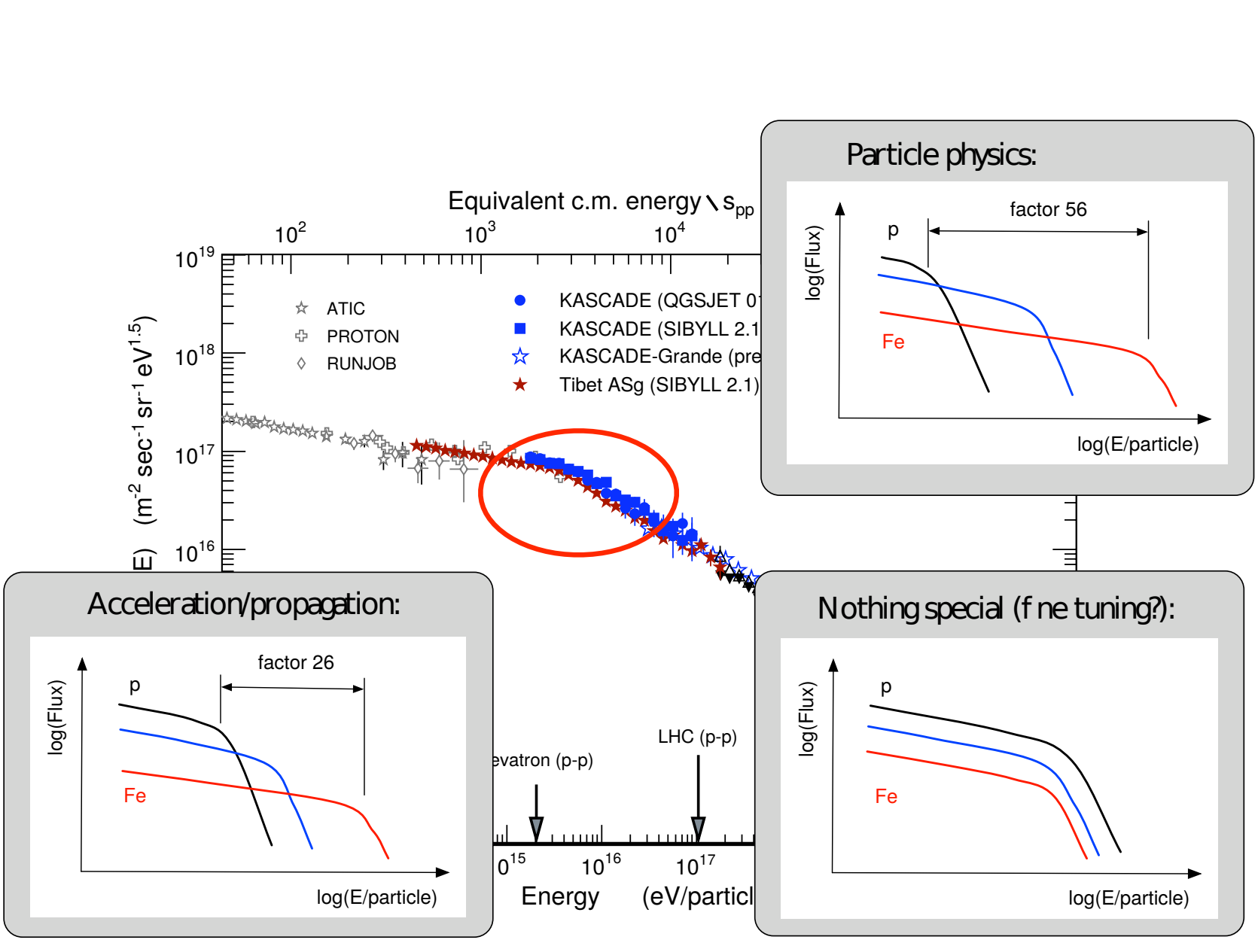

Energy Spectrum at the Knee

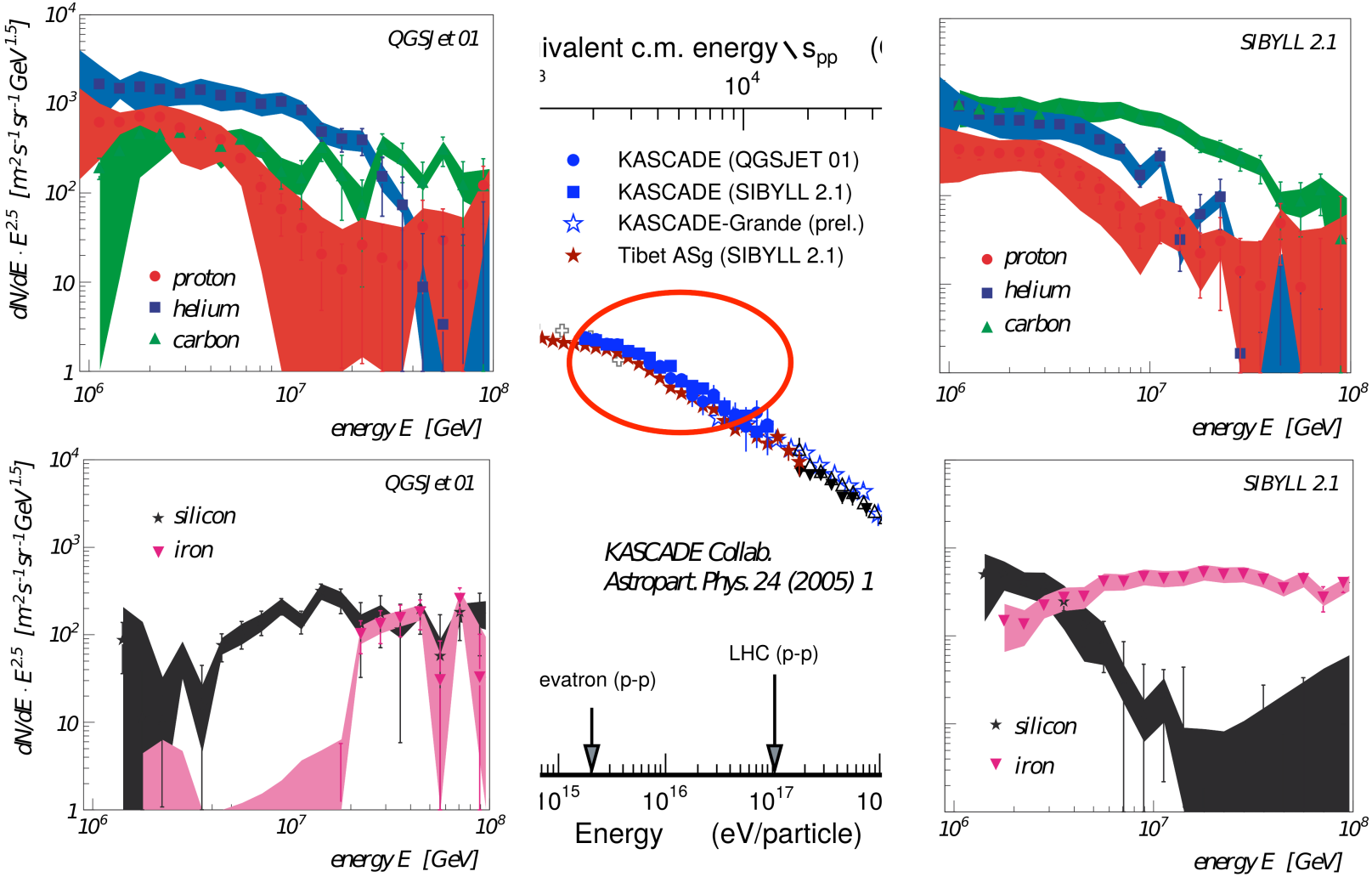

Energy Spectrum Above the Knee

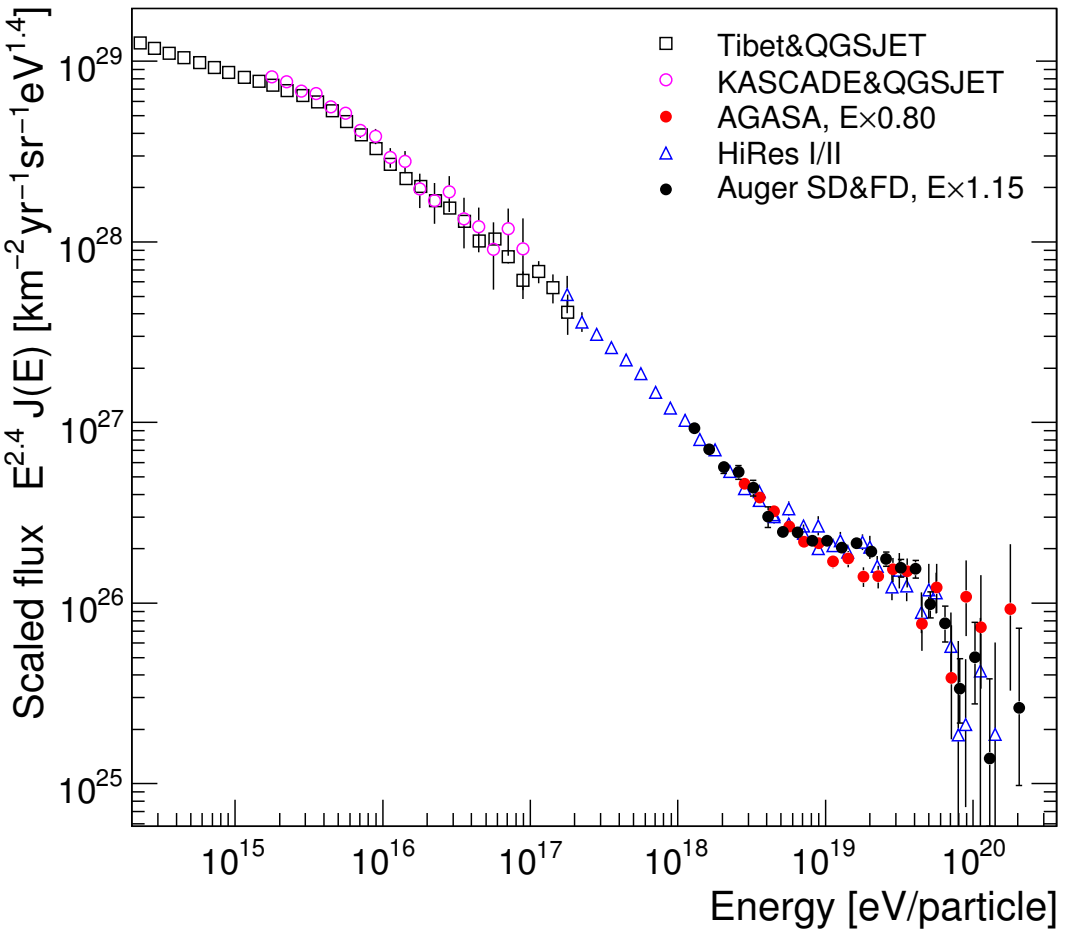

'standard model' of knee:

- maximum energy:
  $\propto Z \cdot E$
- leakage from galaxy:
  $\propto Z \cdot E$

Energy Spectrum Above the Knee

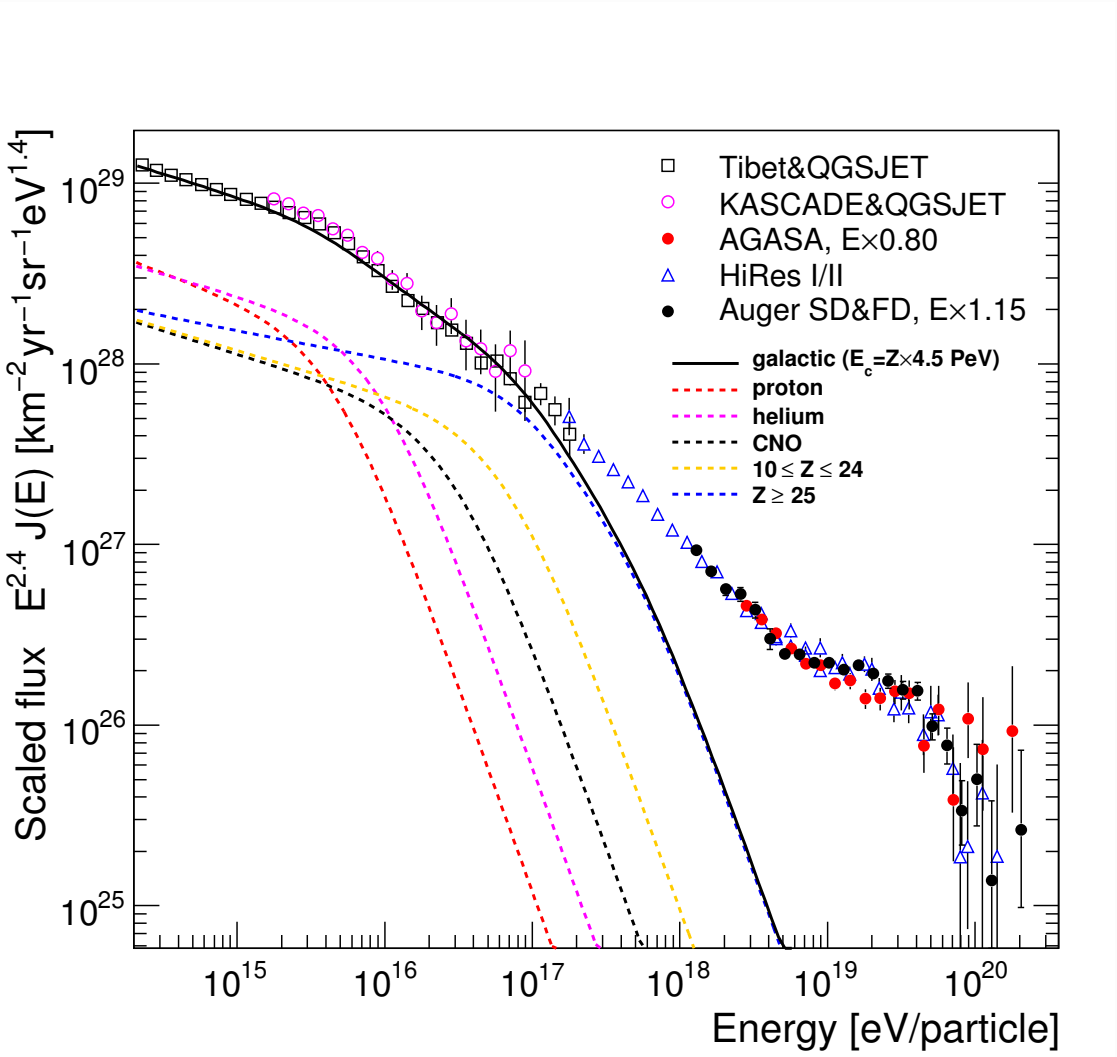

('polygonato' model, Hörandel, APP (2003))

'standard model' of knee:

- maximum energy:
  $\propto Z \cdot E$
- leakage from galaxy:
  $\propto Z \cdot E$

Energy Spectrum Above the Knee

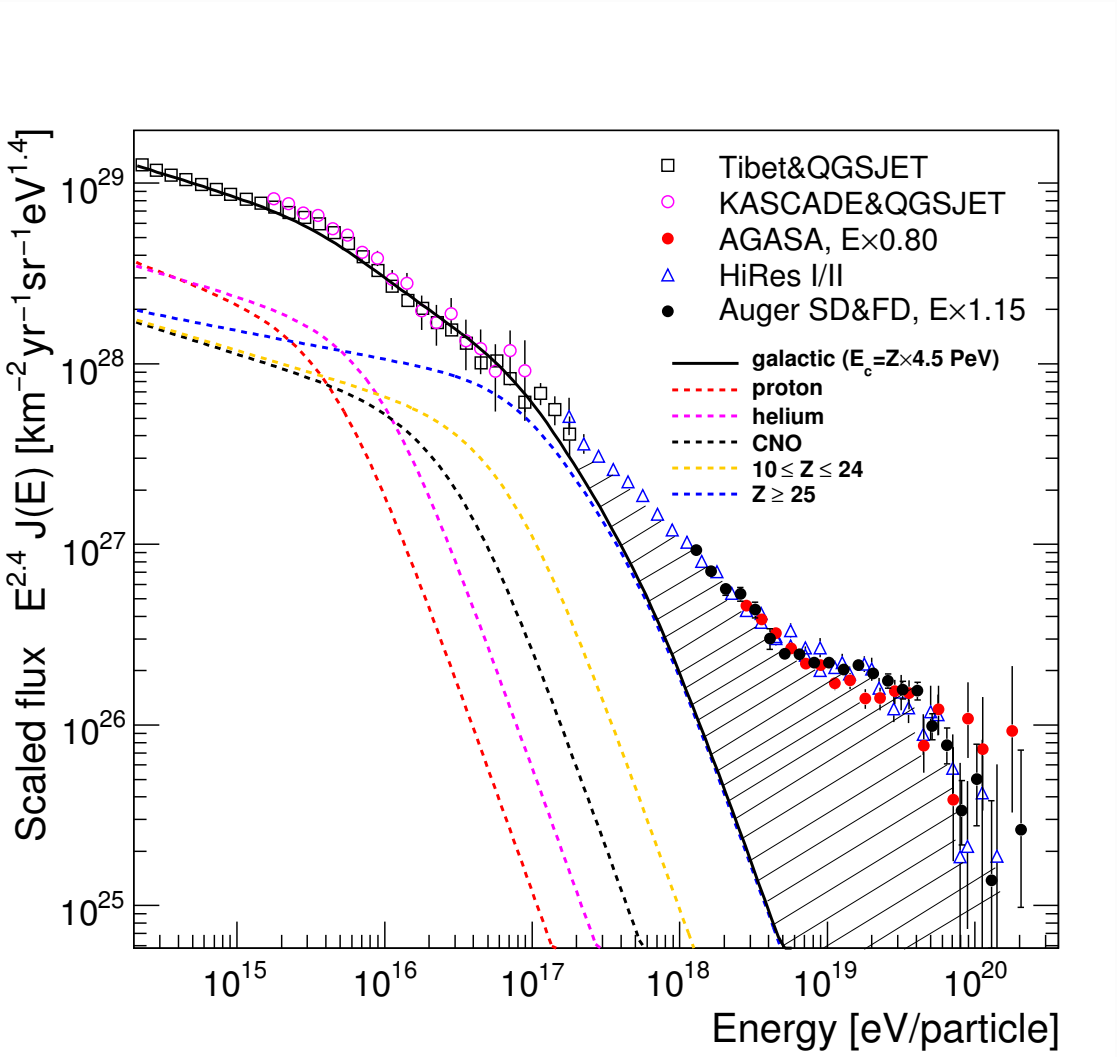

('polygonato' model, Hörandel, APP (2003))

'standard model' of knee:

- maximum energy:
  $\propto Z \cdot E$
- leakage from galaxy:
  $\propto Z \cdot E$

extragalactic stuff!

Propagation of extragalactic protons

redshift

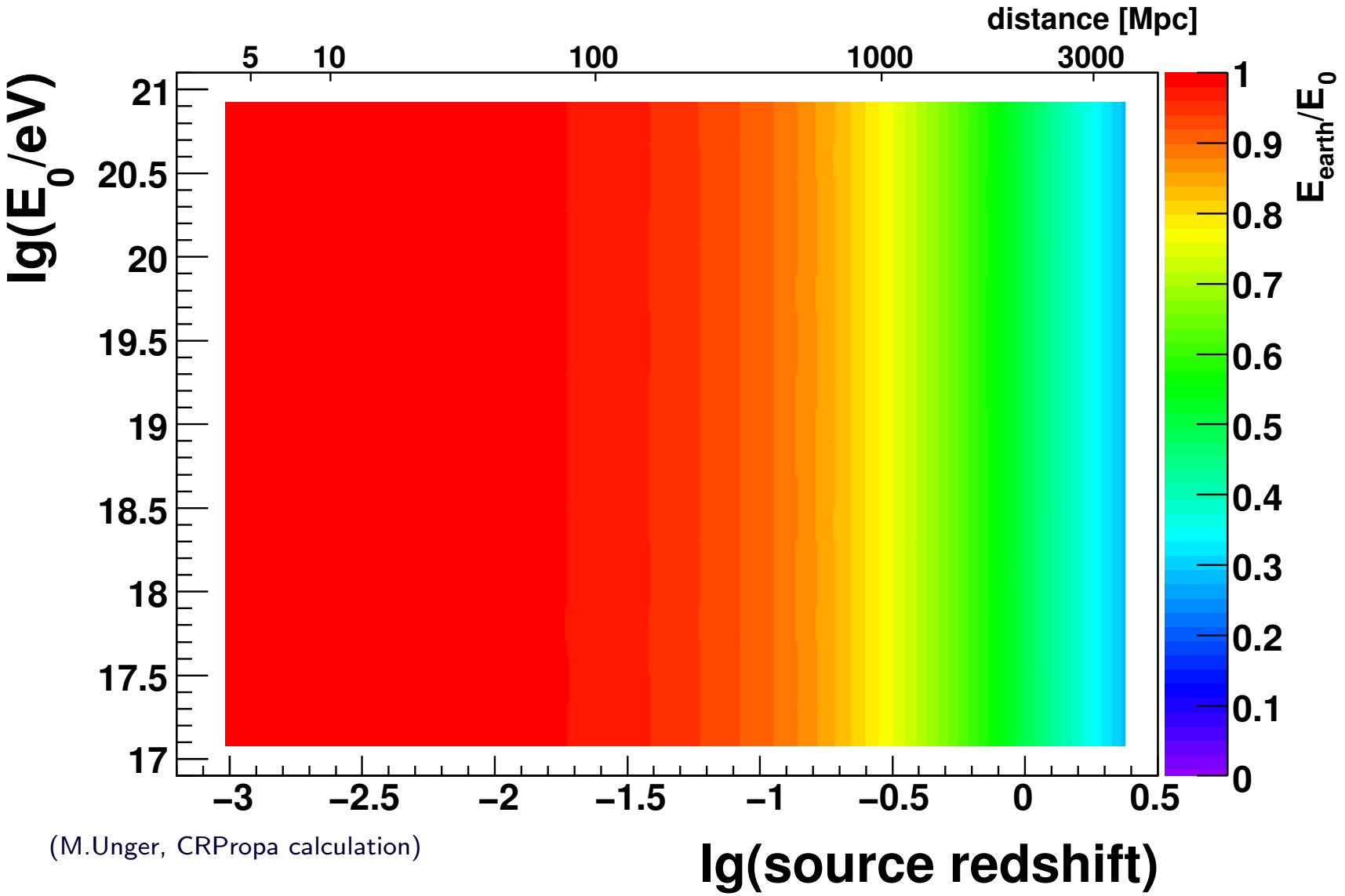

(M.Unger, CRPropa calculation)

Propagation of extragalactic protons

redshift $+ (p + \gamma_{\mathrm{CMB}} \rightarrow p + e^+ + e^-)$

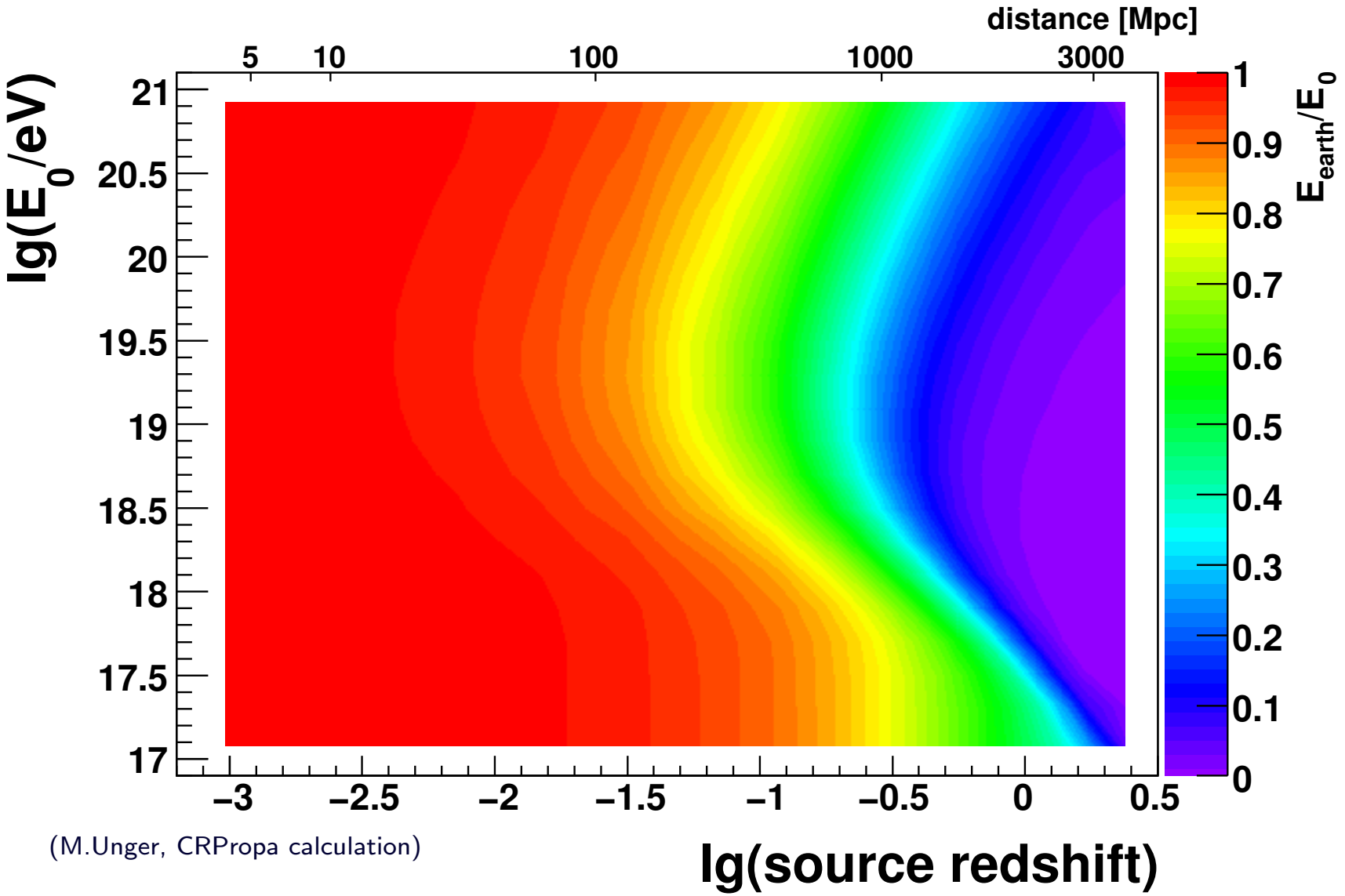

(M.Unger, CRPropa calculation)

Propagation of extragalactic protons

redshift $+ (p + \gamma_{\mathrm{CMB}} \to p + e^+ + e^-) + (p + \gamma_{\mathrm{CMB}} \to p + \pi^0)$

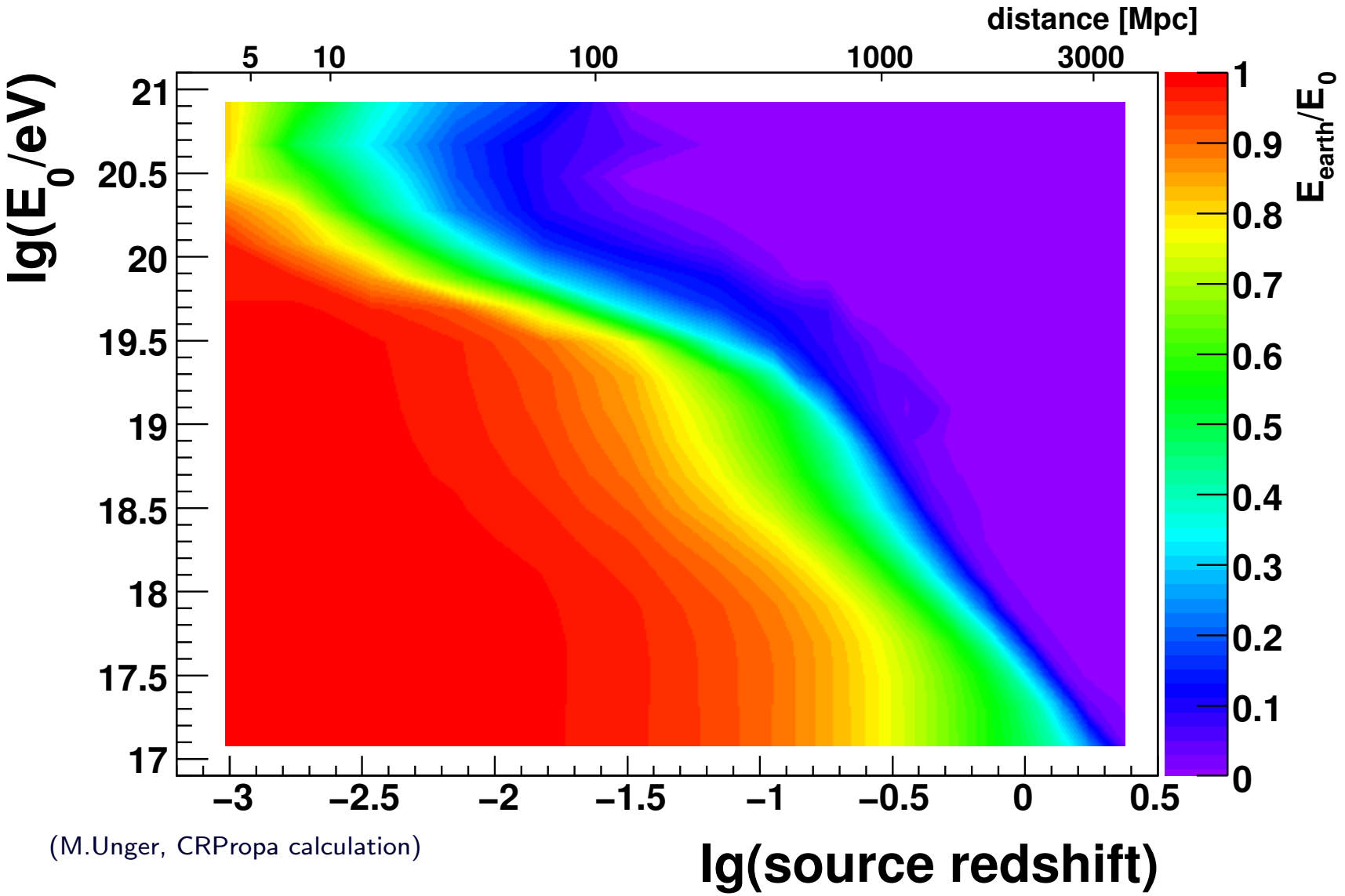

(M.Unger, CRPropa calculation)

The 'Dip' Model

(Berezinsky et al.)

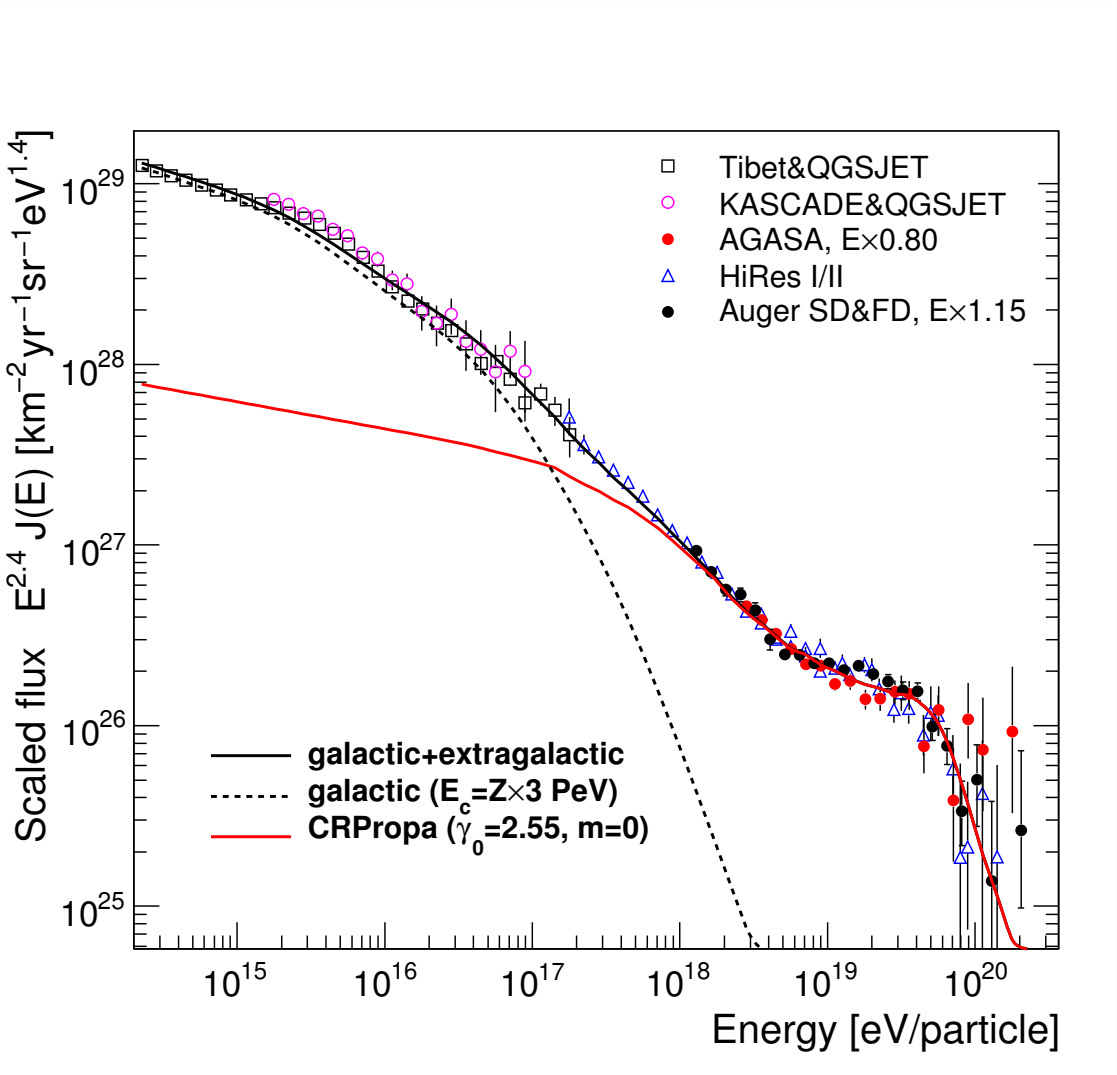

- transition Gal-EGal at 2nd knee $\sim 10^{17}$ eV
- 'standard' galactic component
- spectral features from propagation
- steep source spectra (energy crisis?)
- needs pure EGal p ($\lesssim$ 10% He)

The 'Ankle' Model

(e.g. Bahcall&Waxman 2002, Wibig&Wolfendale 2007)

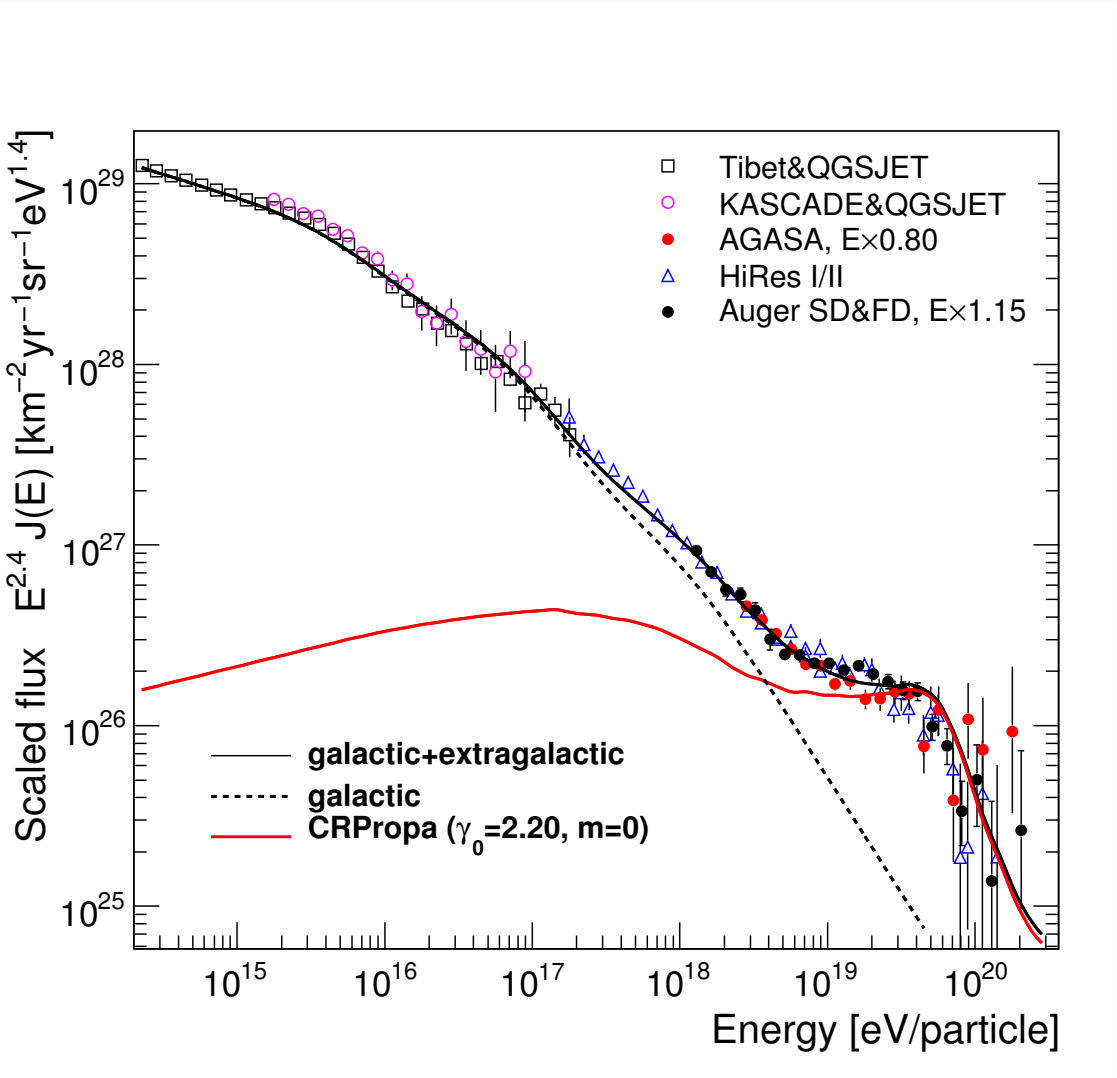

- transition Gal-EGal at several EeV (the ankle!)
- needs powerful galactic accelerators
- flat source spectra

Propagation of extragalactic nuclei

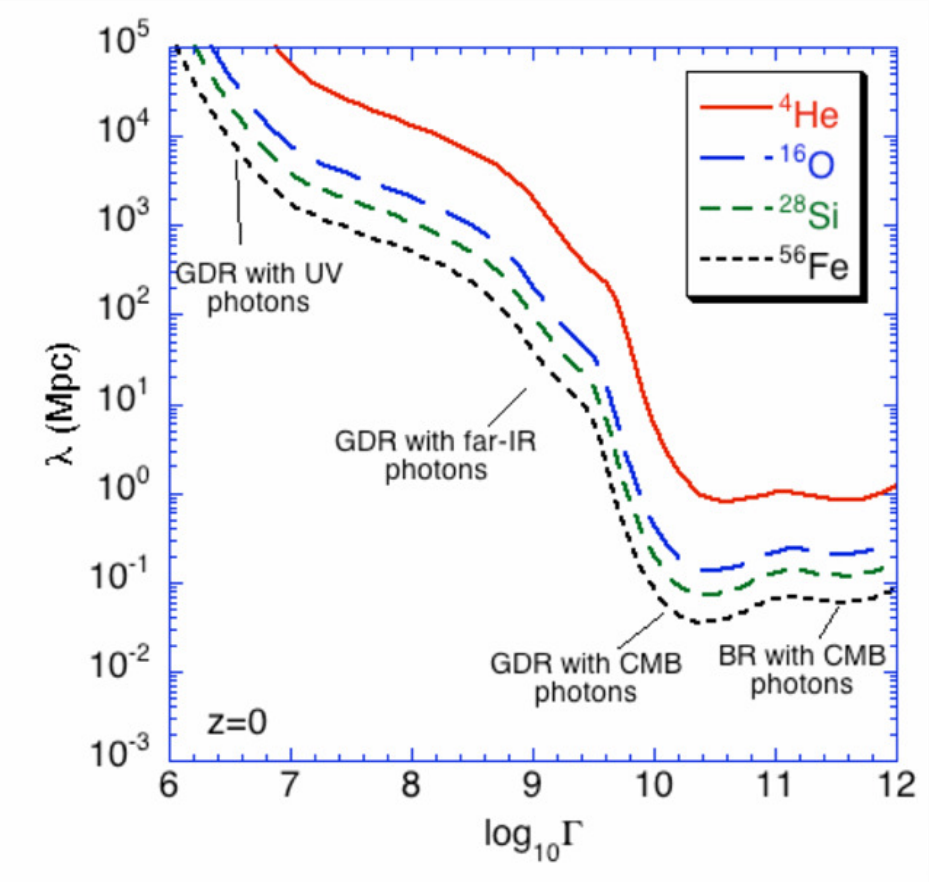

(Allard et al. 2008)

- photodissociation, e.g. $A + \gamma \rightarrow A - 1 + n/p$
- beam composition changes during propagation

Propagation of extragalactic nuclei

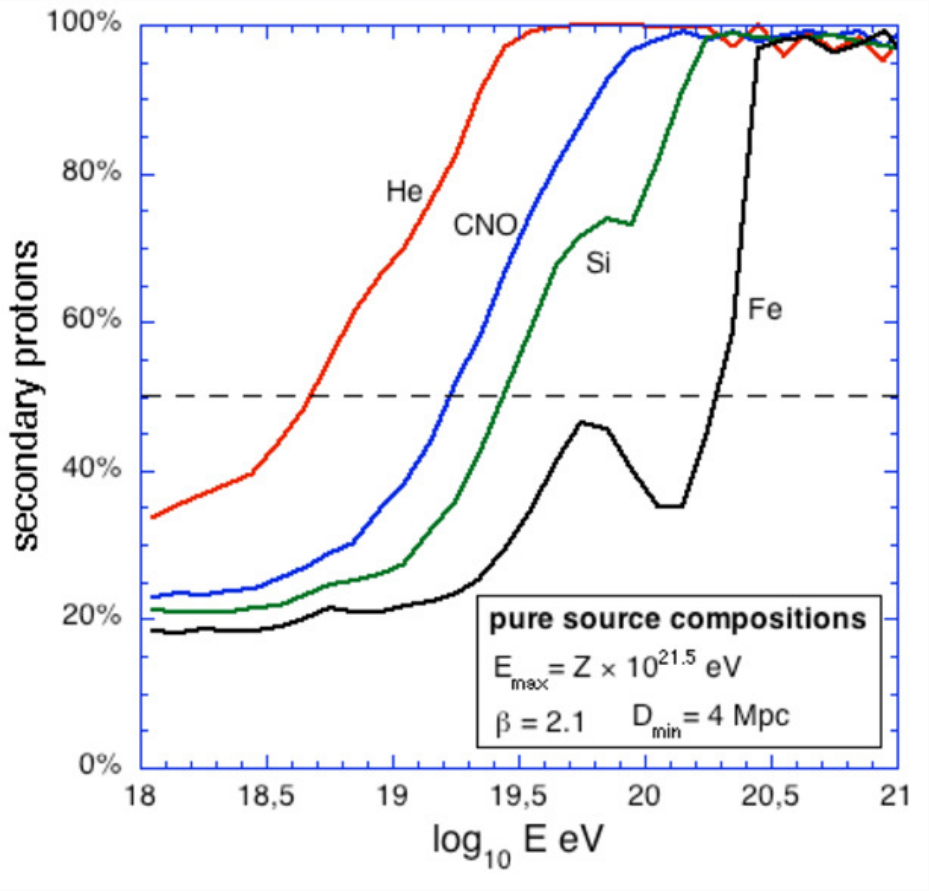

(Allard et al. 2008)

- photodissociation, e.g. $A + \gamma \rightarrow A - 1 + n/p$
- beam composition changes during propagation

Spectrum with extragalactic nuclei

(Allard et al. 2005, 2008)

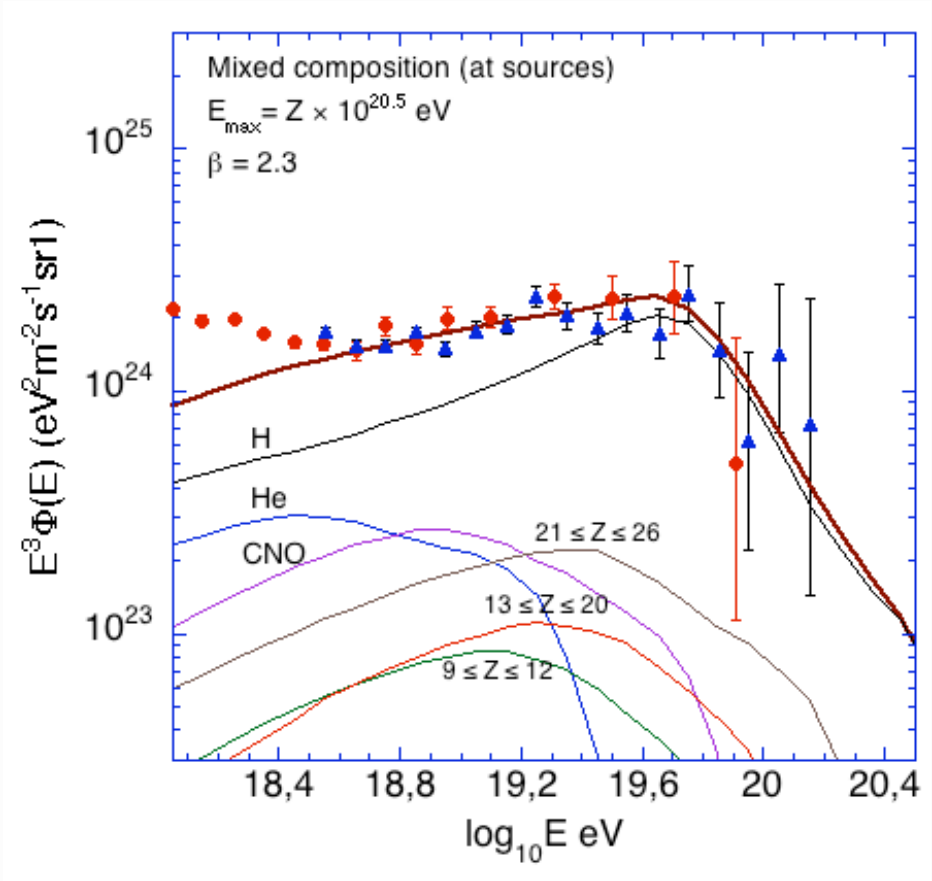

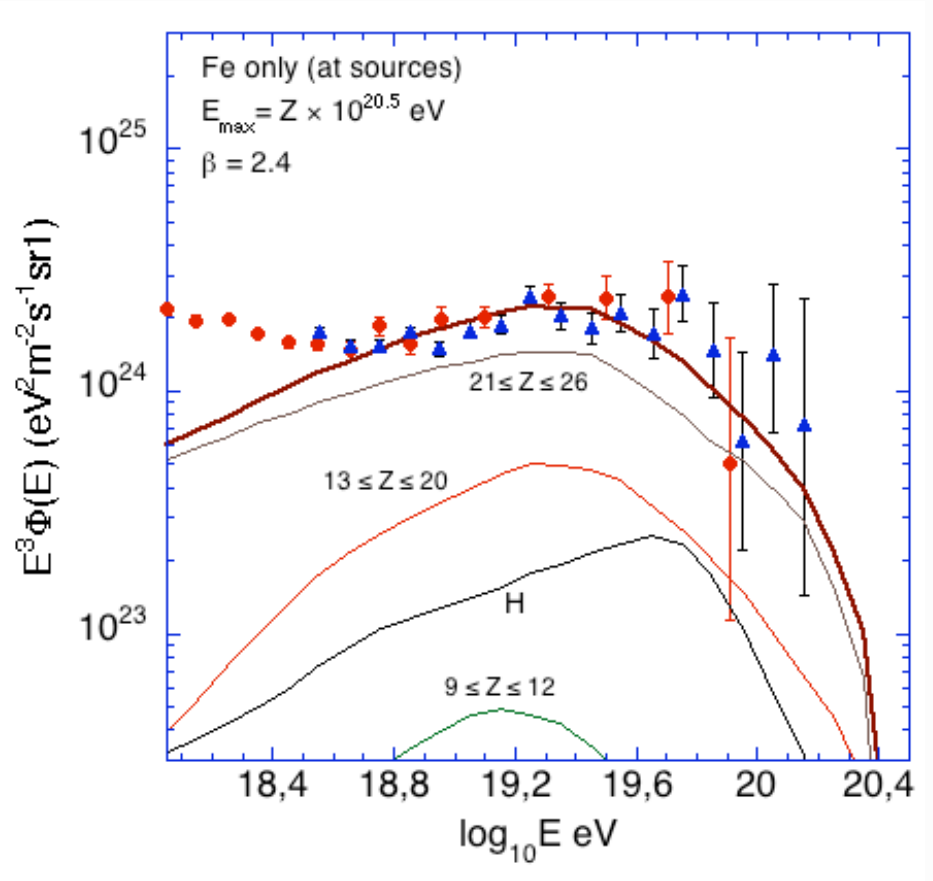

- transition Gal-EGal at around 10^{18} eV

Overview over transition models

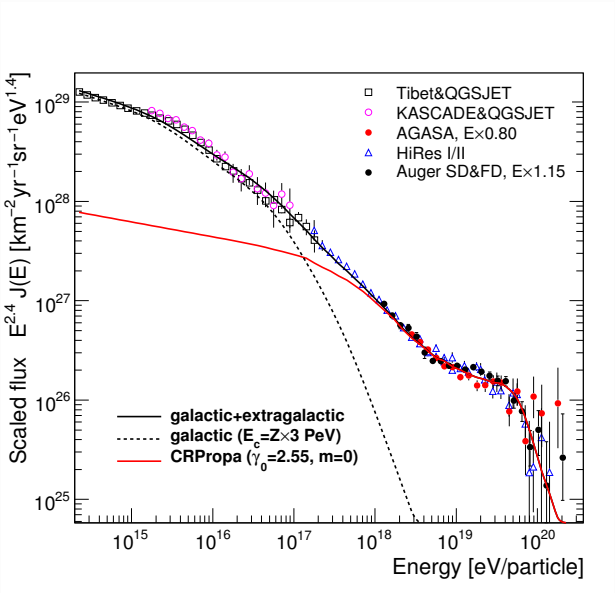

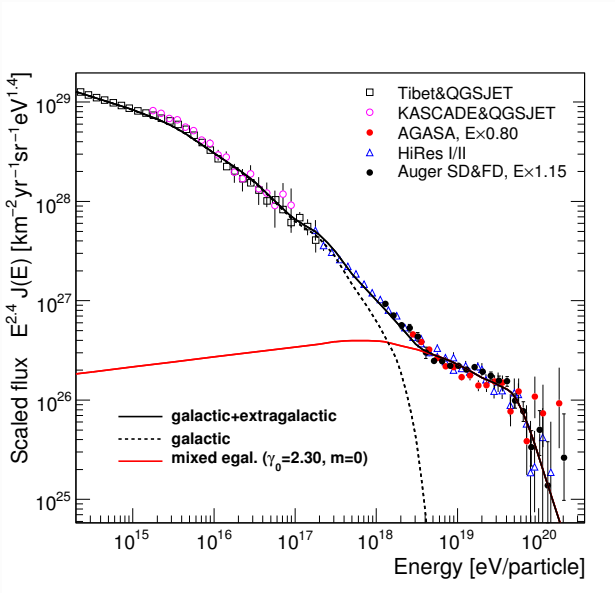

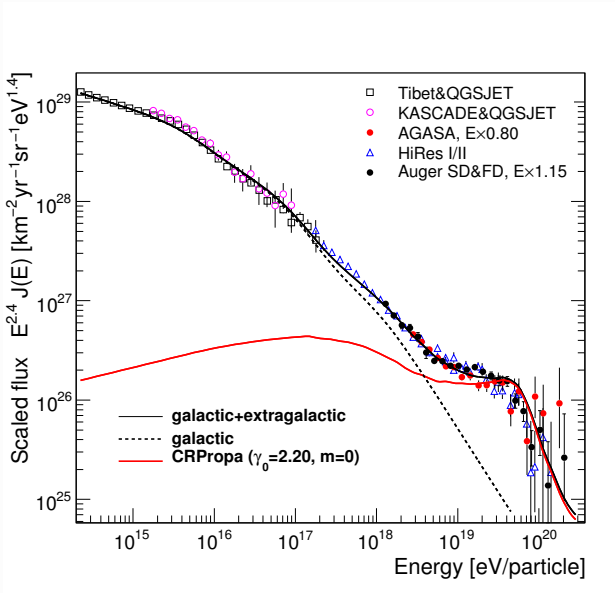

Pierre Auger Observatory

Physics goals: origin and properties of UHECRs
Data taking: since 2004, completed in 2008

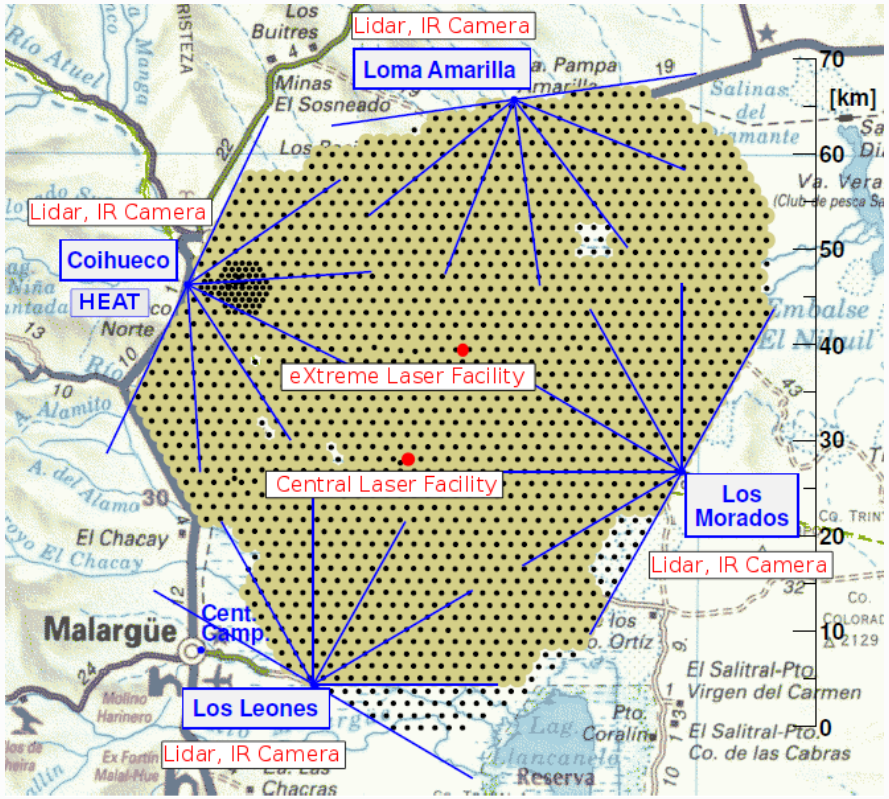

4 Fluorescence detectors

- 10% duty cycle
- 27 telescopes grouped in 5 buildings
- field of view: $(30^\circ \times 180^\circ)$

1663 water Cherenkov detectors

- 100% duty cycle
- 3000 km^2, 1500, 750 m spacing
- distribution of particles on ground

Radio and microwave emissions

- AERA, EASIER, MIDAS, AMBER

Muon counters

- AMIGA

Enhancements of the Pierre Auger Observatory

Infill array

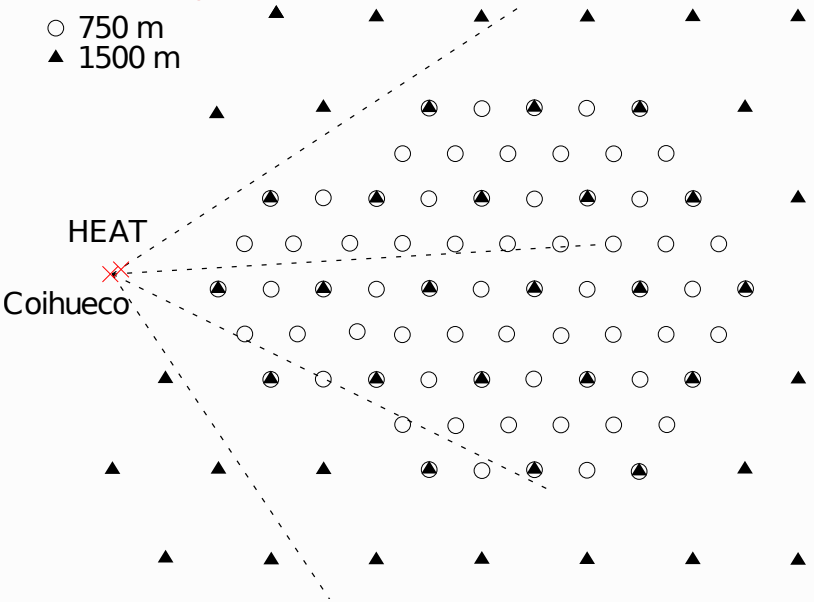

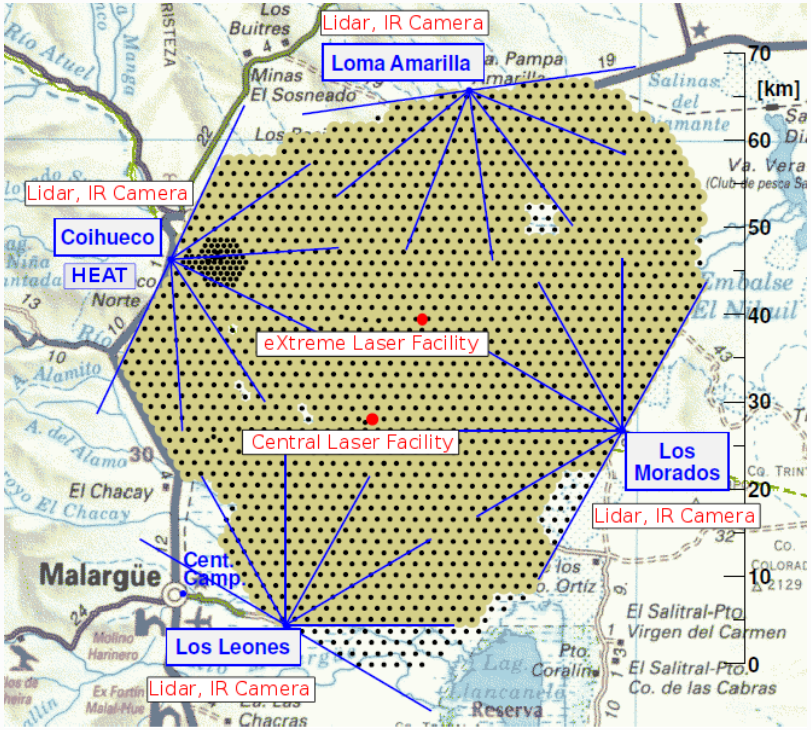

HEAT: High Elevation Auger Telescope

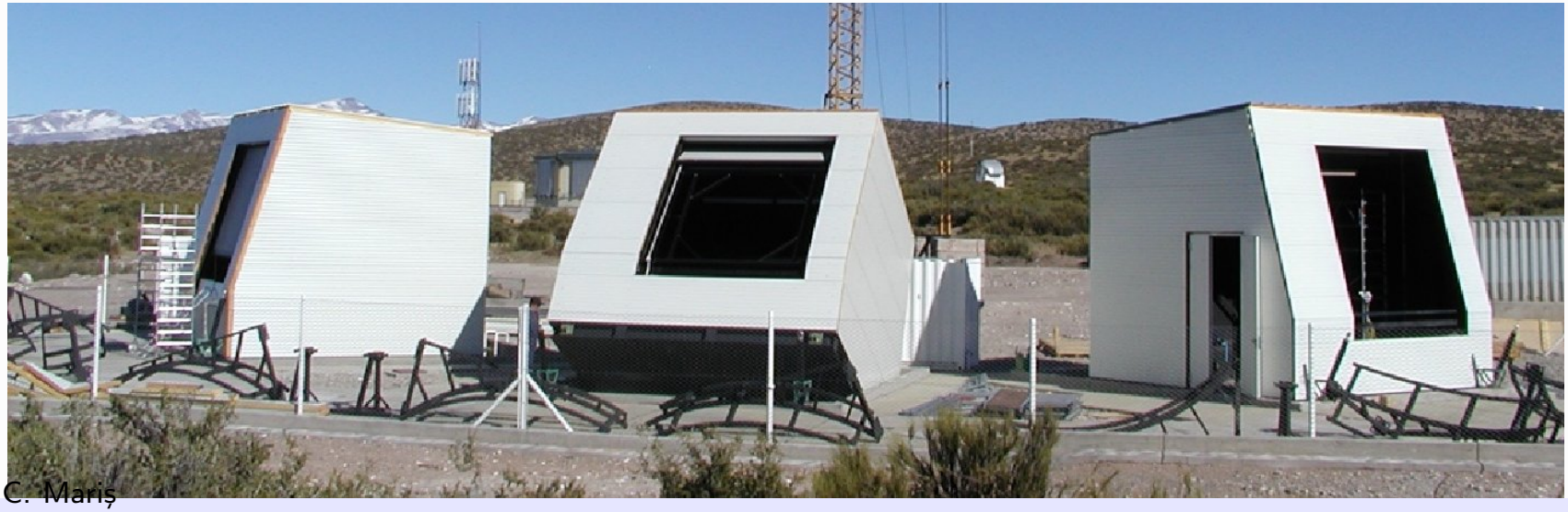

Data sets at the Pierre Auger Observatory

SD vertical ($\theta < 60°$)

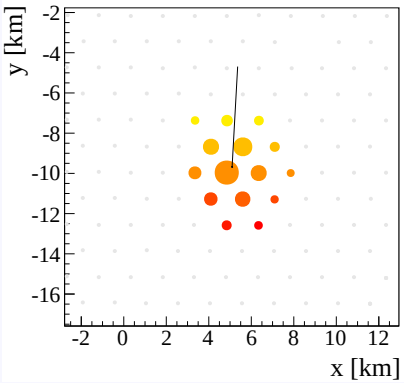

1500 m array

energy threshold:
$E = 3\,\mathrm{EeV}$

geometrical acceptance

SD infill ($\theta < 55°$)

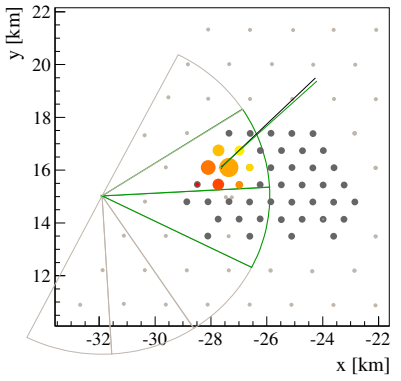

750 m array

energy threshold:
$E = 0.3\,\mathrm{EeV}$

geometrical acceptance

SD inclined ($62° < \theta < 80°$)

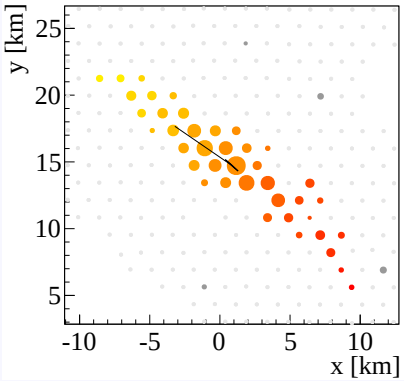

1500 m array

energy threshold:
$E = 4\,\mathrm{EeV}$

geometrical acceptance

Hybrid (FD + 1 SD station)

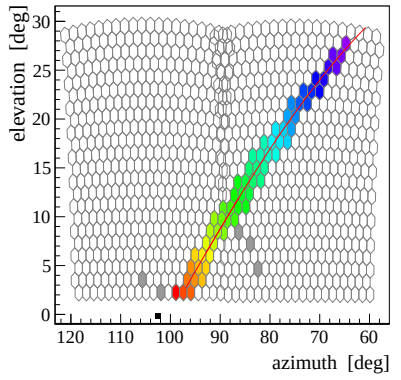

24 telescopes

energy threshold:
$E = 1\,\mathrm{EeV}$

acceptance from simulations

Air showers reconstruction

Event 201022604036, energy 72 ± 1 EeV, 54 degrees

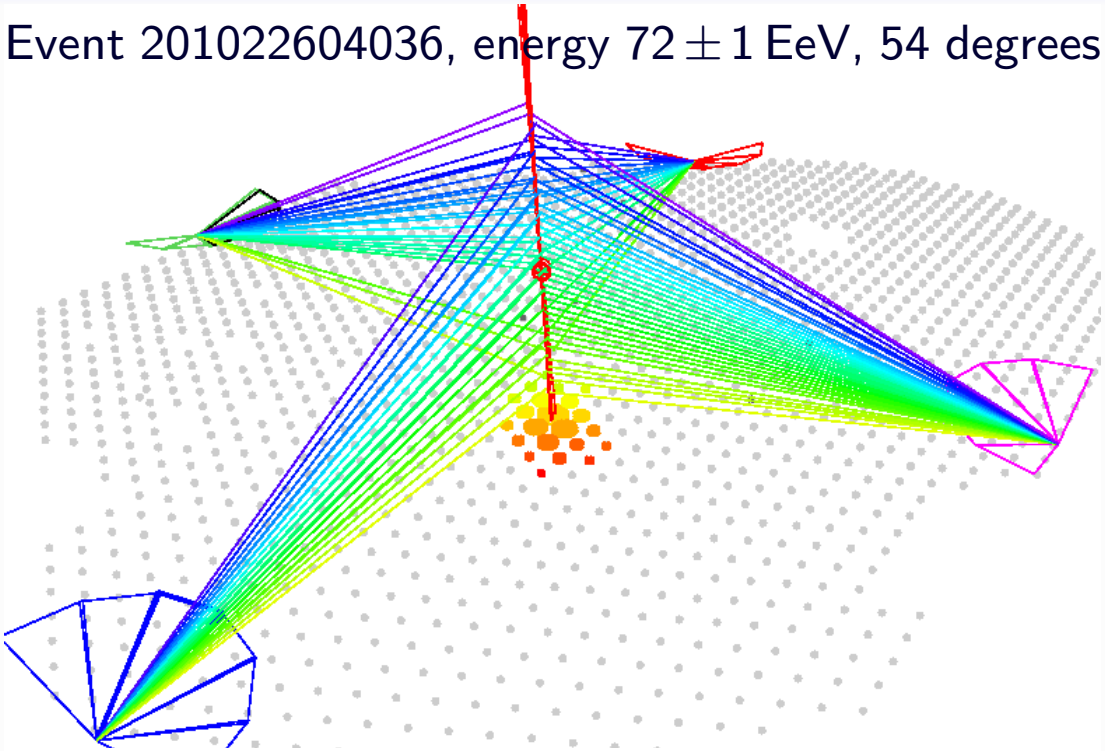

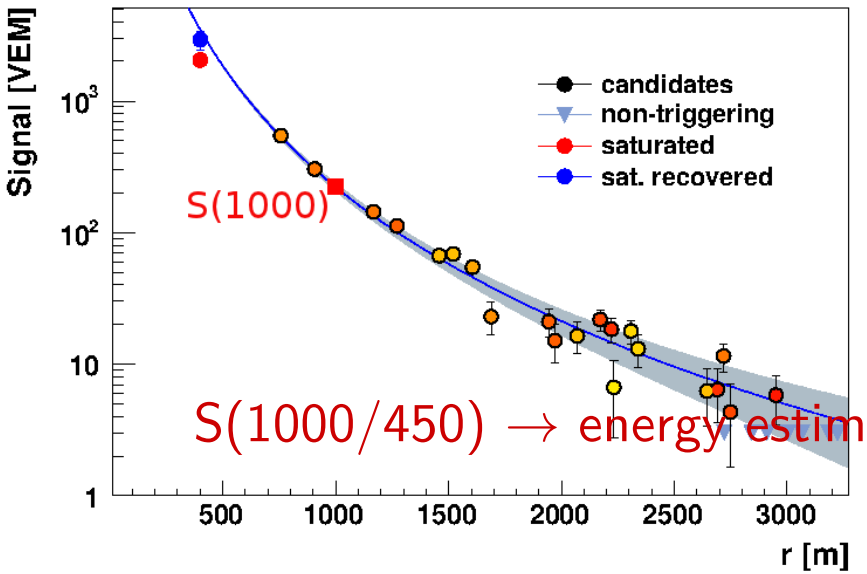

S(1000/450) → energy estimator

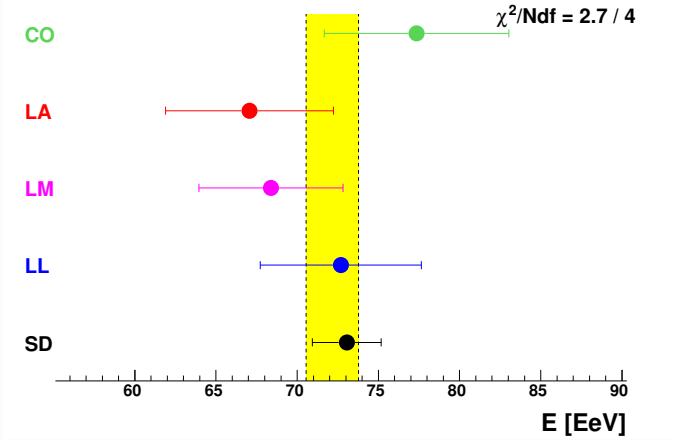

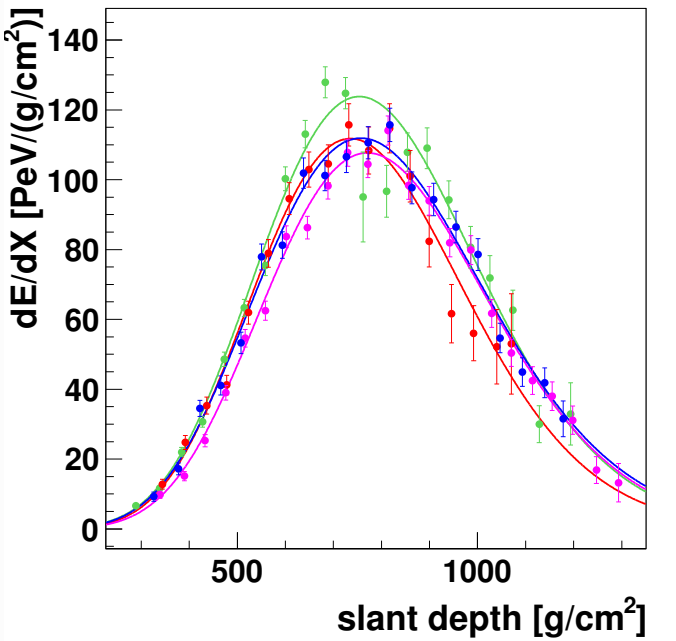

Energy: $\int$Gaisser-Hillas + invisible energy correction (10% @ 1 EeV, 8.5%@100 EeV)

How is the measurement of the energy spectrum done?

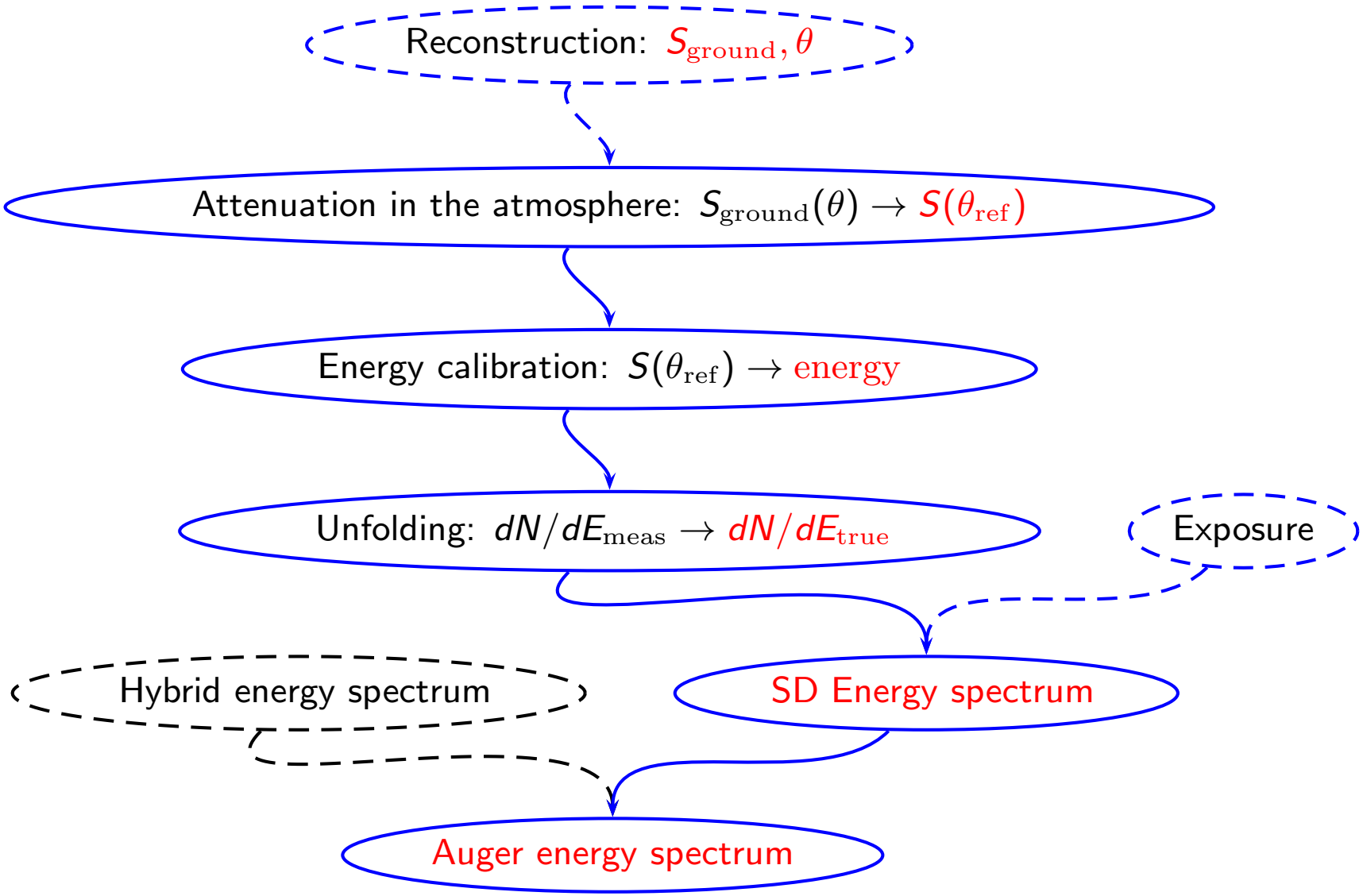

Attenuation in the atmosphere

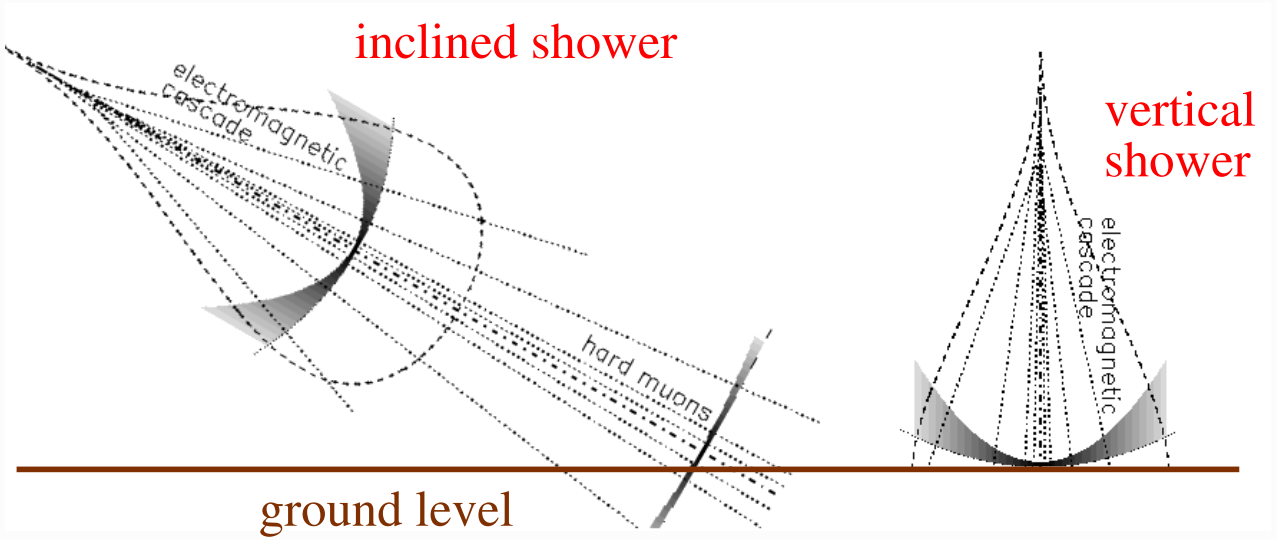

Method of Constant Intensity

integral cosmic ray flux is isotropic (local coordinates)

$$\frac{d\Phi}{d\Omega} \propto \frac{d\Phi}{d\cos\theta} \propto \frac{dI}{d\cos\theta A_{eff}} = const$$

intensity I (events above E_0)
projection on flat array geometry: $A_{\mathrm{eff}} = A\cos\theta$

$$\frac{dI}{d\cos^2\theta} = \mathrm{const}$$

S_{ground}:Attenuation in the atmosphere

empirical function
second degree polynomial in $\cos^2\theta$

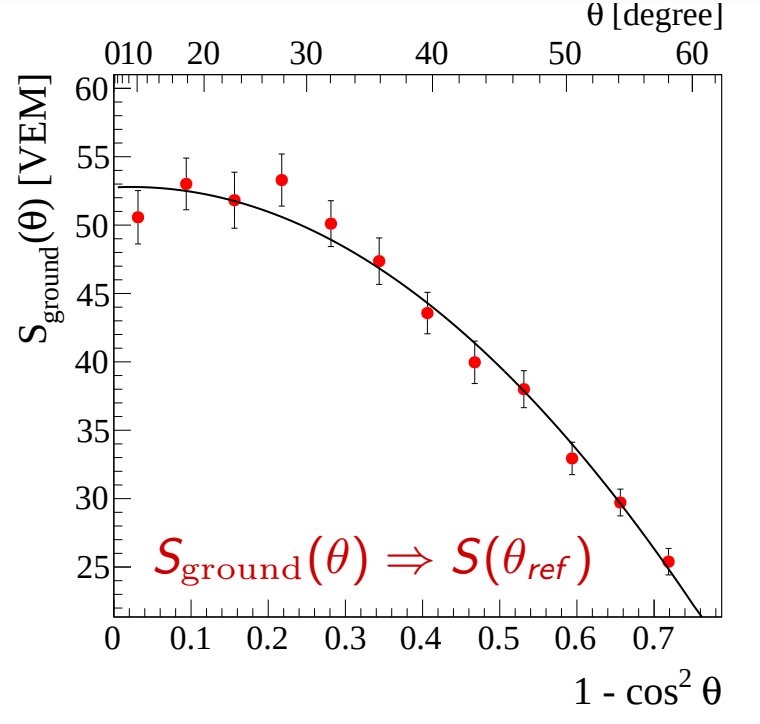

S_{ground}:Attenuation in the atmosphere

empirical function
second degree polynomial in $\cos^2\theta$

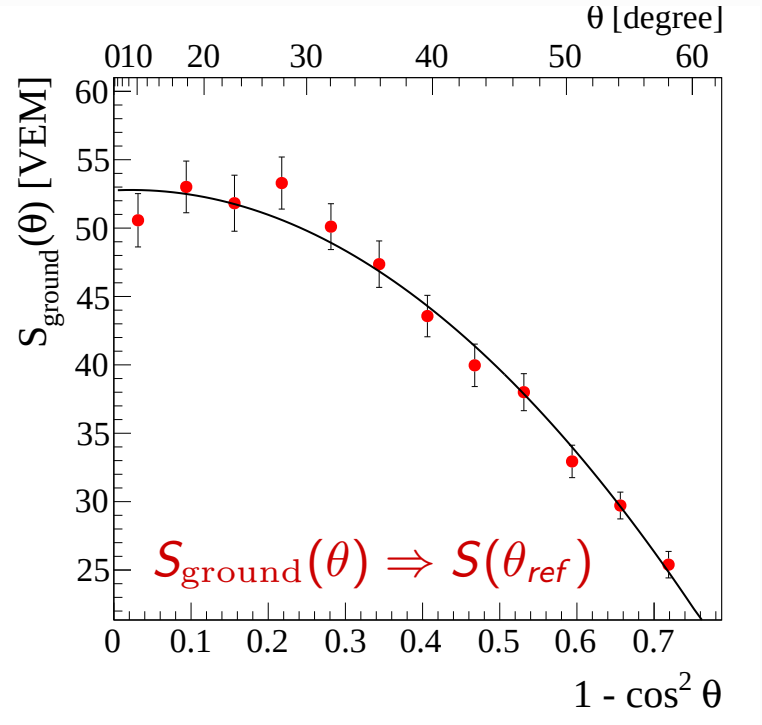

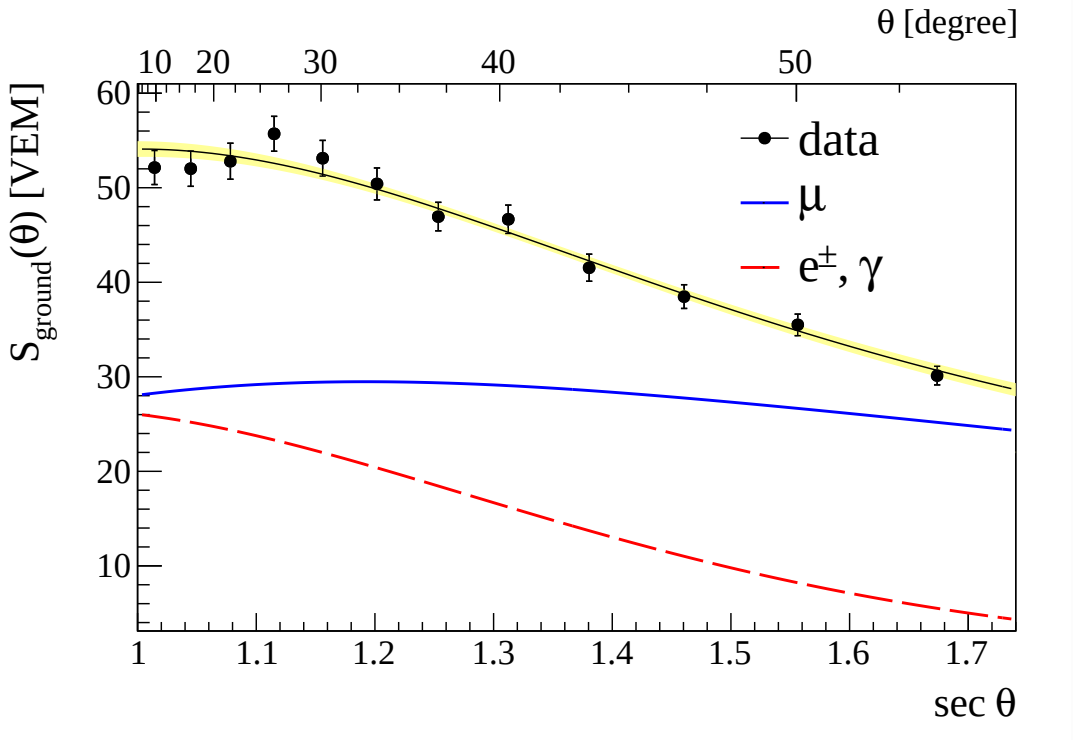

Physical interpretation

$$S_{\text{ground}}(\theta) = N_{\text{e.m.}} S_{\text{e.m.}}(X(\theta)) g_{e.m.}(\theta) + N_{\mu} S_{\mu}(X(\theta)) g_{\mu}(\theta)$$

- modeling of the attenuation of air-showers and of the detector response
- sensitivity to electromagnetic to muonic ratio

SD inclined events ($62^\circ < \theta < 80^\circ$)

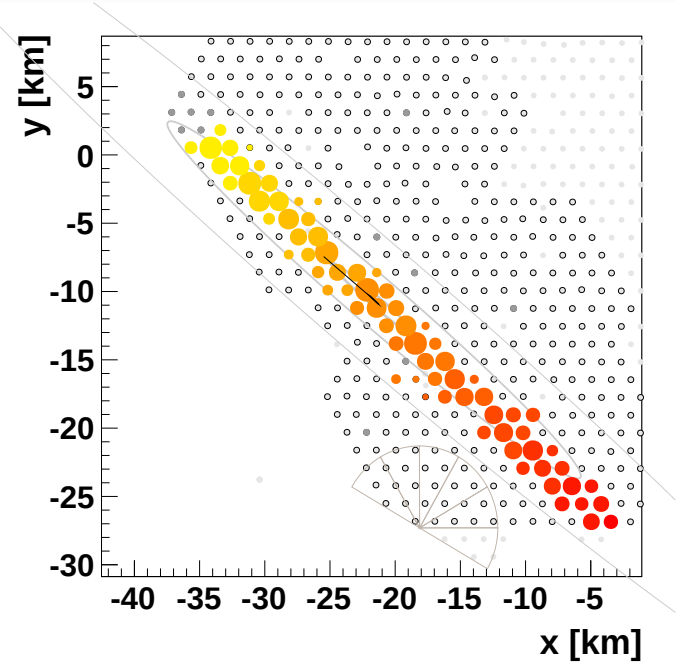

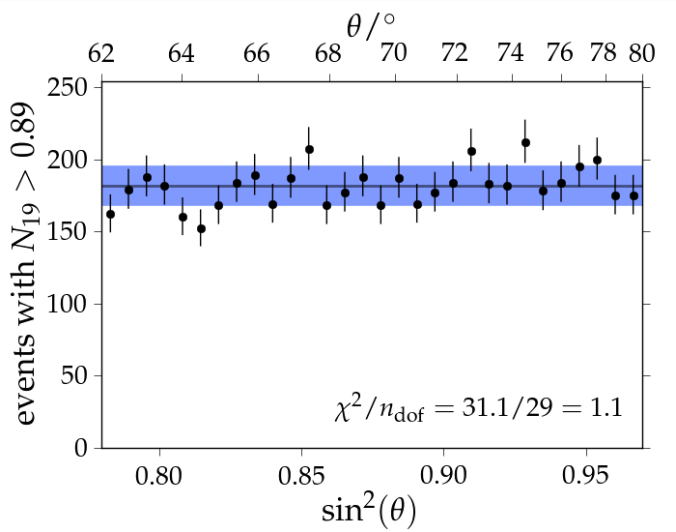

- only muonic component, muon density $n_\mu = f(x, y|\theta, \phi)$
- energy estimator, N_{19}, proportional to the number of muons and independent of the zenith angle $N_{19}(E, A) = N_\mu / N_\mu(10^{19}\,\mathrm{eV}, p, \theta)$
- reconstruction of events based on models for the muon density and on the full simulations (systematic uncertainty $N_{19} < 4\%$)

Energy calibration for the surface detector

- Energy calibration with events recorded by both FD and SD
- High quality events (+ fiducial field of view)

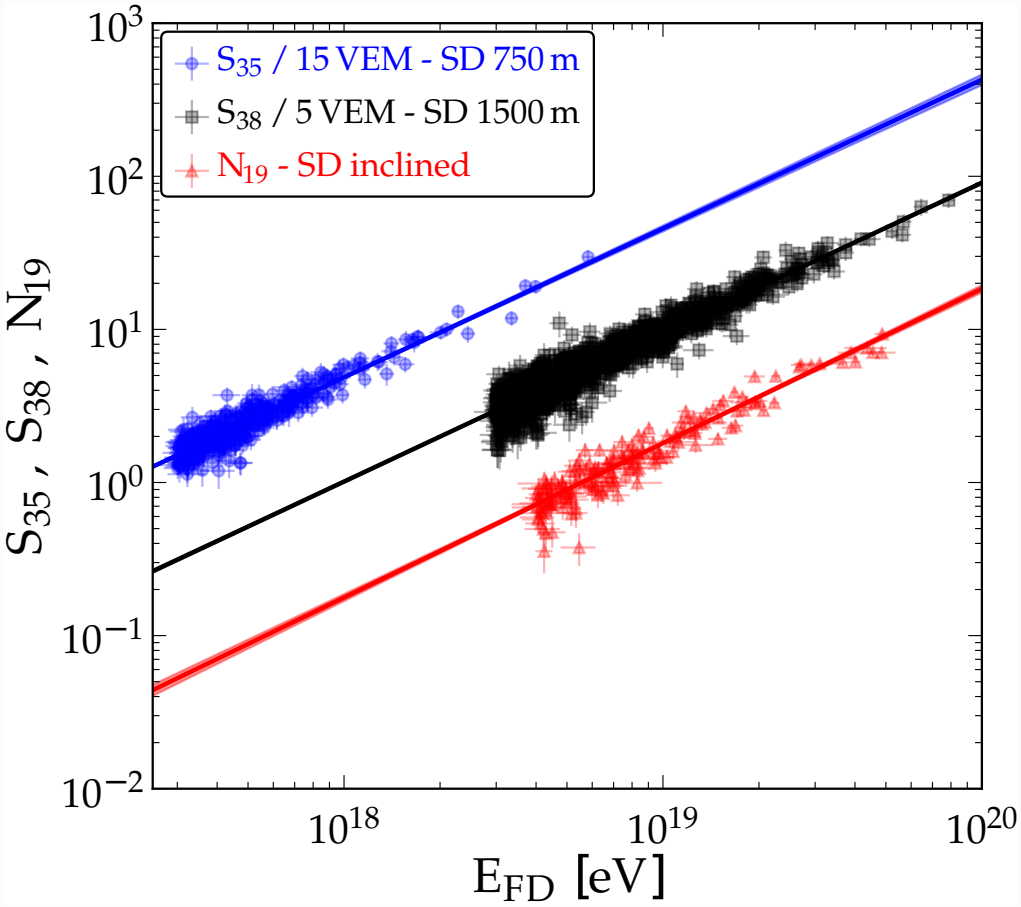

Calibration functions:
$E = A \cdot S^B$

- SD 1500 m:
  $A = (0.190 \pm 0.005)\,\mathrm{EeV}$
  $B = 1.025 \pm 0.007$
- SD inclined:
  $A = (5.61 \pm 0.1)\,\mathrm{EeV}$
  $B = 0.985 \pm 0.02$
- SD 750 m:
  $A = (12.1 \pm 0.7)\,\mathrm{PeV}$
  $B = 1.03 \pm 0.02$

SD energy resolution, 1500 m

obtained from the golden hybrid events

$E > 3\,\mathrm{EeV}$

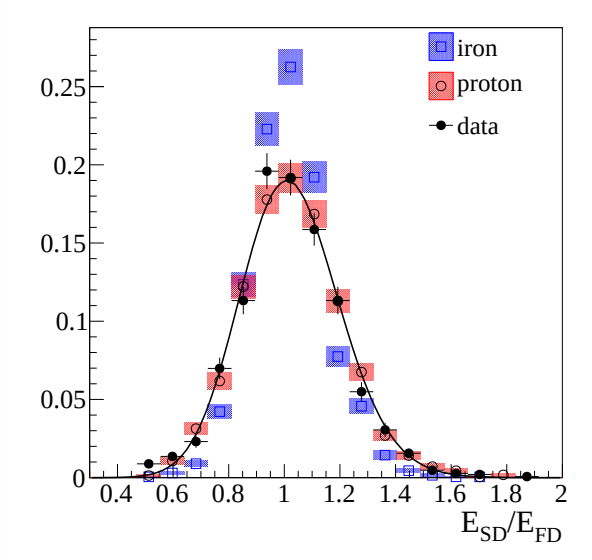

$\sigma_{SD}/E_{SD} = (16 \pm 1)\%$

$6\,\mathrm{EeV} < E < 10\,\mathrm{EeV}$

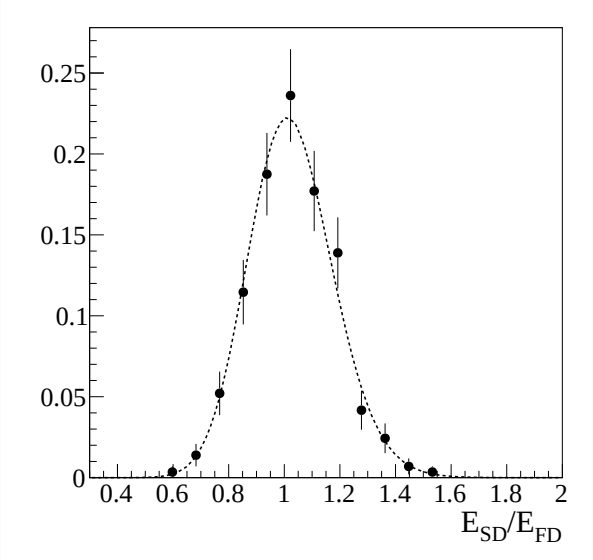

$\sigma_{SD}/E_{SD} = (13 \pm 1)\%$

$10\,\mathrm{EeV} < E$

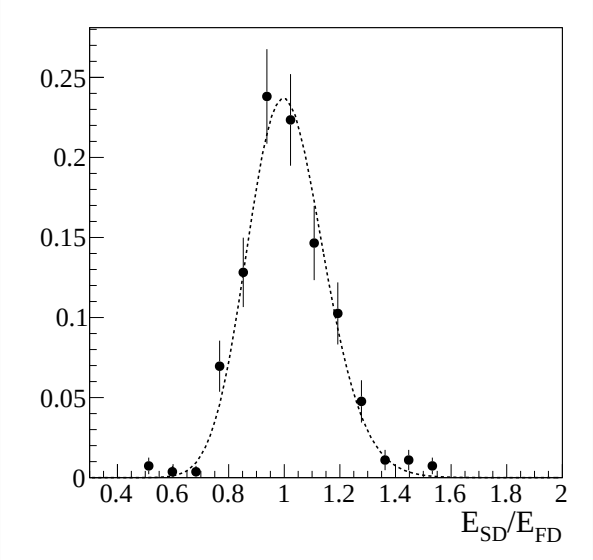

$\sigma_{SD}/E_{SD} = (11 \pm 1)\%$

Contributions:

- shower-to-shower fluctuations $\approx 10\%$
- reconstruction uncertainties 12% at 3 EeV and 6% above 10 EeV
- corrections for resolution effects with a forward folding procedure

Resolution correction through forward folding

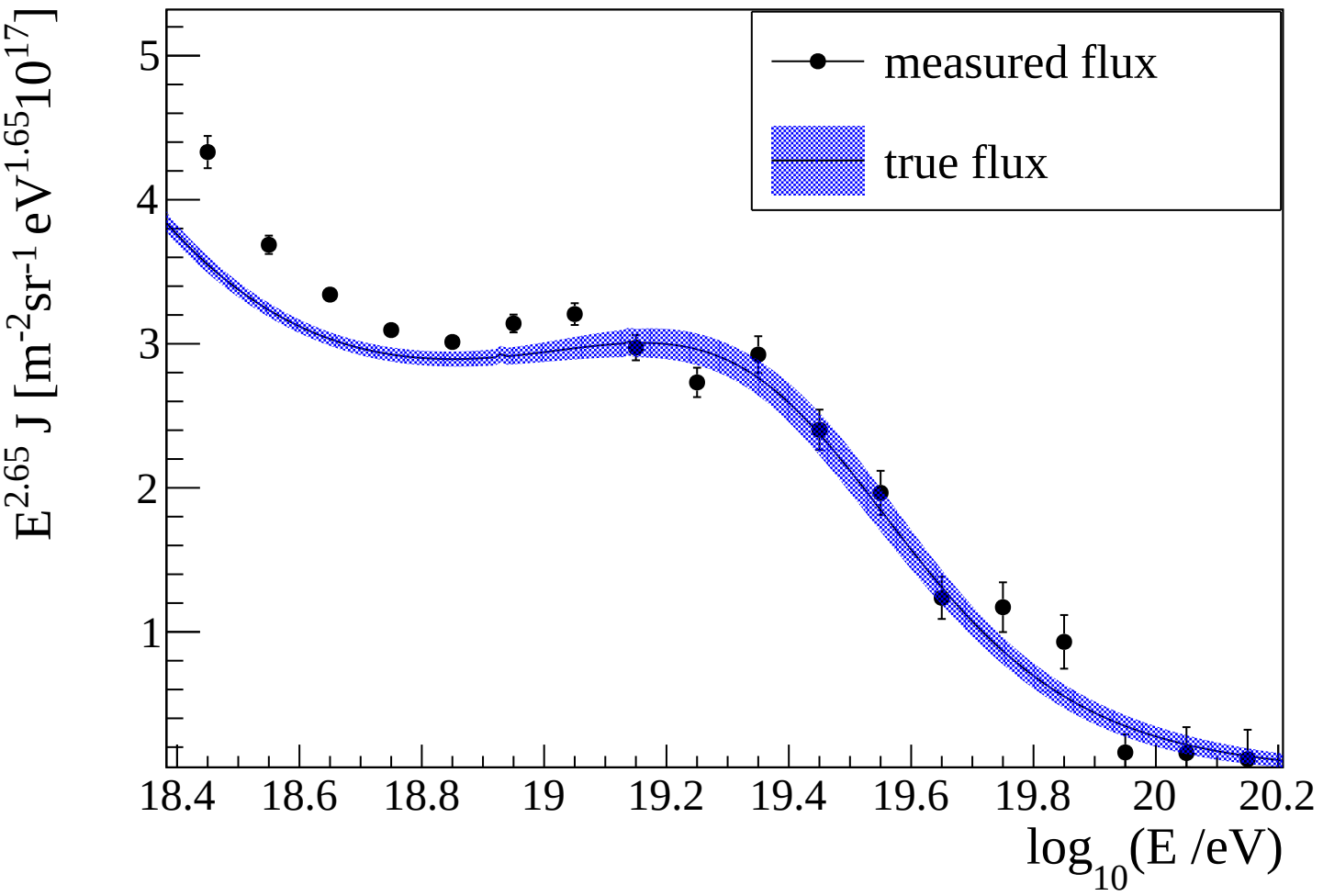

$$J_{\text{meas}} = \mathbf{P}^{-1} \cdot \mathbf{R} \cdot \mathbf{P} J_{\text{true}}$$

trigger efficiency **P**, response matrix **R** (air-showers and detector simulations)

Hybrid exposure

Detector fully efficient above 1 EeV

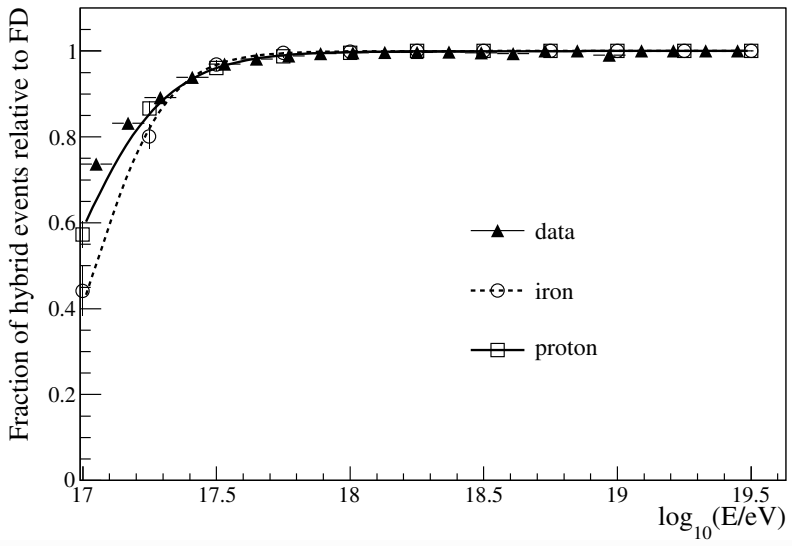

Cross-check with SD data

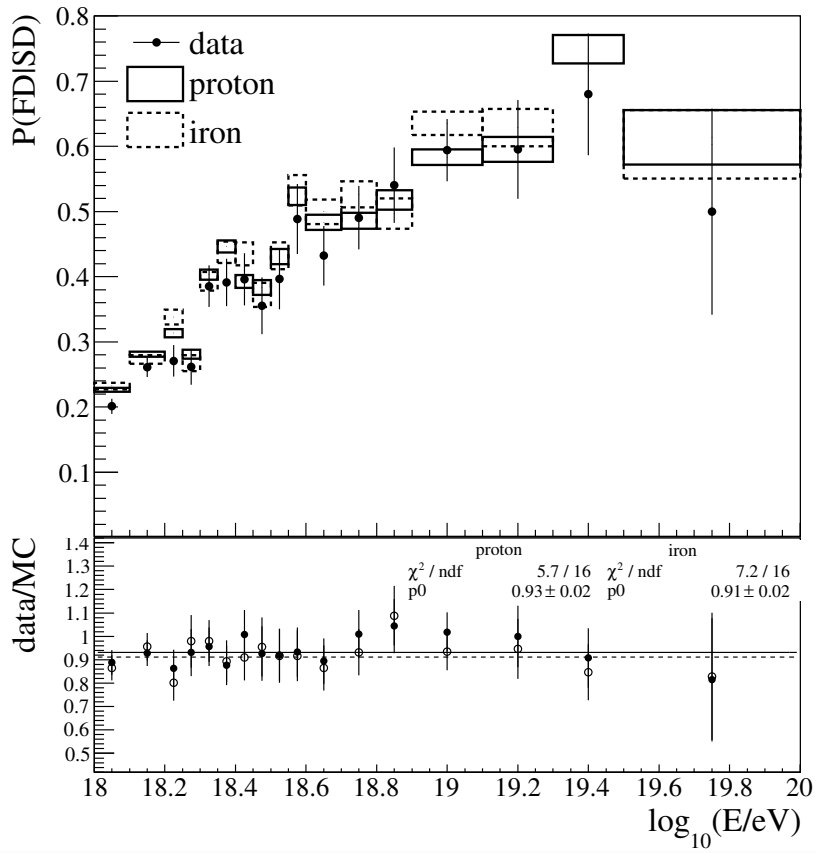

Relative difference to mixed composition

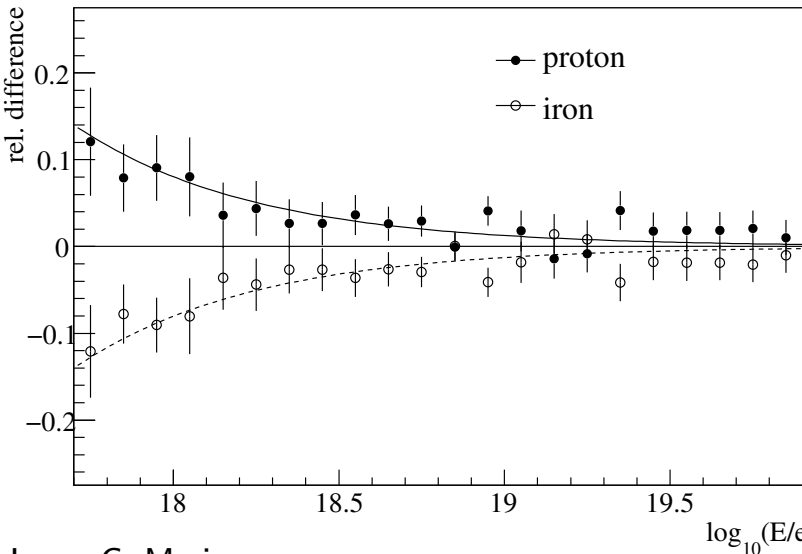

Energy systematics

- energy systematic uncertainty reduced from 22% to 14%
- changes in the energy scale: 15% at 1 EeV and 10% at 10 EeV

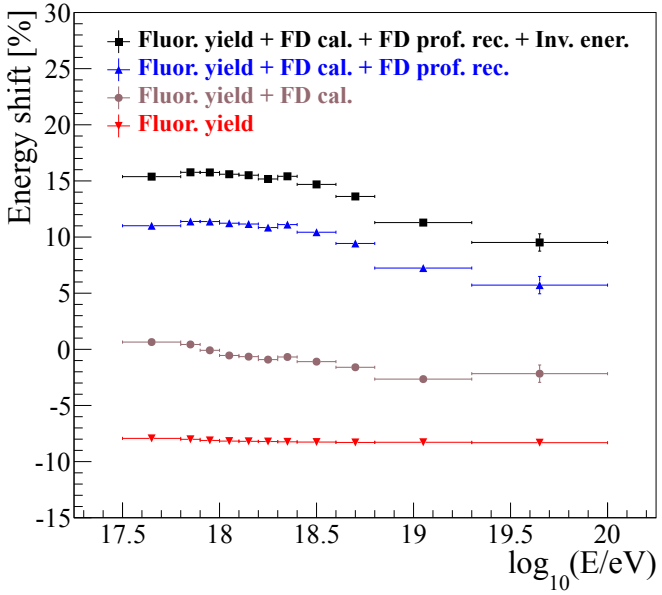

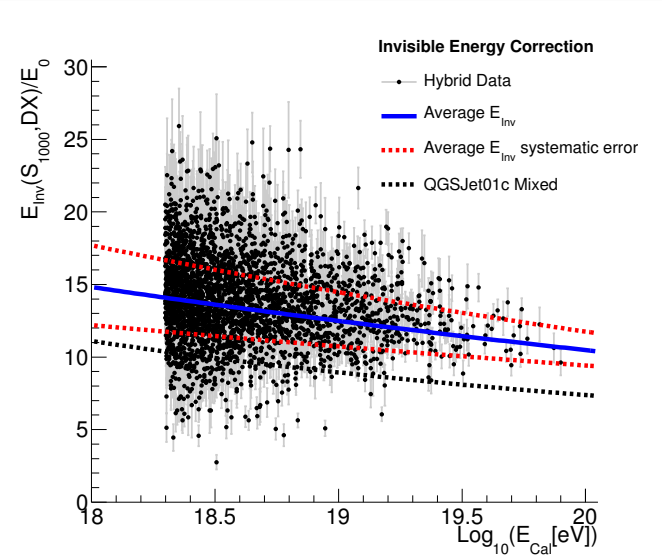

Absolute fluorescence yield	3.4%	
Fluores. spectrum and quenching param.	1.1%	
Sub total (Fluorescence Yield)	3.6%	14%
Aerosol optical depth	3% ÷ 6%	
Aerosol phase function	1%	
Wavelength dependence of aerosol scattering	0.5%	
Atmospheric density profile	1%	
Sub total (Atmosphere)	3.4% ÷ 6.2%	5.1% ÷ 7.6%
Absolute FD calibration	9%	
Nightly relative calibration	2%	
Optical efficiency	3.5%	
Sub total (FD calibration)	9.9%	9.5%
Folding with point spread function	5%	
Multiple scattering model	1%	
Simulation bias	2%	
Constraints in the Gaisser-Hillas fit	3.5% ÷ 1%	
Sub total (FD profile reconstruction)	6.5% ÷ 5.6%	10%
Invisible energy	3% ÷ 1.5%	4%
Statistical error of the SD calib. fit	0.7% ÷ 1.8%	
Stability of the energy scale	5%	
TOTAL	14%	22%

Comparison of exposures

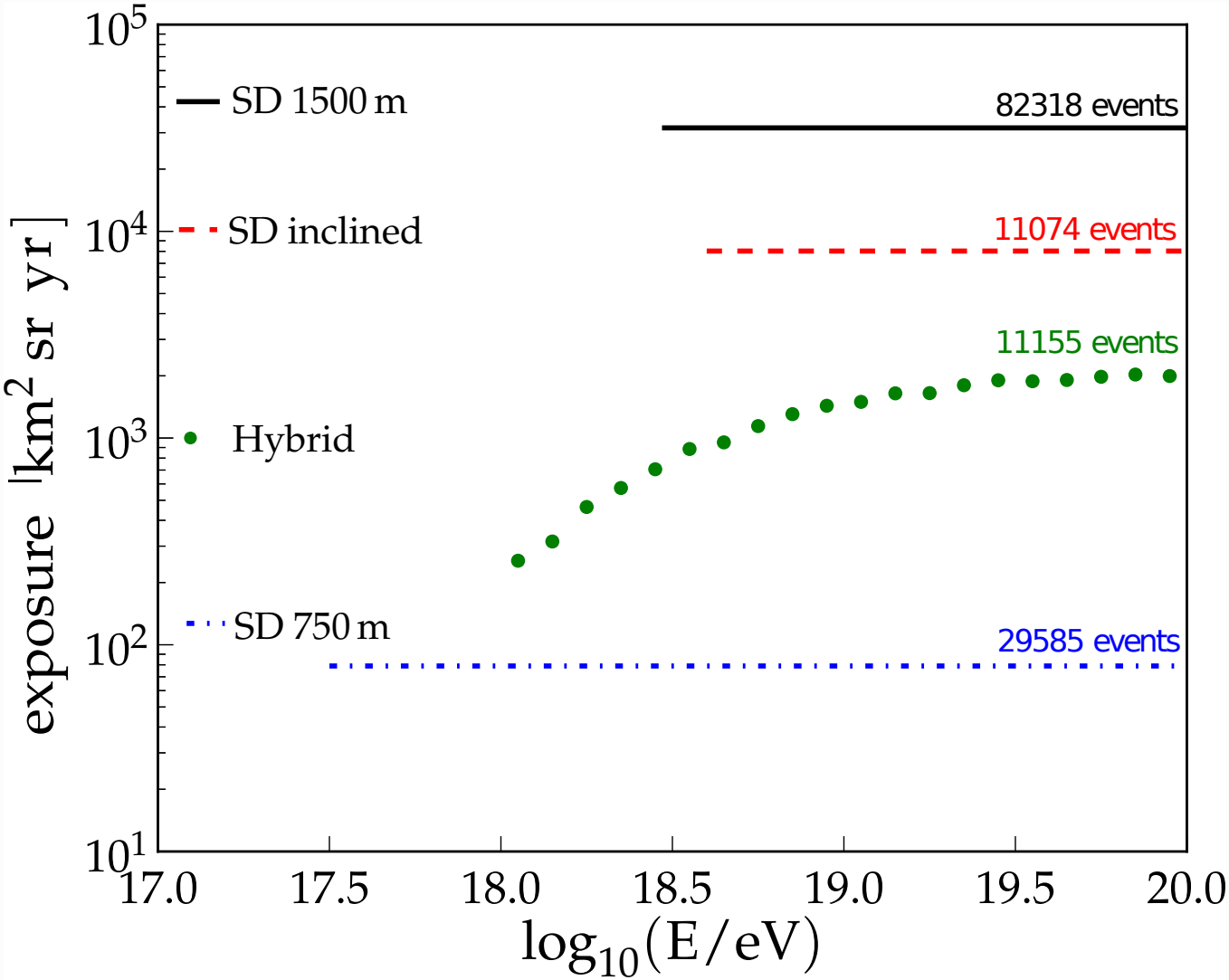

Exposures at 10 EeV: SD vertical 31645 km^2 sr year
Hybrid 1496 km^2 sr year
SD inclined 8027 km^2 sr year
SD infill 79 km^2 sr year

Measurements of the energy spectrum

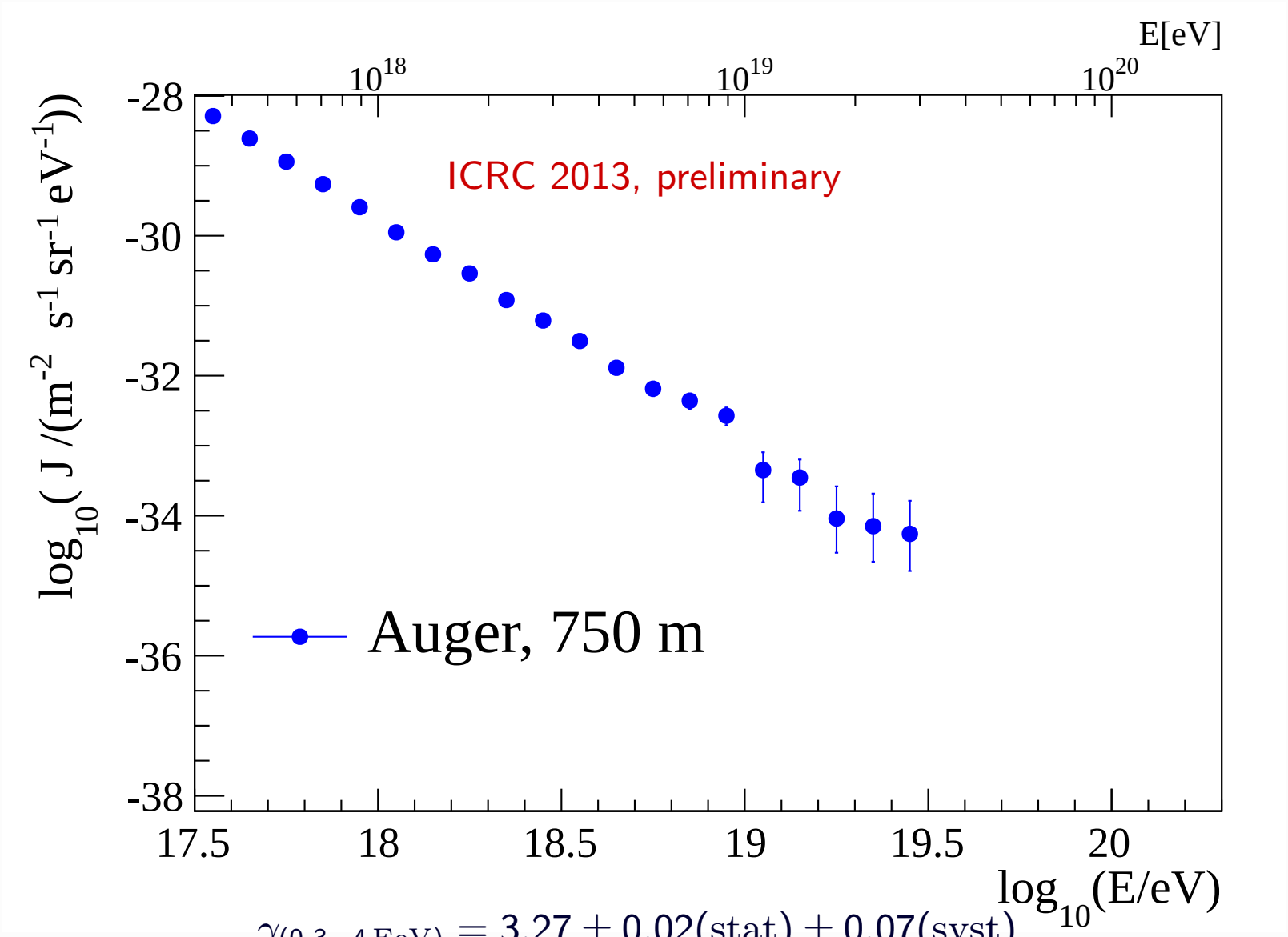

Measurements of the energy spectrum

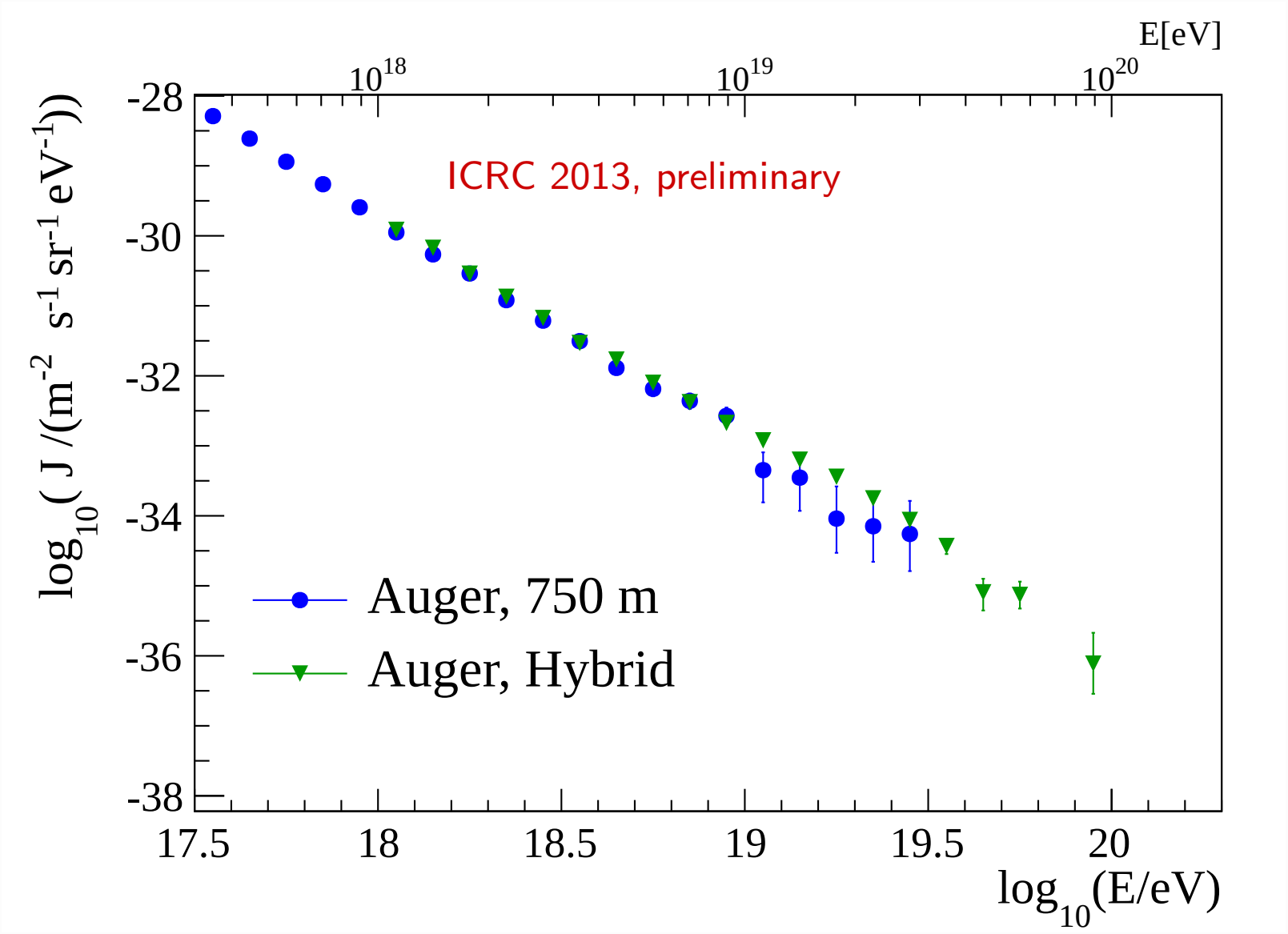

Measurements of the energy spectrum

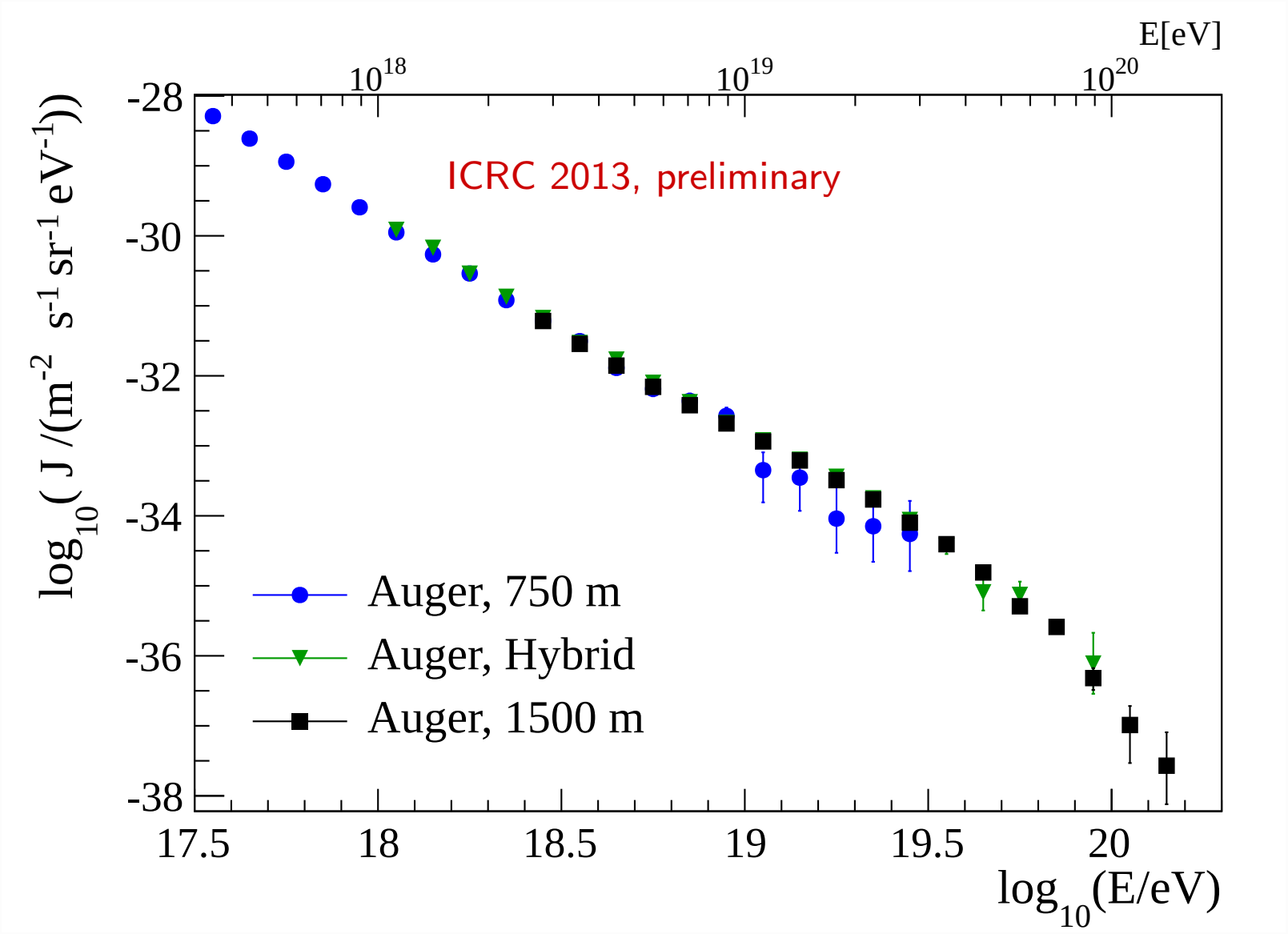

Measurements of the energy spectrum

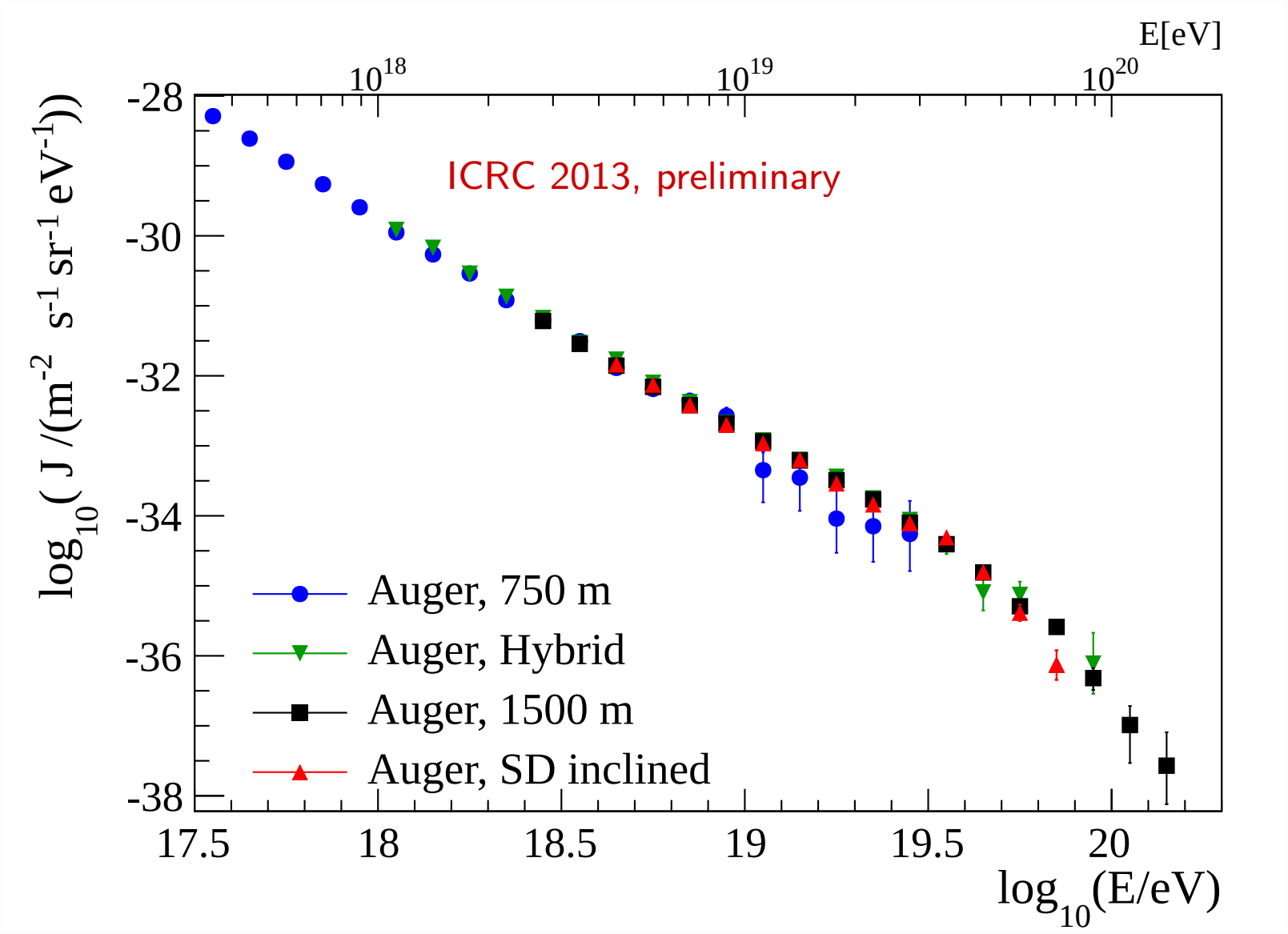

Combined energy spectrum

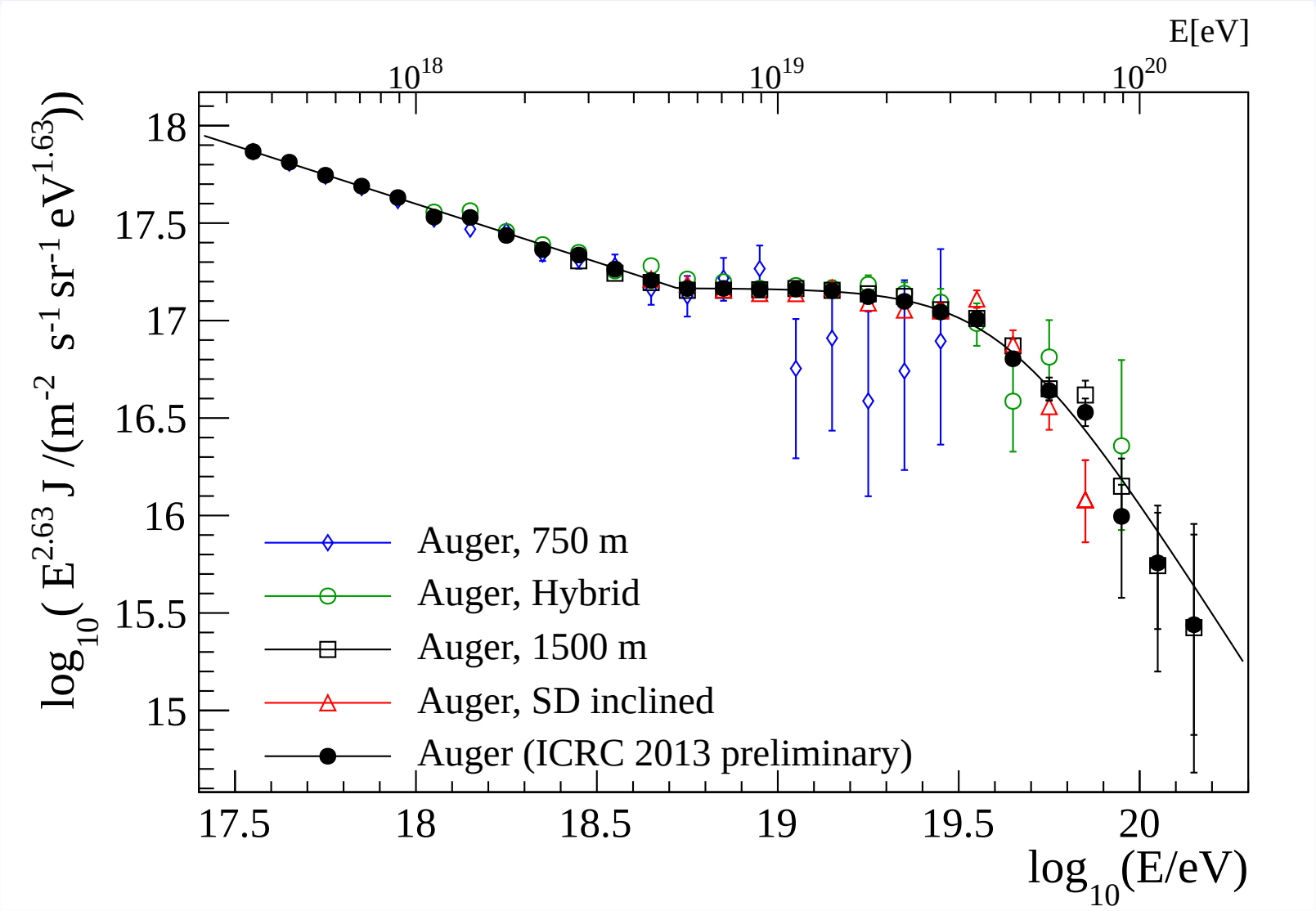

- precise measurement of the spectral features (preliminary)
- $\gamma_1 = 3.23 \pm 0.01$, $\log_{10}(E_{tr}/\mathrm{eV}) = 18.72 \pm 0.01$
  $\gamma_2 = 2.63 \pm 0.02$, $\log_{10}(E_{1/2}/\mathrm{eV}) = 19.63 \pm 0.01$

Comparison with other experiments

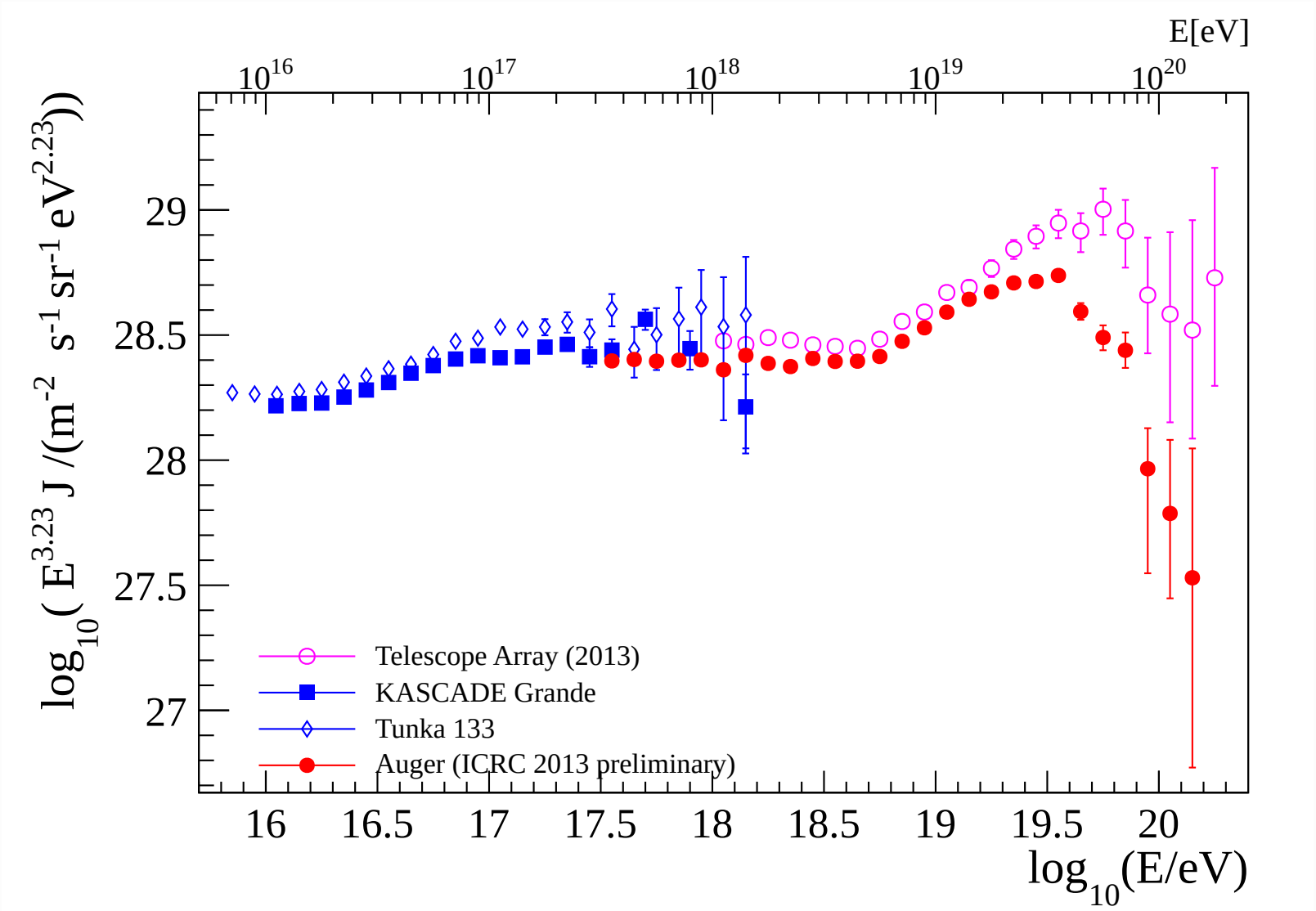

energy systematic uncertainties important

Overview of the spectral features

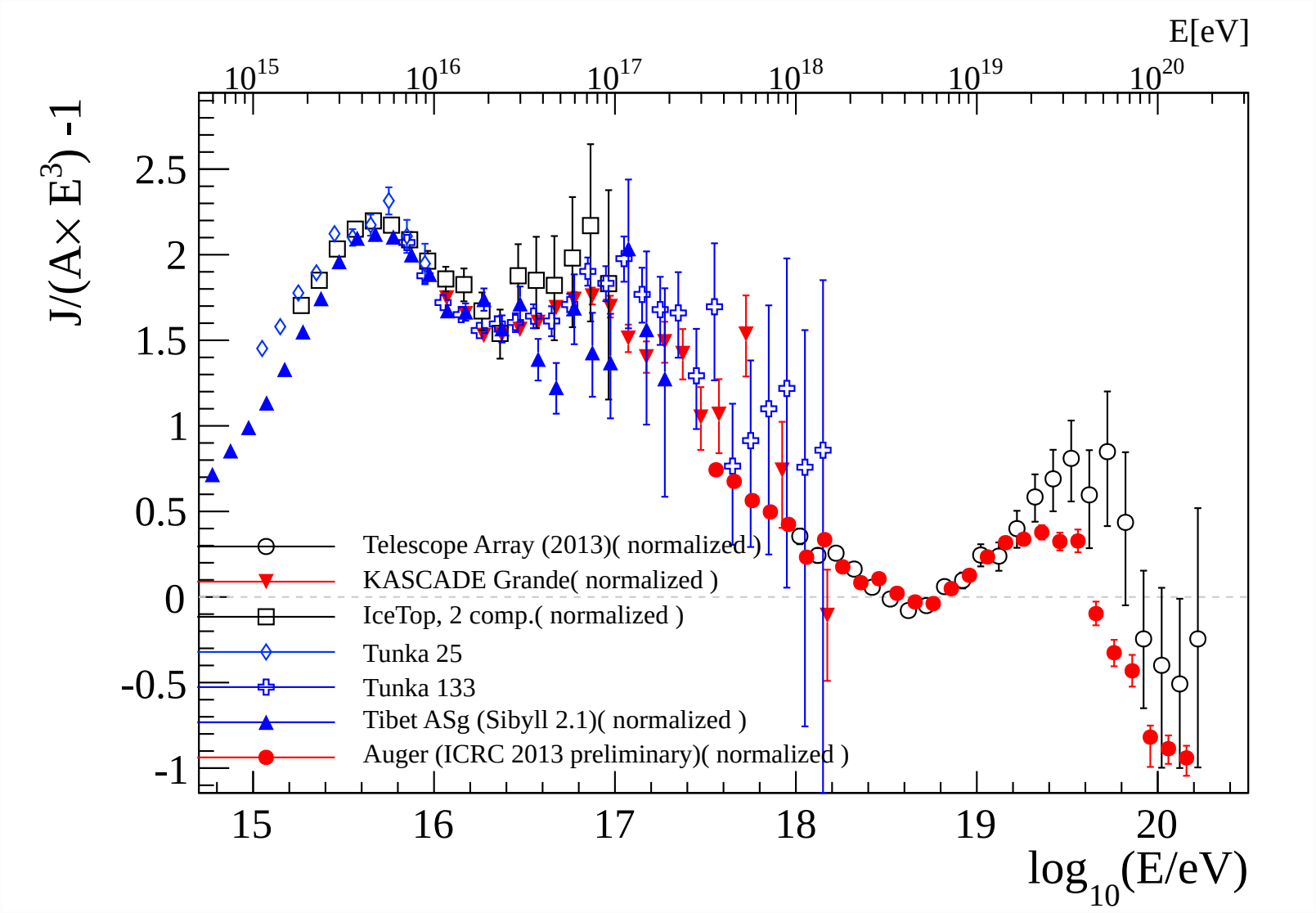

energy systematic uncertainties important

Where do we start from

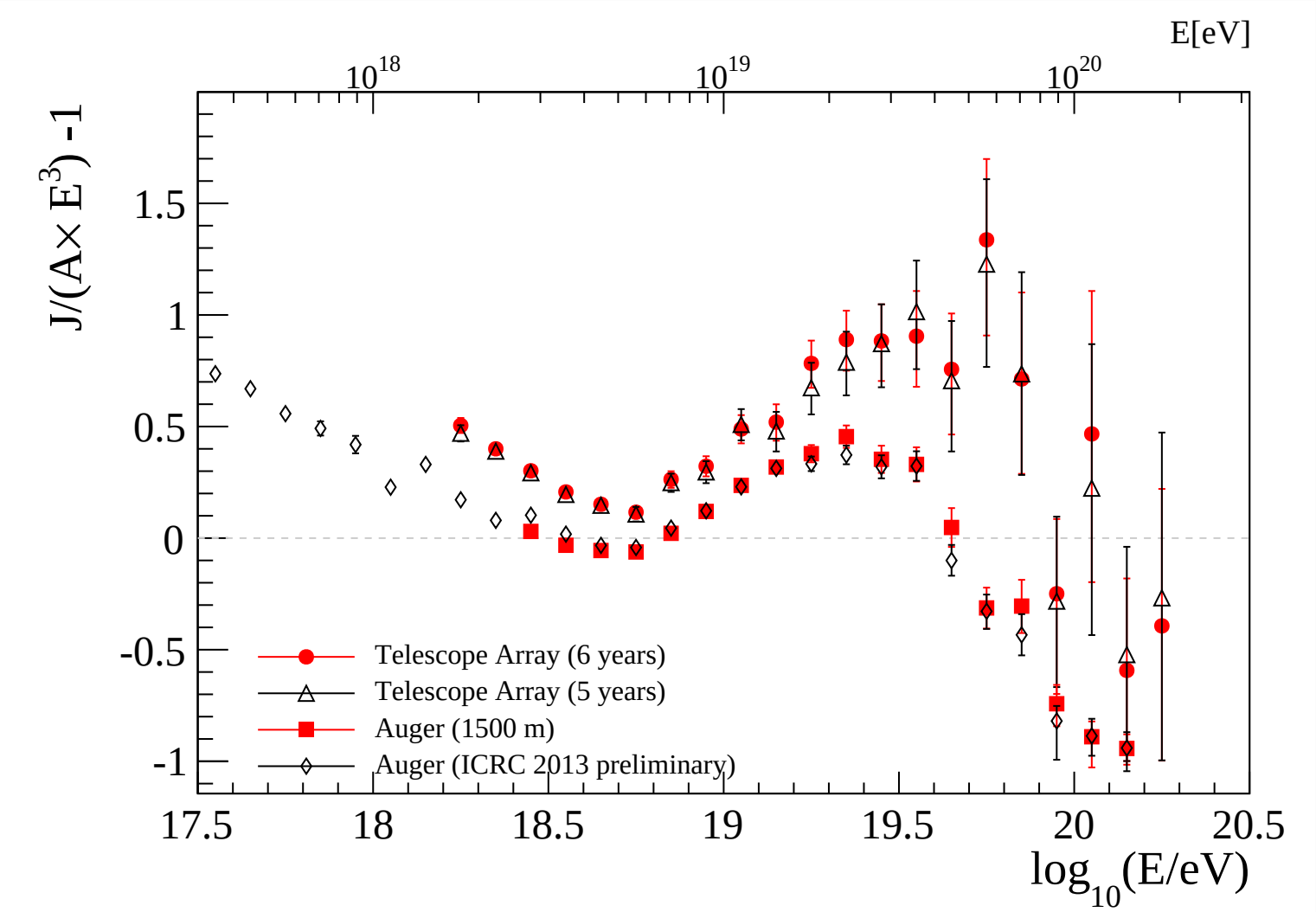

$\Rightarrow$ Can the differences be explained by the systematic uncertainties and differences in the analysis?

Where do we start from

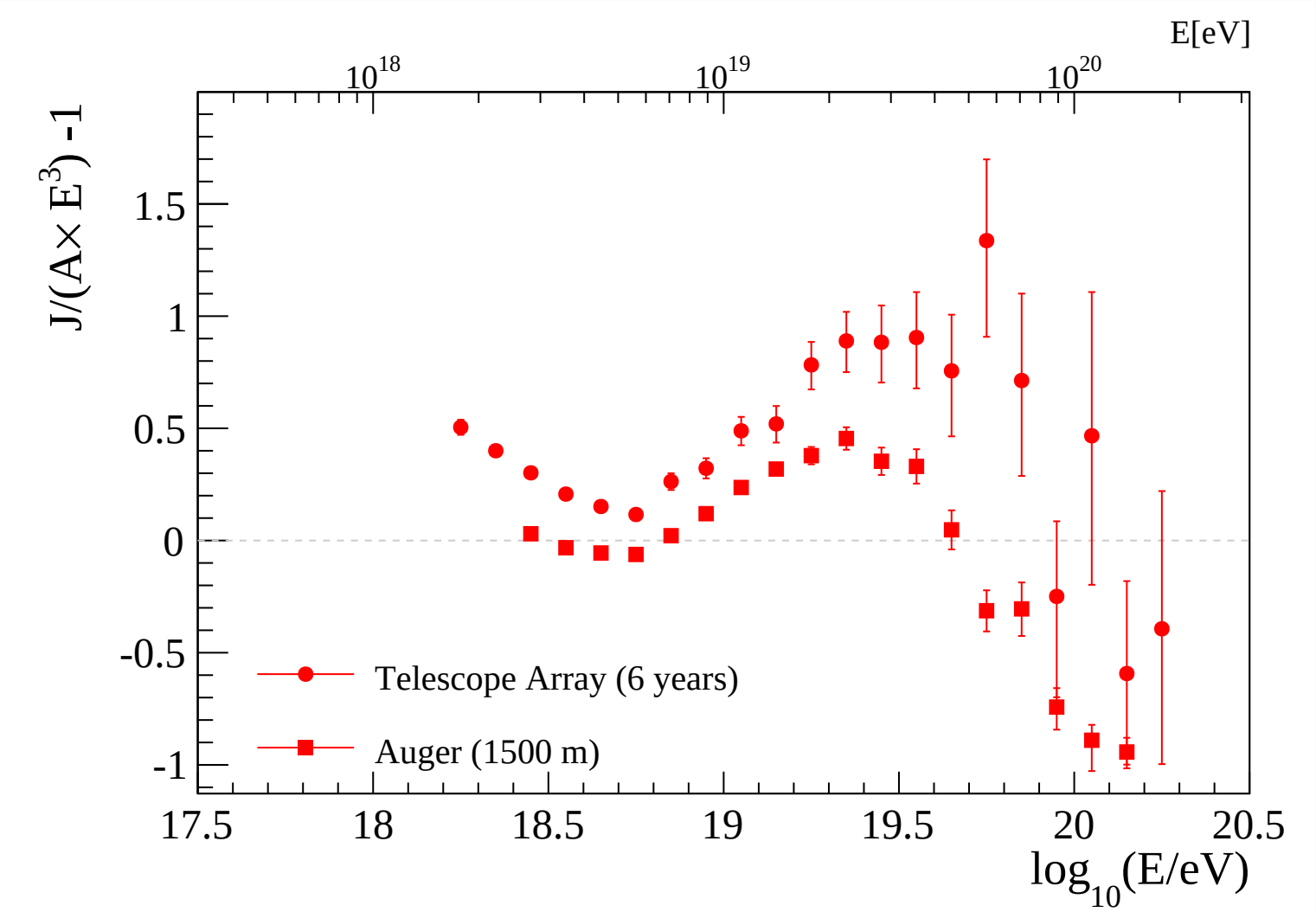

$\Rightarrow$ Can the differences be explained by the systematic uncertainties and differences in the analysis?

Energy calibration and systematic uncertainties

Telescope Array

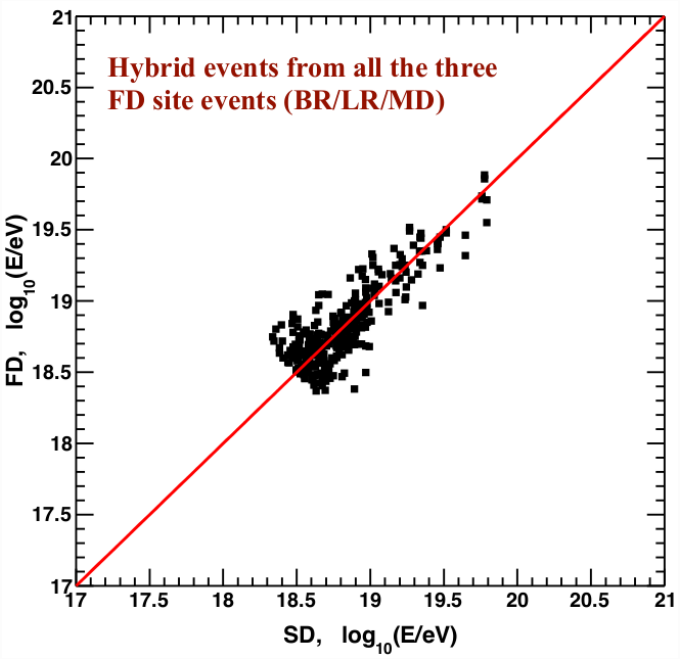

Auger

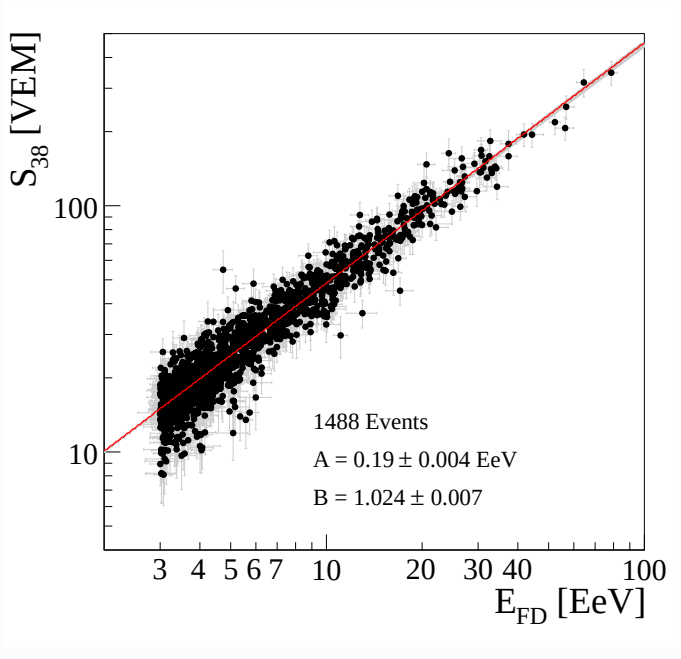

	Auger[%]	Telescope Array [%]
Atmosphere	3.4 - 6.2	11
Detector	9.9	10
Reconstruction	6.5 - 5.6	9
Stability of the energy scale	5	-
Sub-total	13	17
Invisible energy	3 - 1.5	5
Fluorescence yield	3.6	11
Total	14	21

Invisible energy

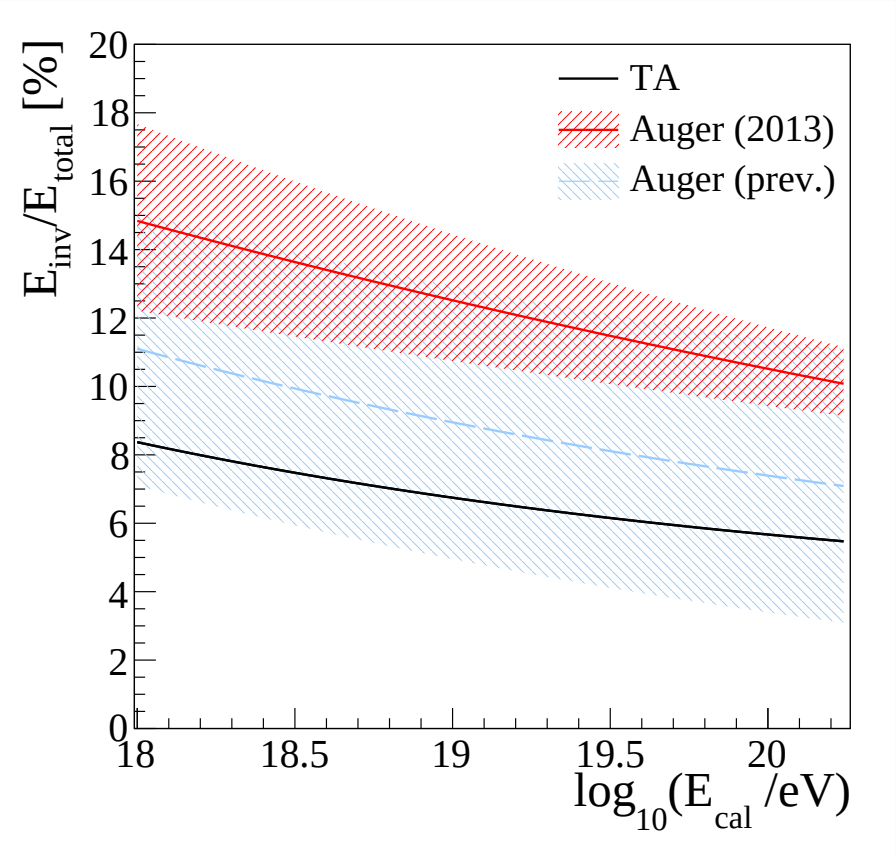

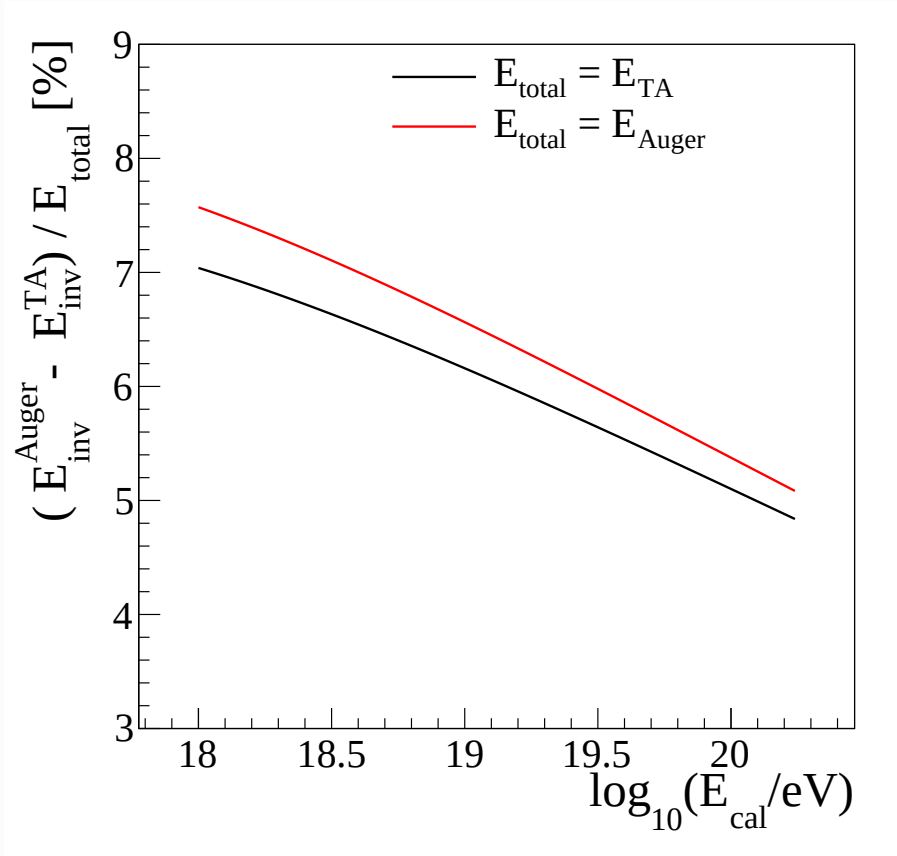

- Auger (prev): mixed composition (H. M. J. Barbosa et al.,Astropart. Phys. 22 (2004) 159)
- Auger (2013): data driven (M. Tueros ICRC 2013 #0705 arXiv:1307.5059)
- Telescope Array: proton composition (Astropart. Phys. 61 (2015) 93-101)

Fluorescence yield

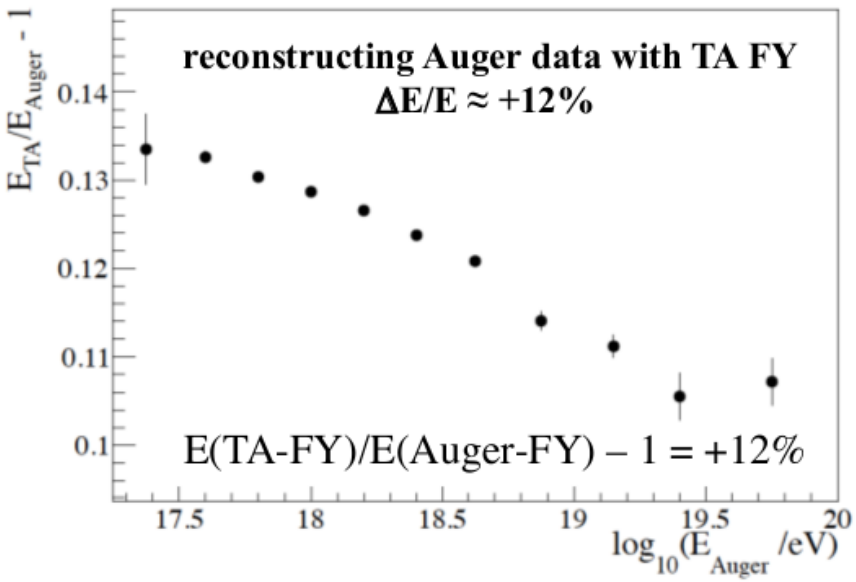

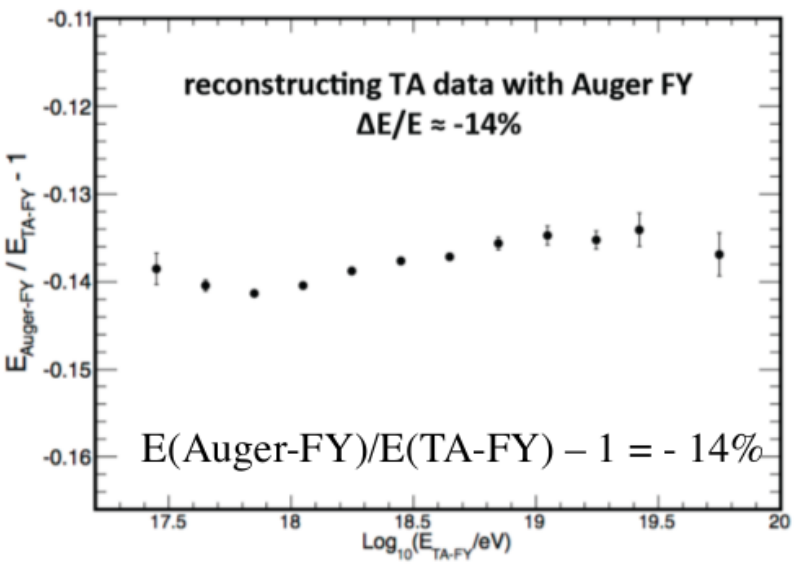

	E(TA-FY)/E(Auger-FY) - 1	E(Auger-FY)/E(TA-FY) - 1
Auger	+12%	-11%
TA	+16%	-14%

- Auger: AIRFLY (spectrum, absolute intensity, (p,T,h) dependency)
- TA: spectrum- FLASH, absolute intensity- Kakimoto, (p,T)- Kakimoto
- optical efficiency ($\approx$ 2%), wavelength dependence of the Rayleigh/ aerosol scattering cross-section, FD-shower distance, Cherenkov fraction...

Energy changes with TA settings

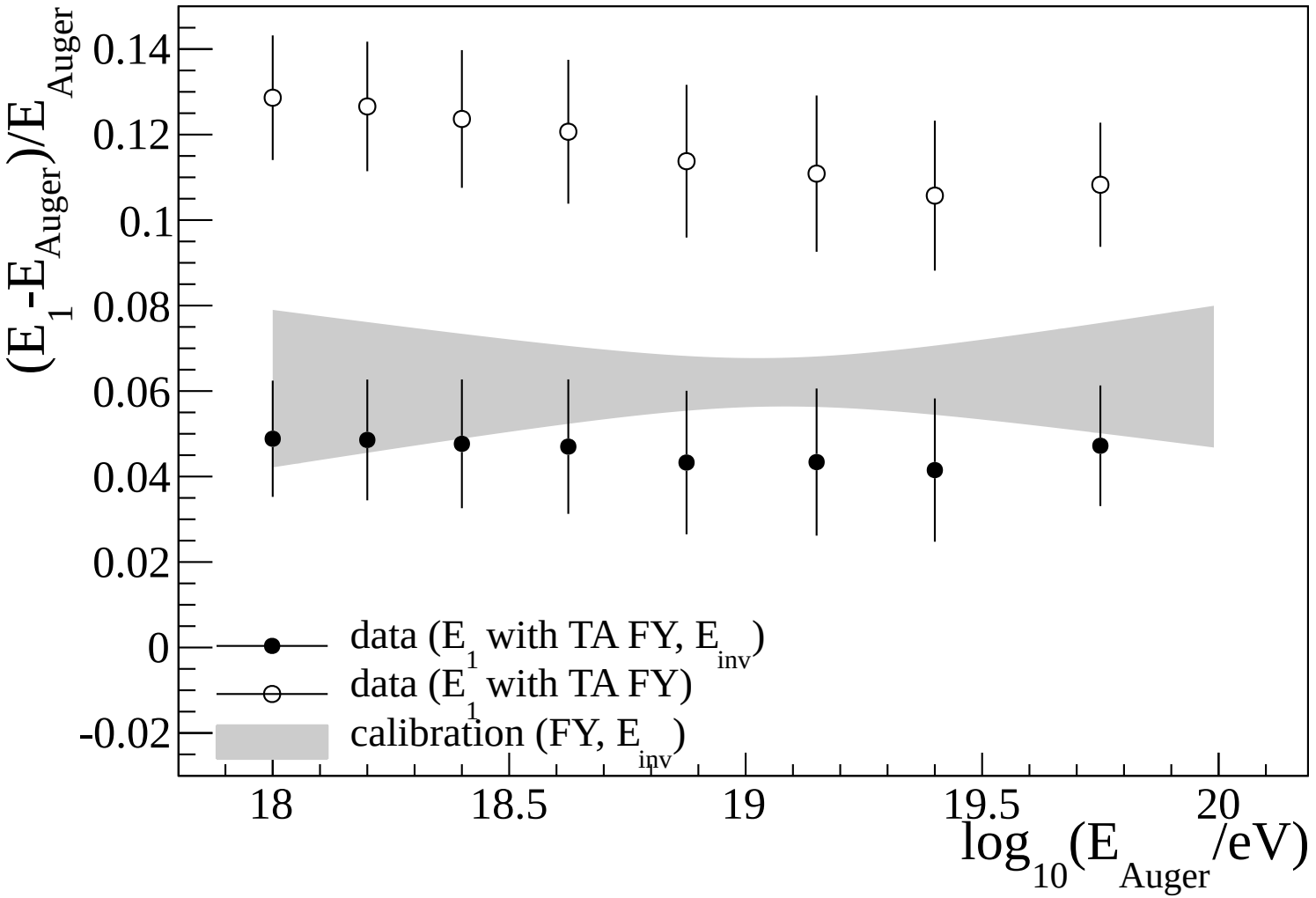

$\Rightarrow$ Using the TA FY and the TA invisible energy the Auger energy scale would change by 6%

Energy spectra

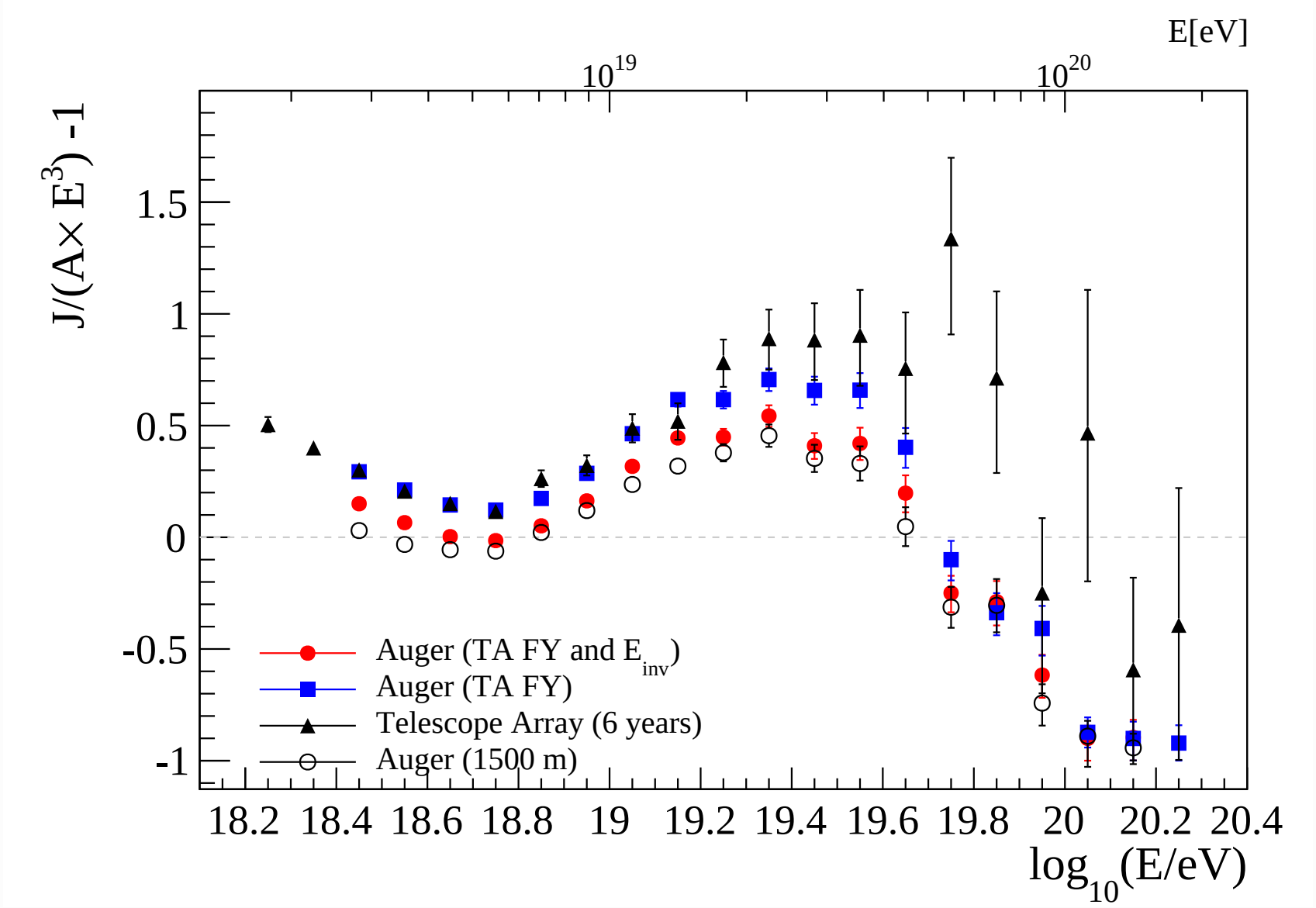

Energy spectra

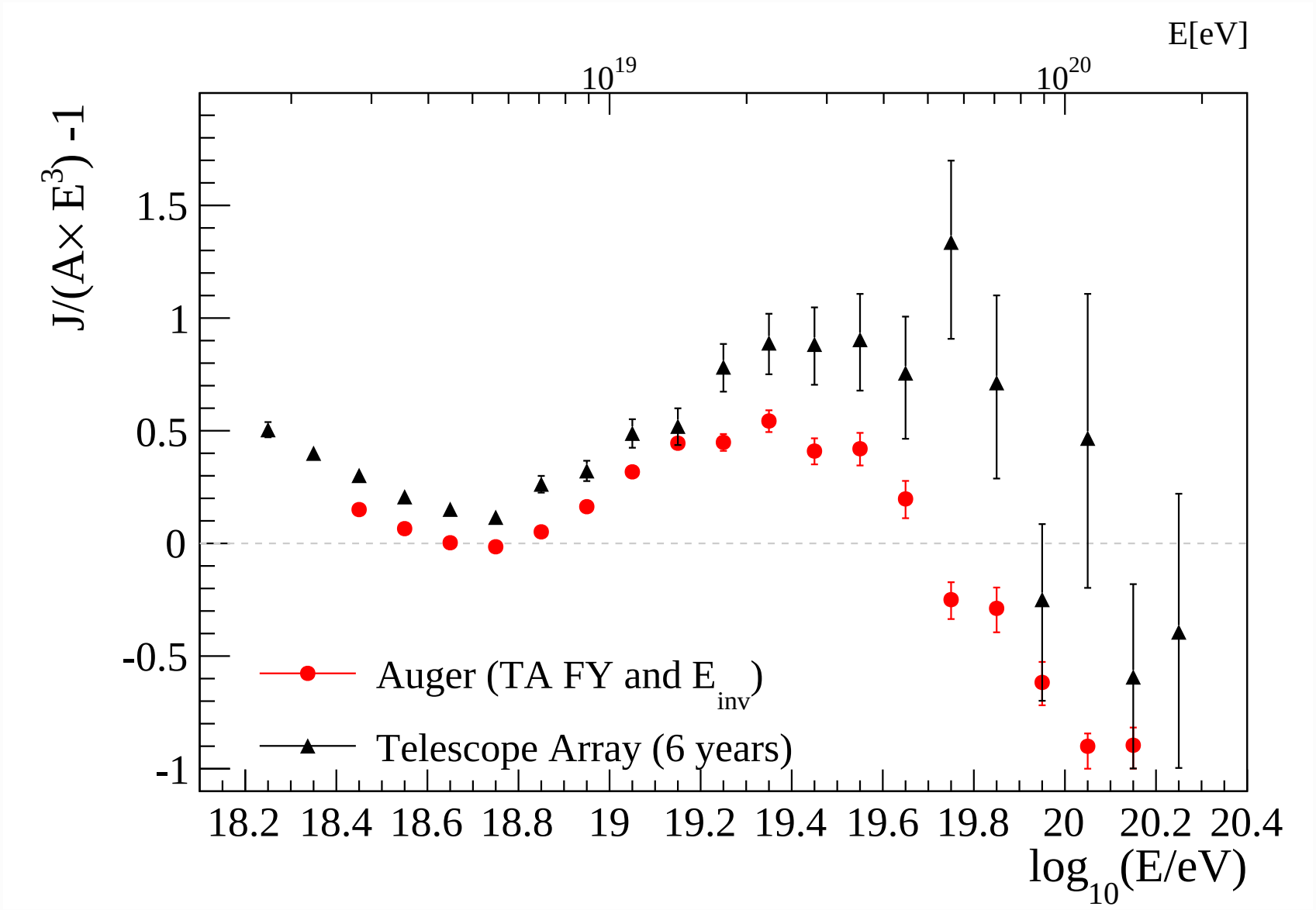

The ankle energy region

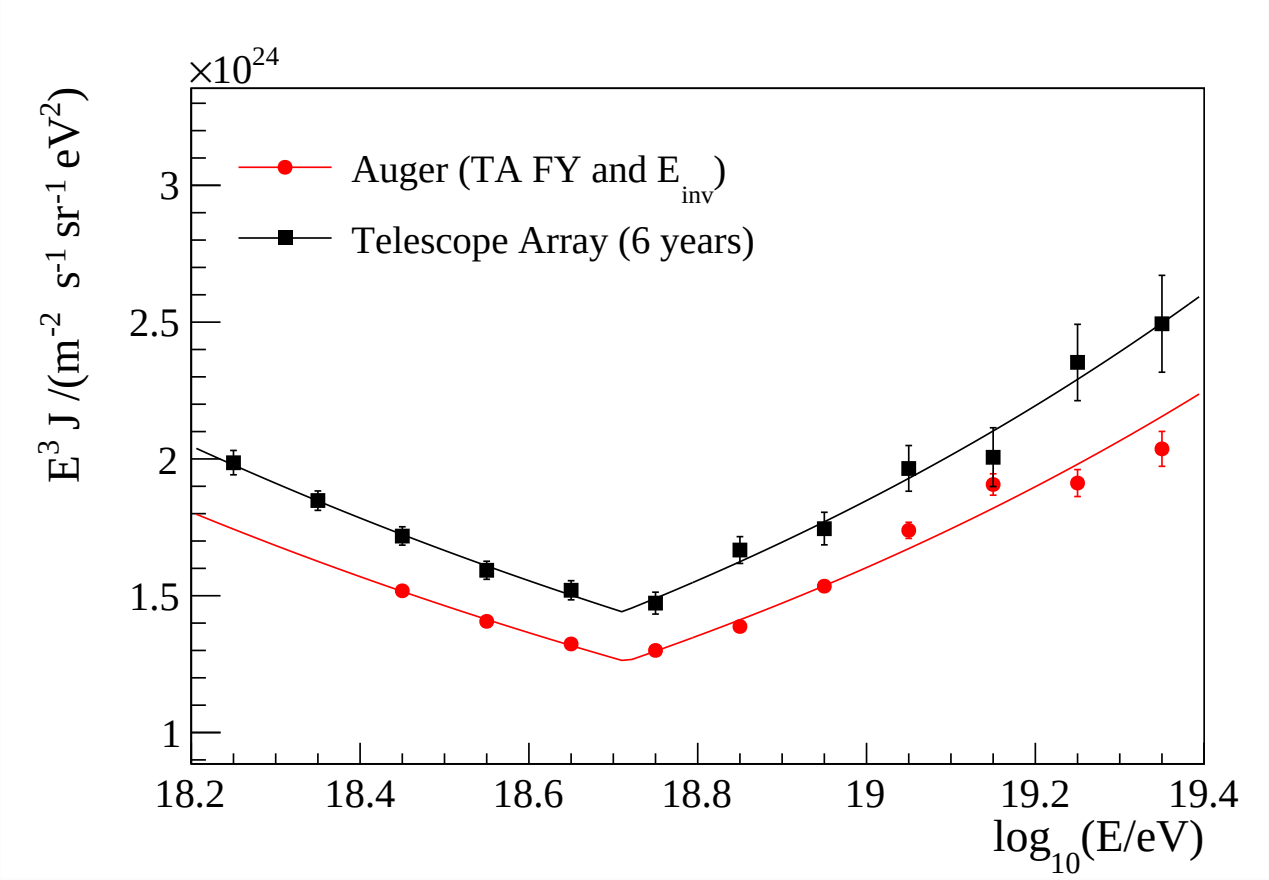

- $\log_{10}(E_{TA}/eV) = 18.70 \pm 0.02$, $\log_{10}(E_{Auger,TAset}/eV) = 18.71 \pm 0.004$
- $\gamma_{TA} = -3.30 \pm 0.03$, $\gamma_{Auger,TAset} = -3.30 \pm 0.03$
- $\gamma_{TA} = -2.67 \pm 0.03$, $\gamma_{Auger,TAset} = -2.63 \pm 0.02$

Spectral features

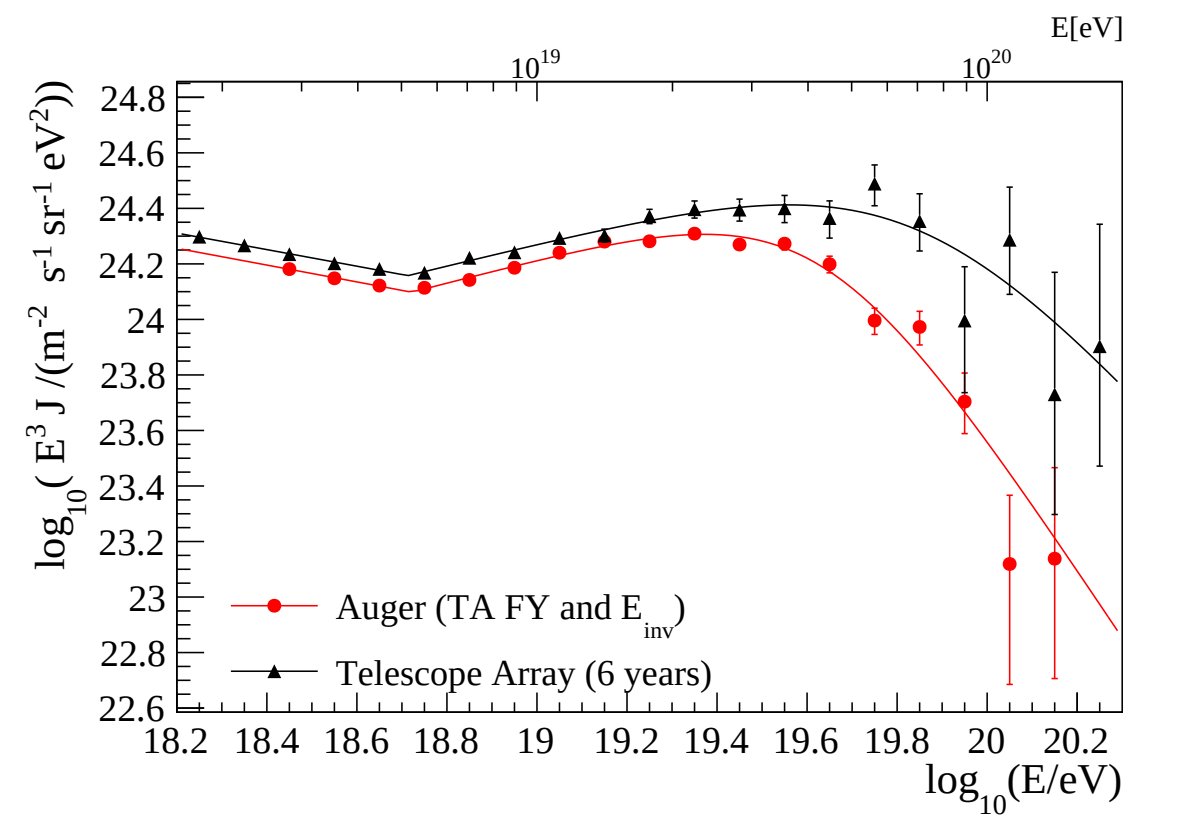

Auger (TA FY and inv. en):

$\gamma_1 = -3.30 \pm 0.03$, $\gamma_1 = -2.57 \pm 0.02$

$\lg(E_1/eV) = 18.72 \pm 0.01$

$\lg(E_{1/2}/eV) = 19.64 \pm 0.01$

Telescope Array:

$\gamma_1 = -3.30 \pm 0.03$, $\gamma_2 = -2.62 \pm 0.05$

$\lg(E_1/eV) = 18.71 \pm 0.02$

$\lg(E_{1/2}/eV) = 19.88 \pm 0.06$

Normalizing the energy spectra (constant energy shift)

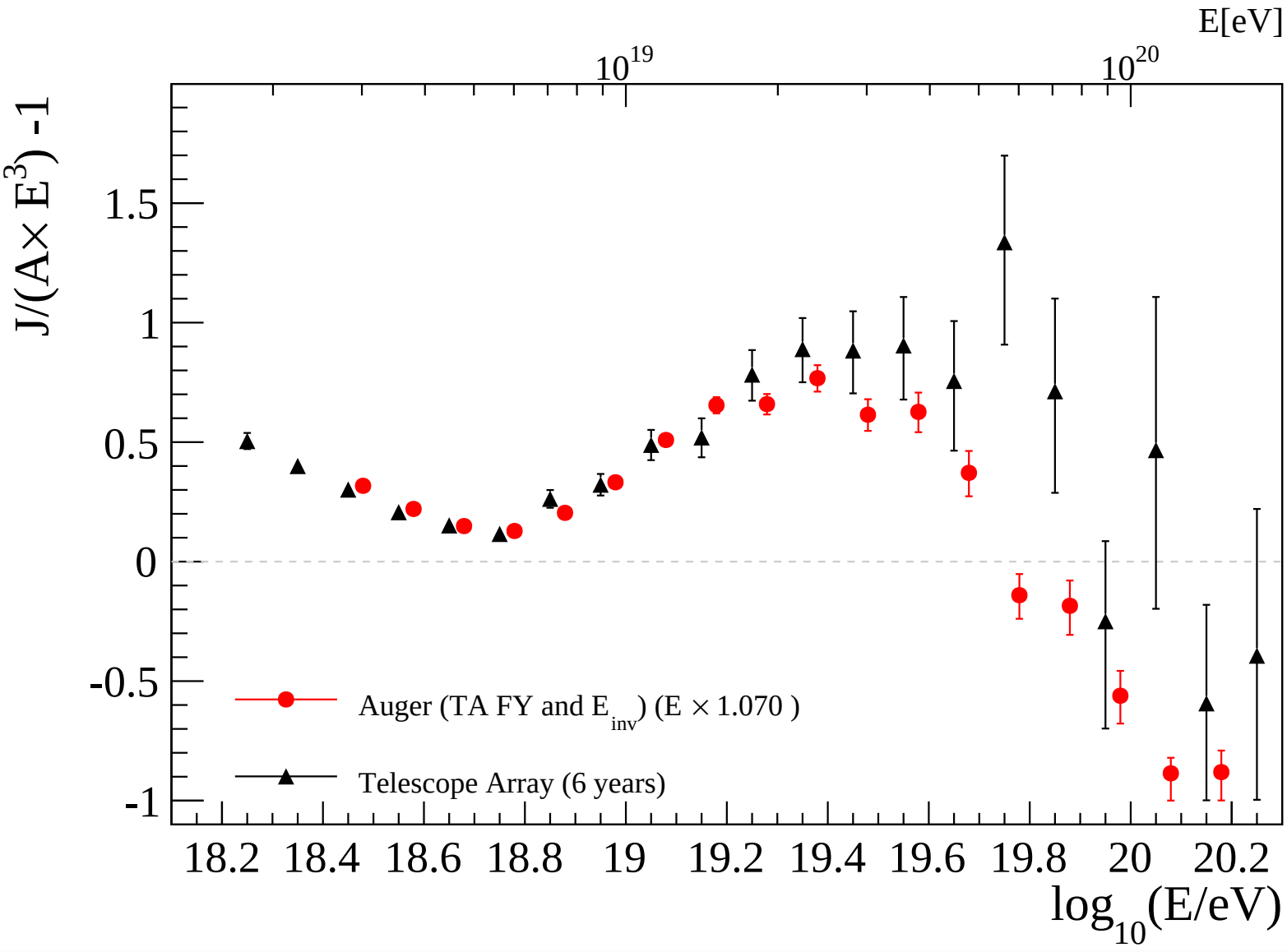

$\Rightarrow$ 7% difference on energy ($\chi^2/\mathrm{ndof} = 1.6$)

Normalizing the energy spectra (constant energy shift)

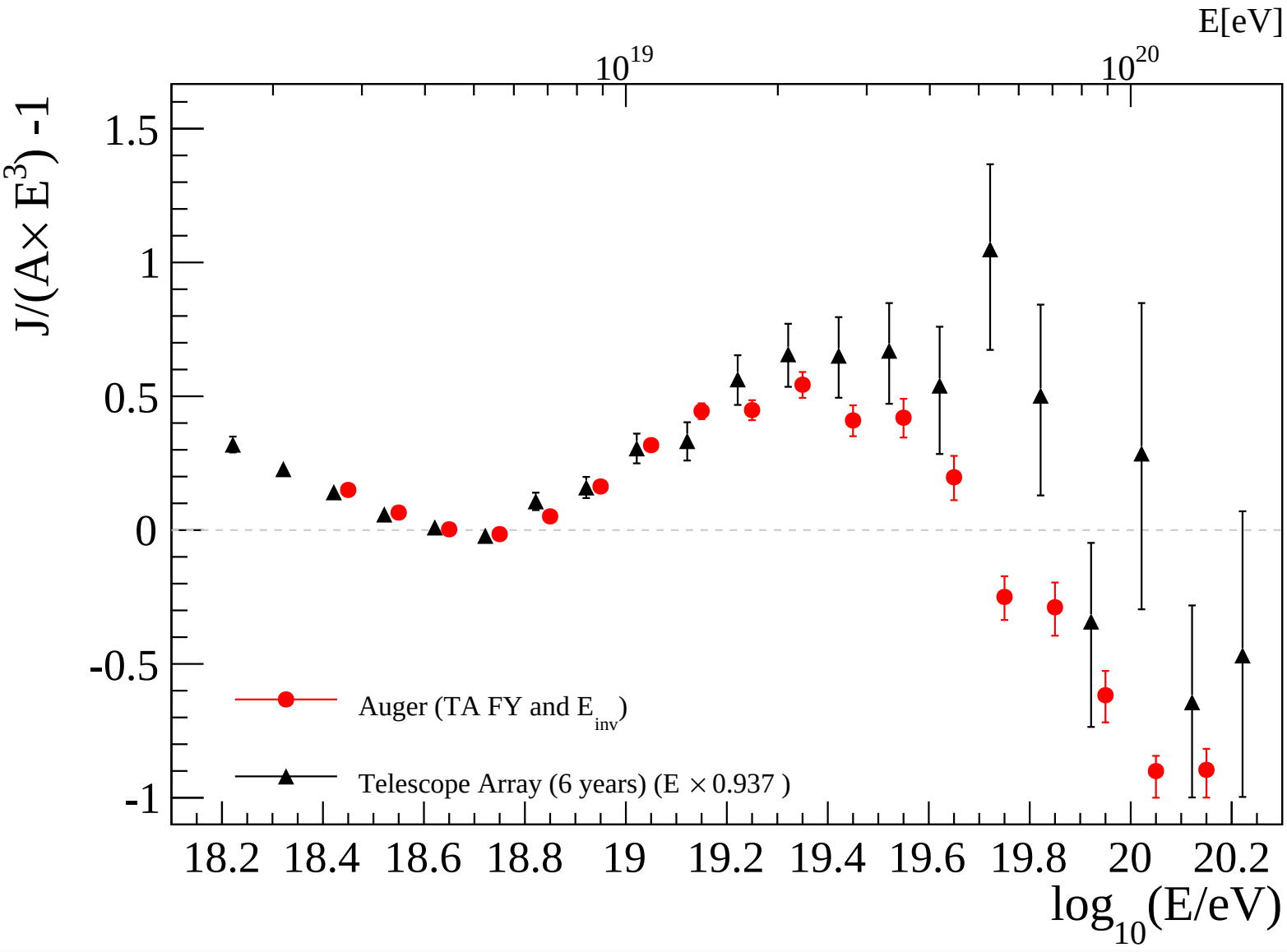

$\Rightarrow$ 7% difference on energy ($\chi^2/\mathrm{ndof} = 1.6$)

Energy dependent normalization

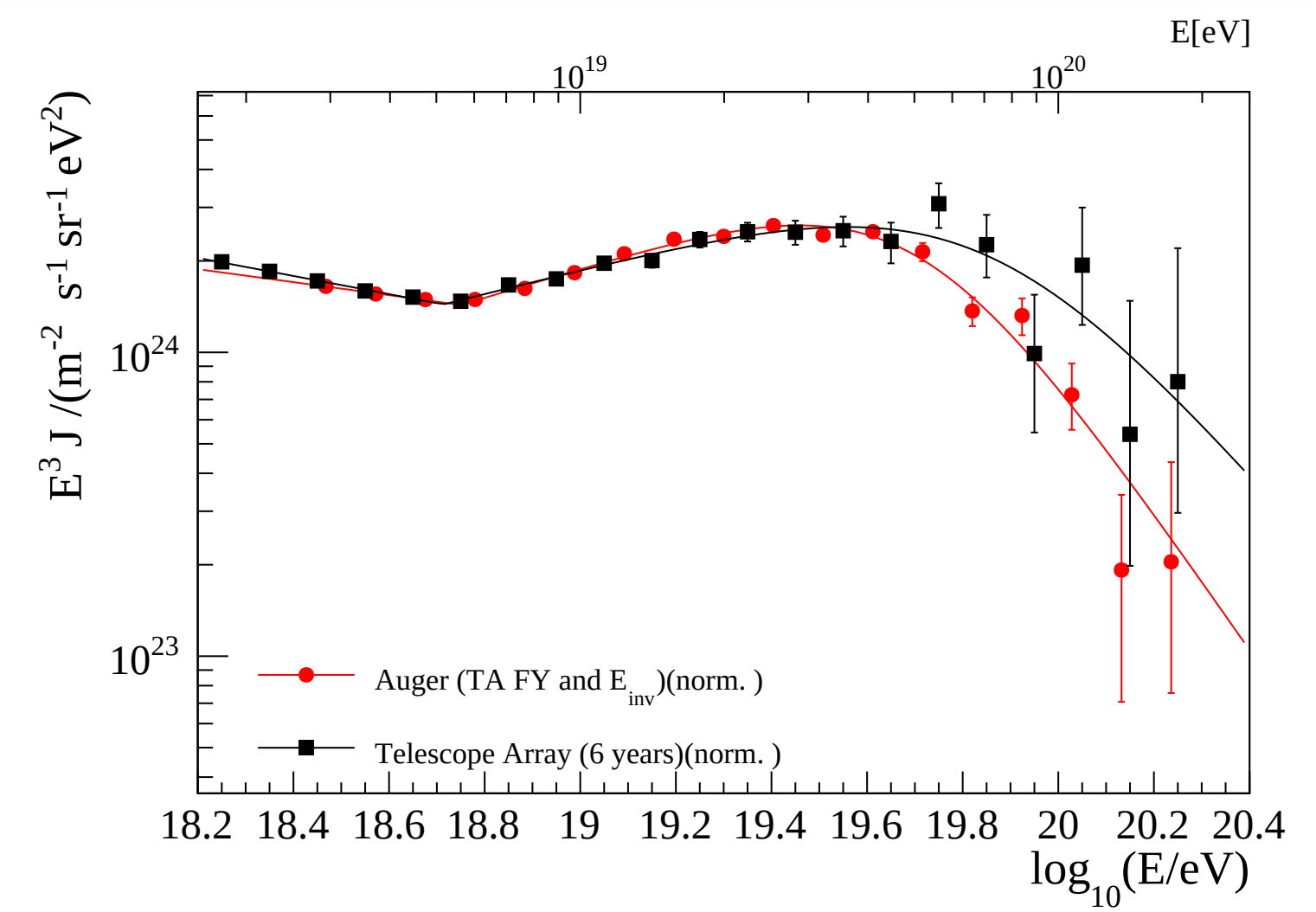

$\lg(E) = a + b \cdot \lg(E)$, $\chi^2/\mathrm{ndof} = 0.75(\mathrm{Prob} = 0.85)$

Energy dependent energy scaling

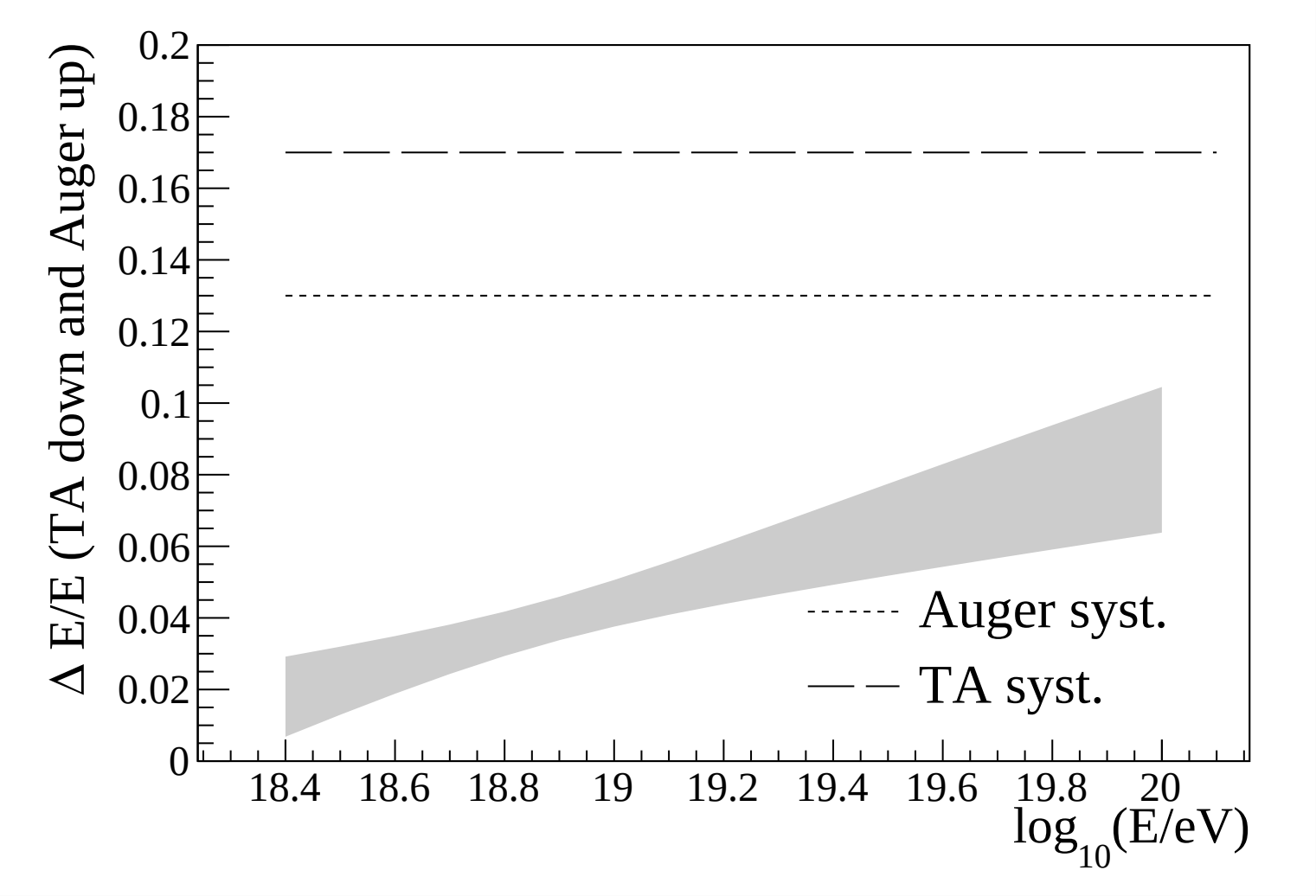

- after using the same FY and invisible energy, dividing the contribution naively in two
- can we find these systematic uncertainties dependency?

Is the TA hot-spot causing the flux differences?

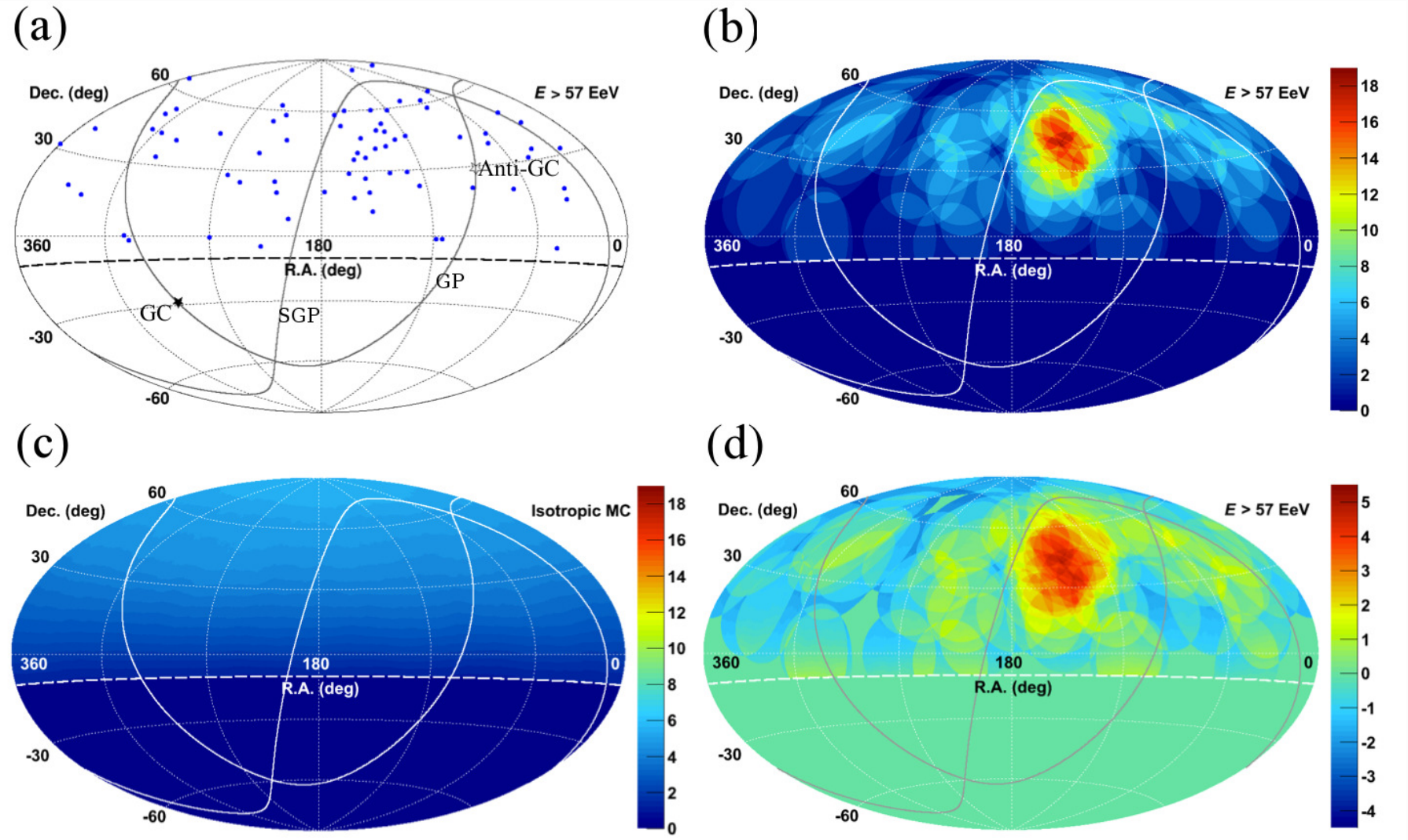

Declination dependent exposure

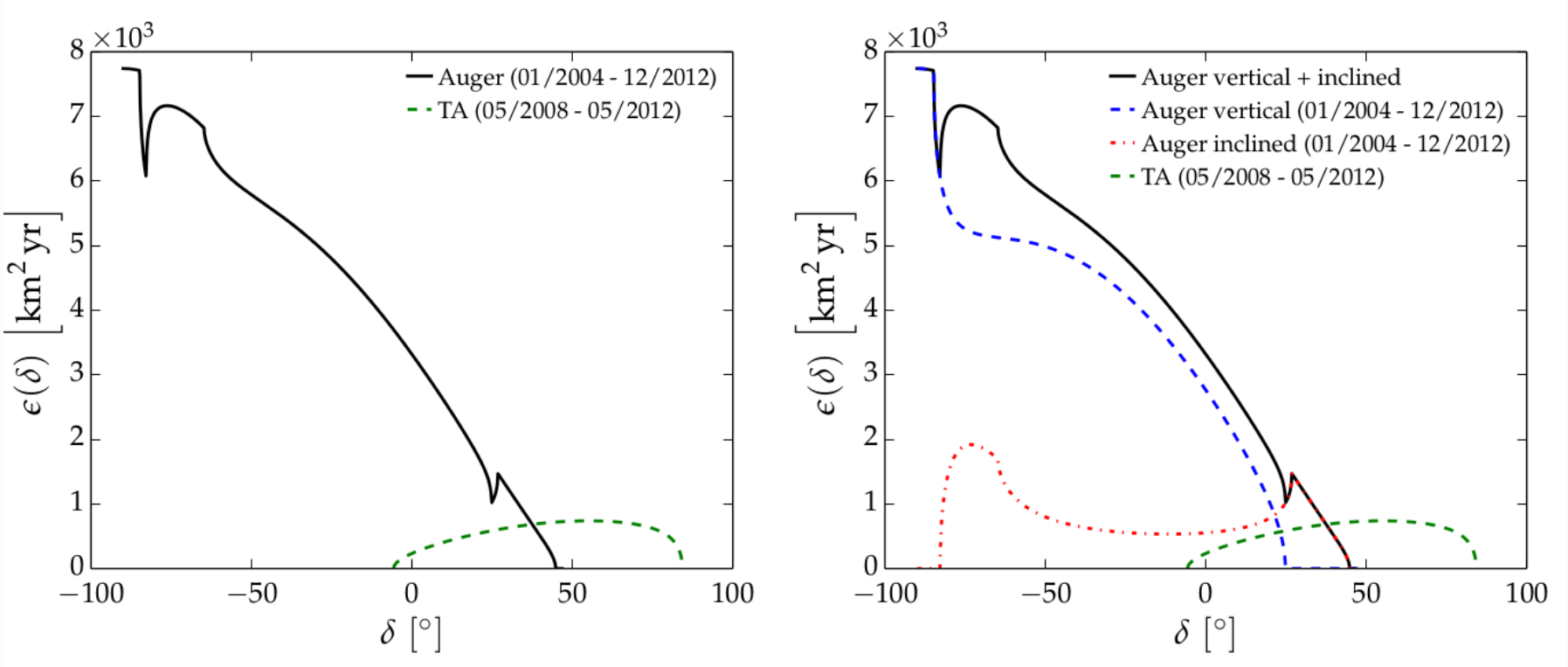

- TA: 05/2008 - 05/2012, Auger: 01/2004-12/2012
- Auger: divide the data set in four sky regions of equal exposure
- TA: divide the data in off/on-source and in two declination bands

Auger energy spectrum in the common sky

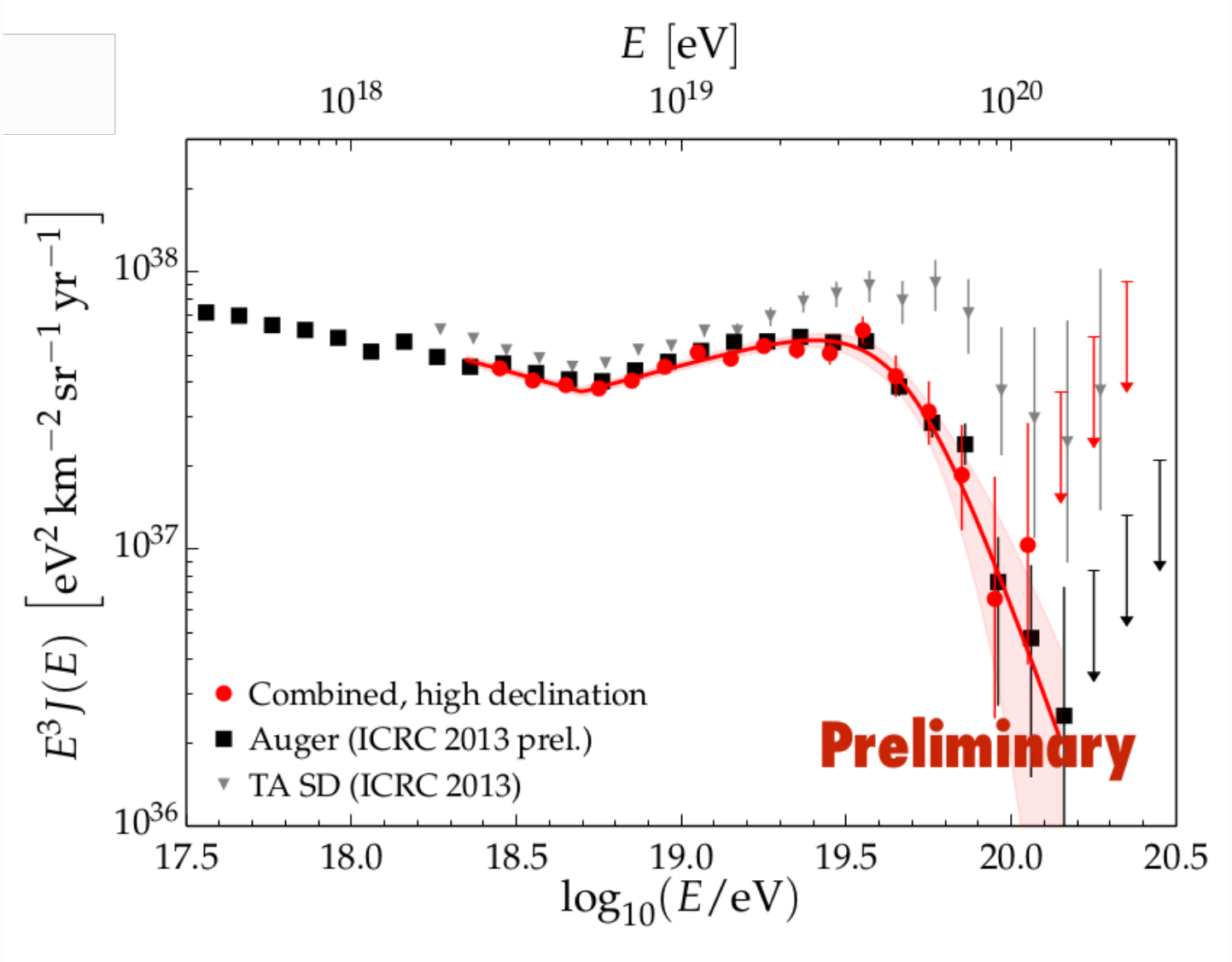

$\Rightarrow$ No difference observed with the Auger data ($0 < \delta < 45$)

TA: On/off source definition

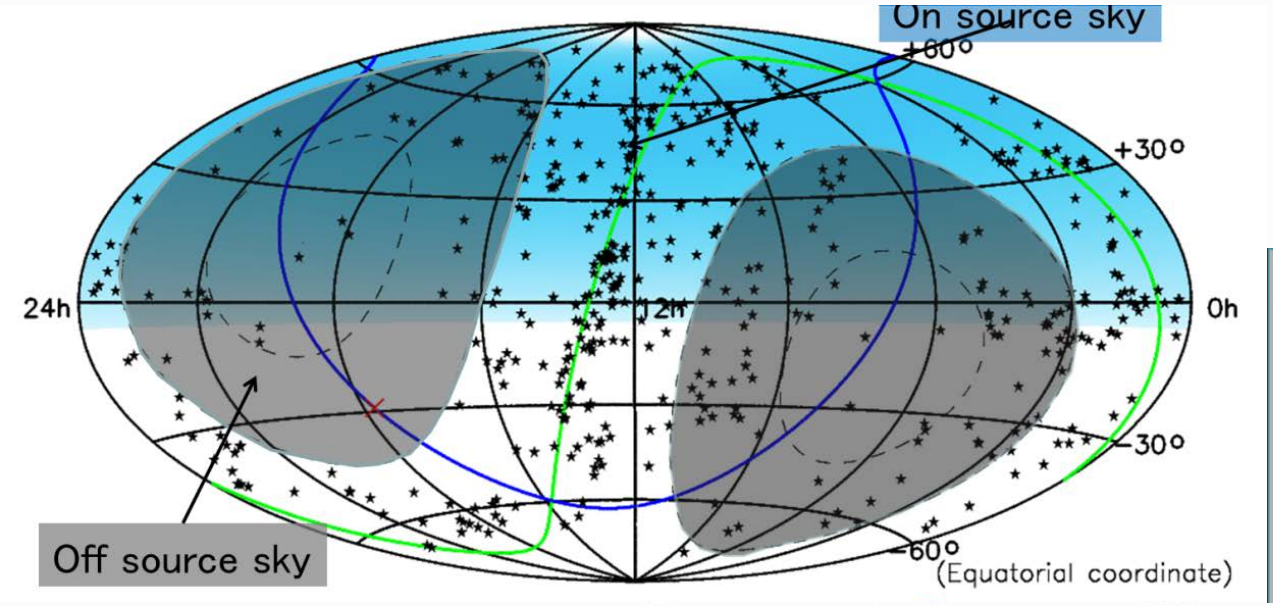

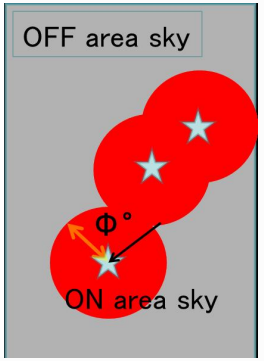

- On source 1: super galactic plane $\pm 30°$
- On source 2: VCV catalogue, $11°$ around sources (after scan to maximise N_{on}/N_{off})

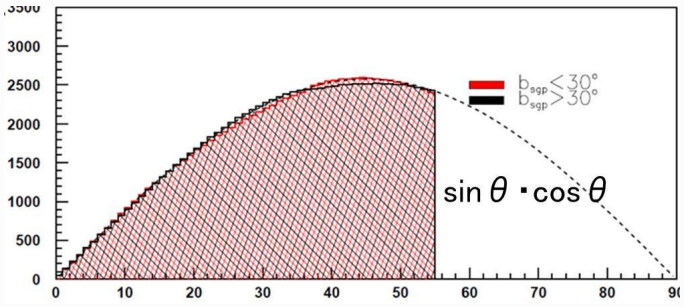

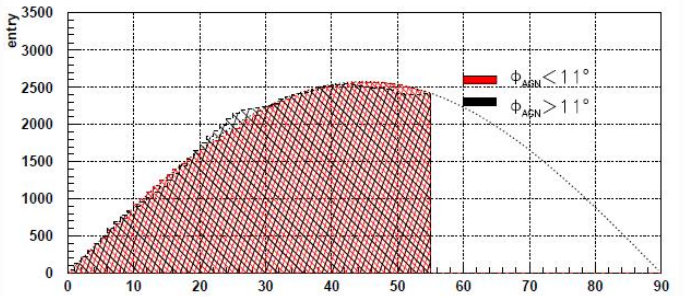

TA on/off sources, preliminary

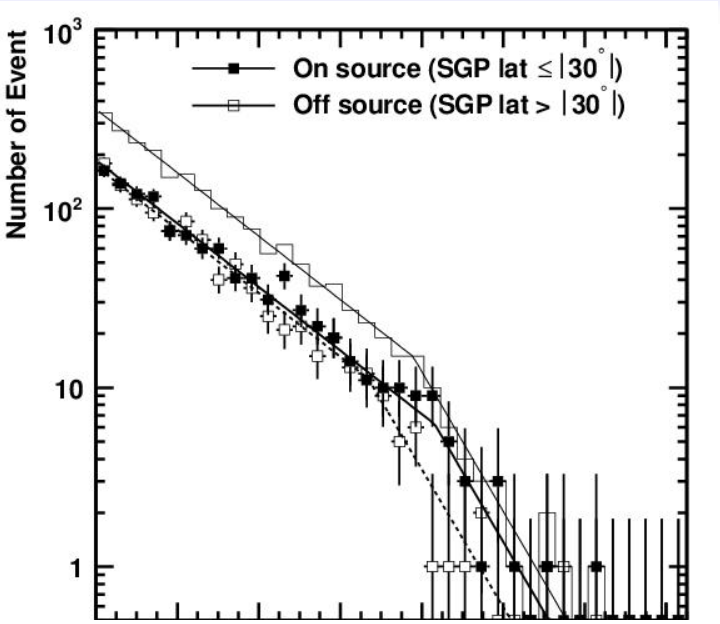

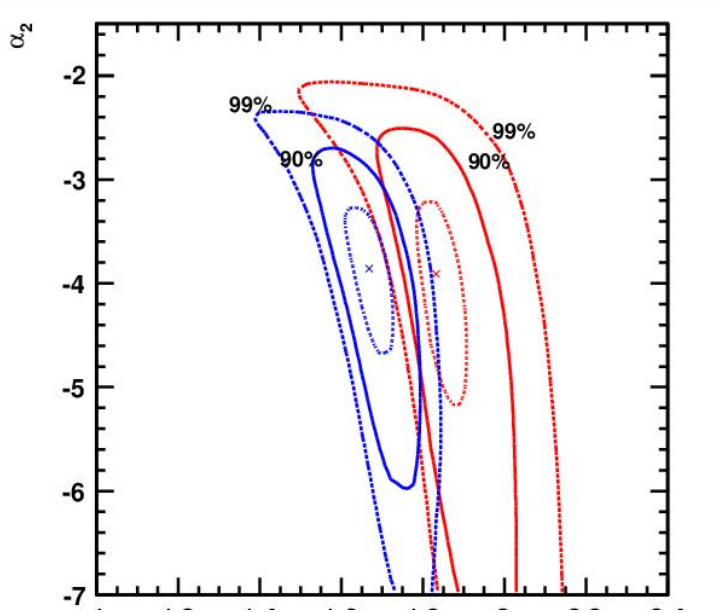

$\frac{N_{off}(E>E_b)}{N_{all}(E>E_b)} = 0.34$
(exp. 0.48)
P = 0.0006

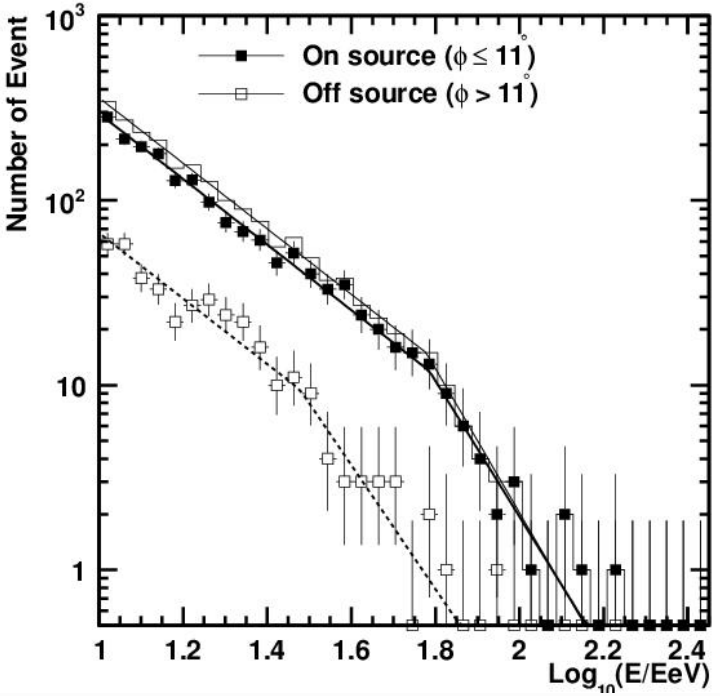

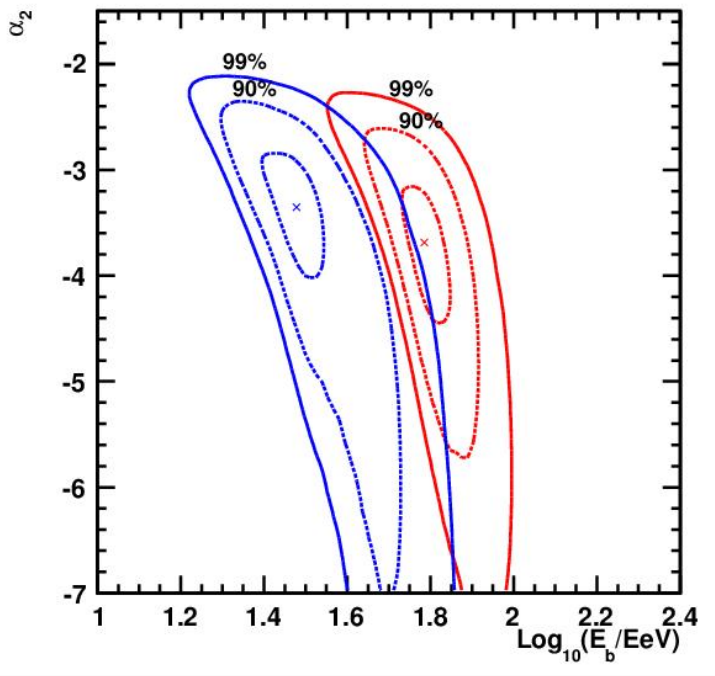

$\frac{N_{off}(E>E_b)}{N_{all}(E>E_b)} = 0.12$
(exp. 0.19)
P = 0.015
(with scan penalty)

Common sky TA-Auger ($\delta < 26^\circ$), preliminary

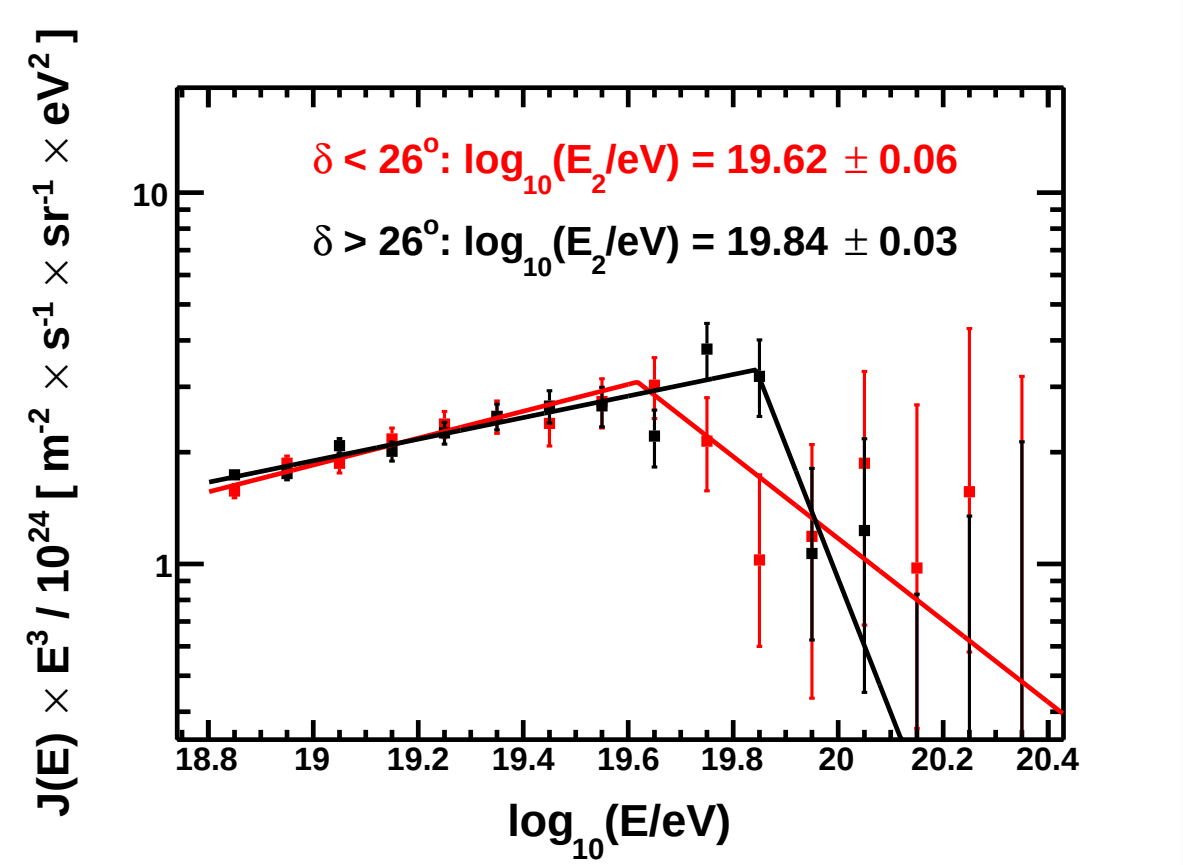

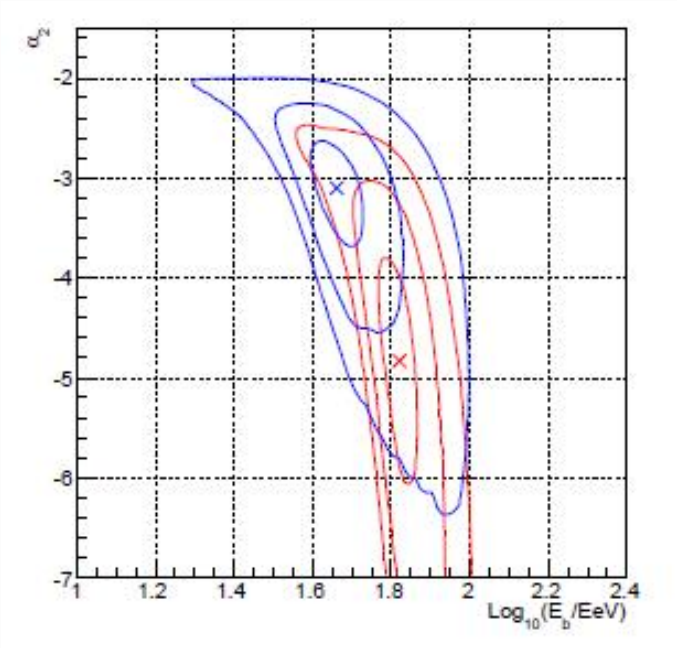

$\Rightarrow$ indication for a flux difference ($\approx 3\sigma$)

Summary

Features of the energy spectra

- all of them indicate the acceleration and propagation mechanisms
- changes of spectral slopes at the knee, ankle and a flux suppression

Still lots of things to solve

- where is the transition from galactic to extragalactic component
- is there a second knee? If so is it produced by Fe?
- is there a flux difference between the North and South at the high energies?
- ....